The LHCb detector performance and upgrade and BR($\Lambda_b \to \Lambda_c^* D_s^{(*)}$ / $\Lambda_b \to \Lambda_c D_s^{(*)}$) measurement

F. Borgato

27th July 2023

My PhD thesis

- General **introduction** on **LHCb detector and the Upgrades**
- What was done for the **current LHCb detector and collaboration**?
  - RICH Upgrade 1 commissioning
  - BR($\Lambda_b \to \Lambda_c^* D_s^{(*)}$ / $\Lambda_b \to \Lambda_c D_s^{(*)}$) measurement
- What was done for the **LHCb detector Upgrades**? Timing!
  - RICH LS3 enhancements
  - VELO Upgrade 2 R&D

Lot of stuff! But there is real work in all these sections

RICH Upgrade 1 commissioning

- Talk at LHCb week RICH parallel session (Feb 2023)
- Talk at Marseille LHCb week RICH parallel session (Sept 2023)

Threshold scans analysis

Threshold scans analysis are a fundamental tool to **optimize the detector performance** since it allows to:

- choose the **optimal threshold** of operation
- **fine tune** the **HV**
- check the **aging** of the sensors

Steps completed/ongoing on RICH1 and RICH2 data:

- compare the **Quality Assurance anode gains** with the **ComLab ones** ✅
- develop the **tools for the threshold scan at P8** ✅
- check the **detector status before** the start of **Run3** ✅
- calculate **k-factors** with **ComLab and P8** thr. scan data ⭐
- **compare PDM to PDM gains** to **fine tune the HV** and increase the **detector uniformity** ⭐

For more details, see the LHCb week presentation

Today's presentation

Quality Assurance data

During the **MaPMTs Quality Assurance** phase, the **gain of all the sensor anodes were extracted** using an **electronics different from the current RICH** one (that was not available at the time).

Thus the QA gains are an **independent gain measurement** that can **validate** what was observed during the **ComLab Commissioning** phase.

The considered **HV** is the one at which **RICH1 and RICH2 are currently operated**.

In particular in the **QA data** it is possible to observe an **enhanced gain** for the **bordering anodes of MaPMTs ECR-type**.

1	2	3	4	5	6	7	8
9	10	11	12	13	14	15	16
17	18	19	20	21	22	23	24
25	26	27	28	29	30	31	32
33	34	35	36	37	38	39	40
41	42	43	44	45	46	47	48
49	50	51	52	53	54	55	56
57	58	59	60	61	62	63	64

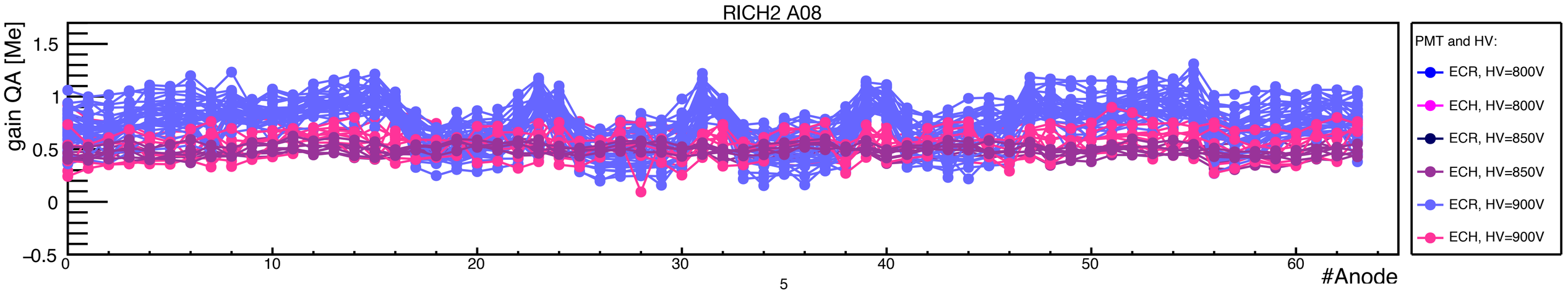

ComLab threshold and DAC scans

In the **ComLab** a **full set of scans** was taken. This means:

- One **integrated charge spectrum** for **each anode** (threshold scan)
- One **DAC scan for each anode** , to correlate threshold and charge

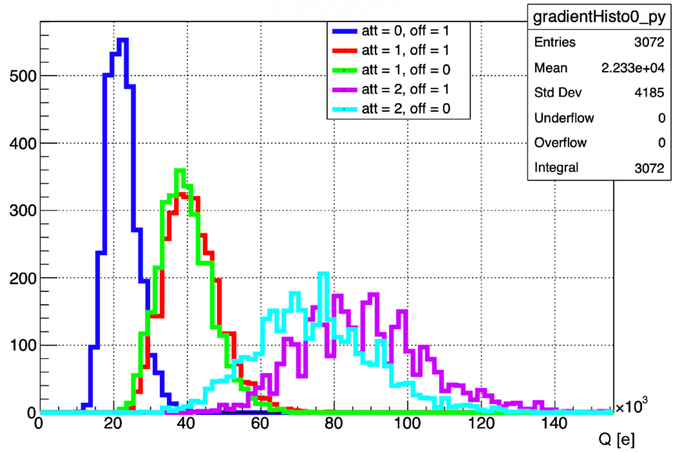

x4 ! **CLARO asic** has **two possible configuration parameters**:

- **Attenuation** (equal to 1,2 ; amount of charge for each threshold step, att=1 approximately 40ke)
- **Offset** (equal to 0,1 ; shift of CLARO baseline)

In **one RICH1 column** there are:

64 anodes per PMTs, 72 PMTs R-type 4 CLARO config.
≈ **18k config. to test**

In **one RICH2 column** there are:

64 anodes per PMTs, 16 PMTs H-type & 32 PMTs R-type 4 CLARO config. ≈ **12k config. to test**

The phase space is big, so a stable methodology to find the best CLARO configuration for each anode is needed.

Starting from DAC scans checks

From the **DAC scans**, the **CLARO available range of charge** for a **certain attenuation, offset** combination was observed and it was checked that the **QA gain is contained in such a range**.

RICH2 A01 PDM0 EC0 PMT0

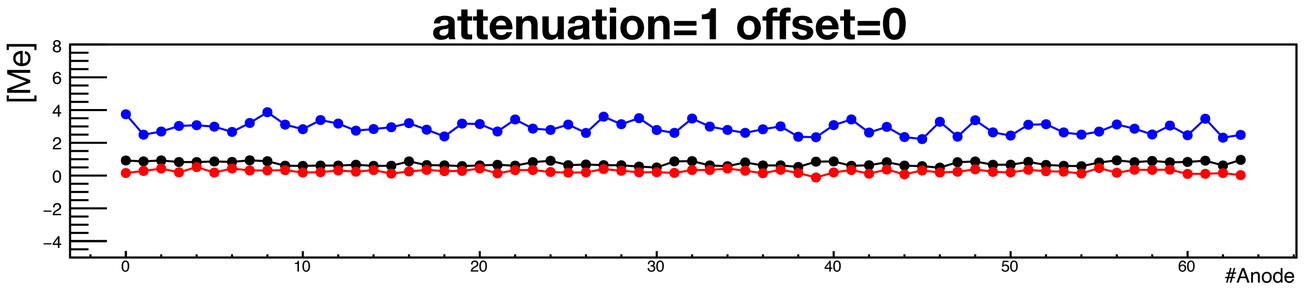

RICH2 A01 PDM0 EC0 PMT0

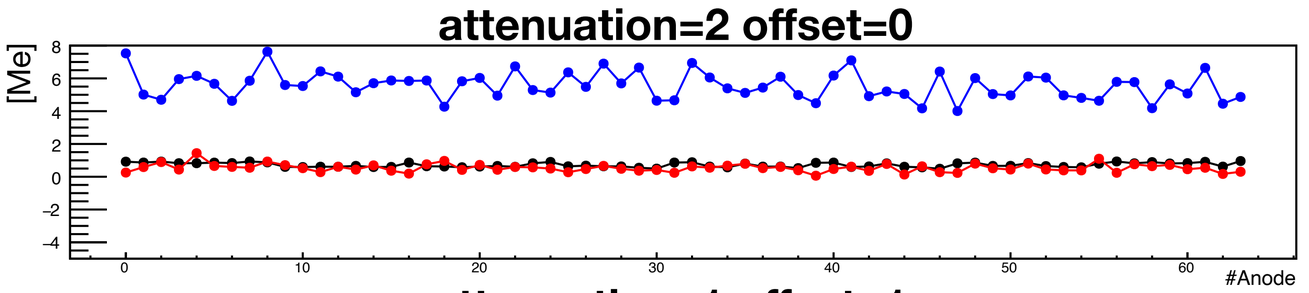

RICH2 A01 PDM0 EC0 PMT0

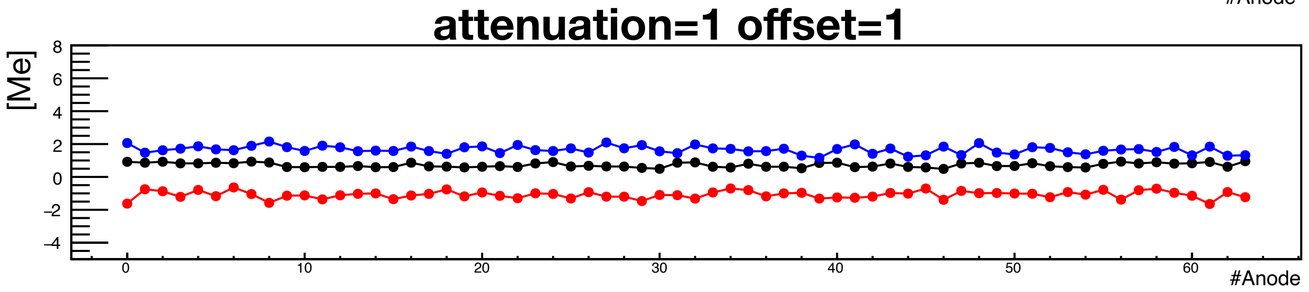

RICH2 A01 PDM0 EC0 PMT0

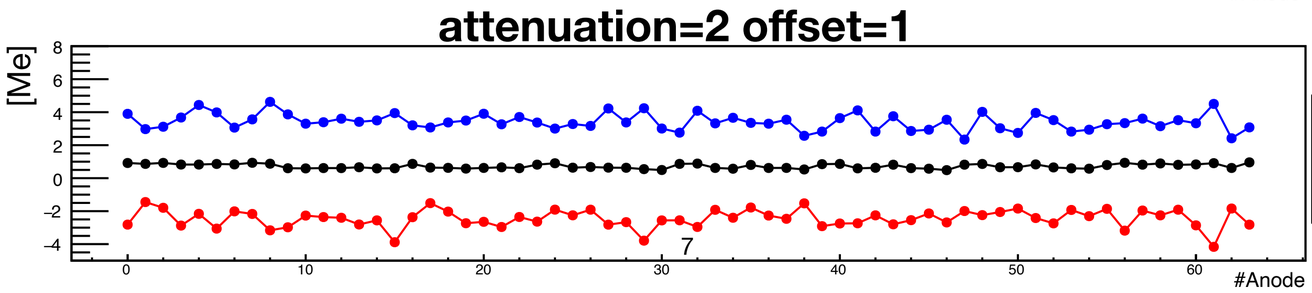

Threshold scans analysis

Integrated spectrum charge from the **threshold scan** with **different CLARO configurations** for one anode of column A01:

att=1 off=0

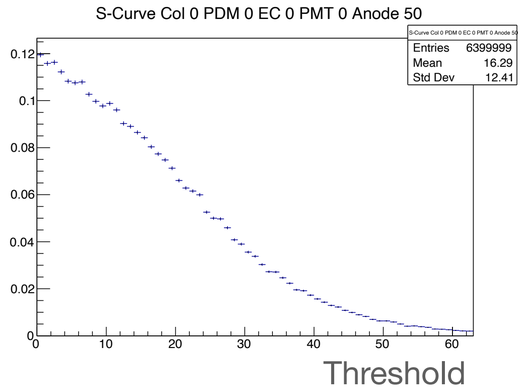

att=2 off=0

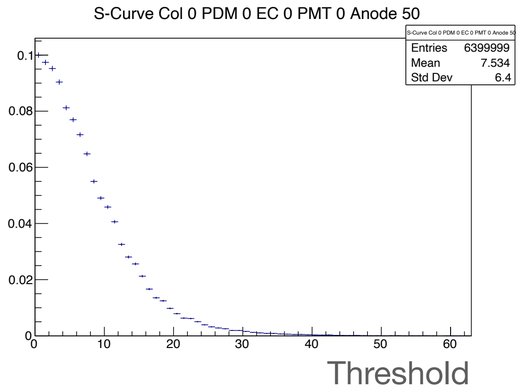

att=1 off=1

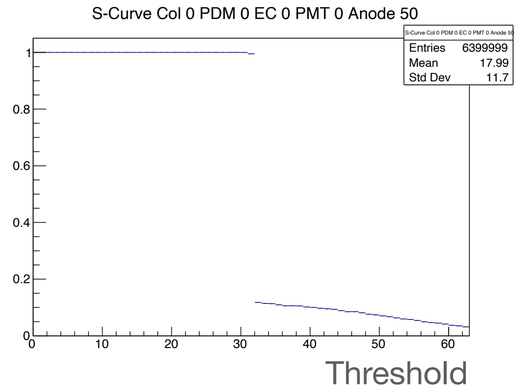

att=2 off=1

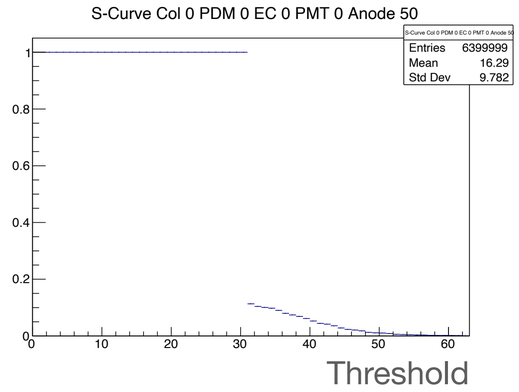

With offset=0, the threshold range does not allow to reach the baseline.

In order to **extract the anode gain** from these data, I **look for the flex in the integrated spectrum** (which is the maximum of the charge distribution itself).

Threshold scans analysis

Integrated spectrum charge from the **threshold scan** with **different CLARO configurations** for one anode of column A01:

att=1 off=0

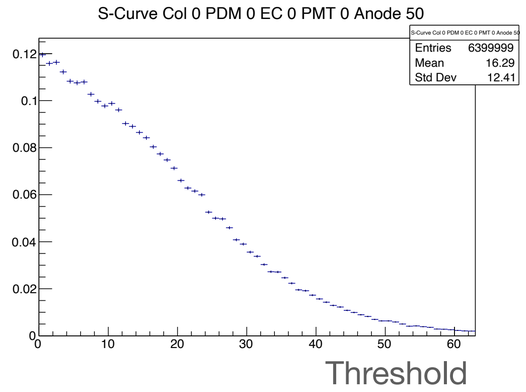

att=2 off=0

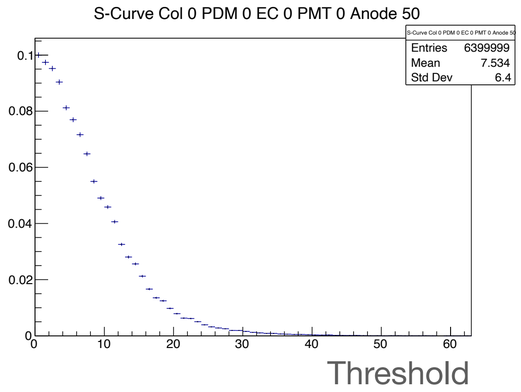

att=1 off=1

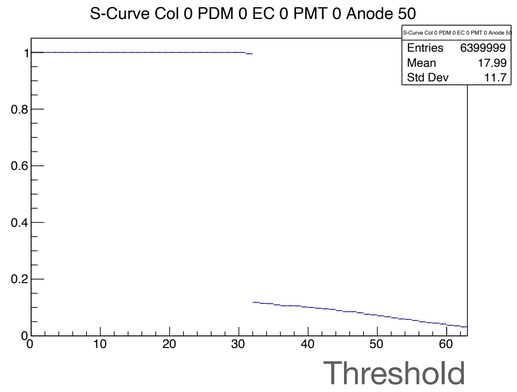

att=2 off=1

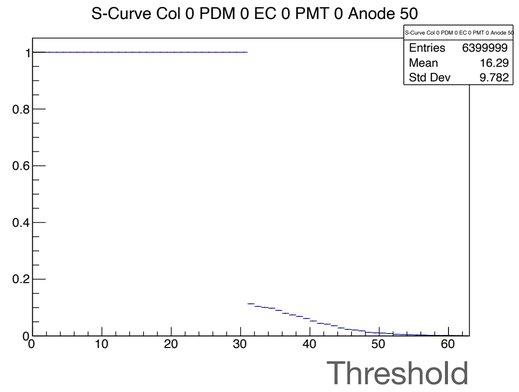

I **fit the integrated charge spectrum** with an erf function to extract the flex.
When offset=1, I exclude the baseline points.

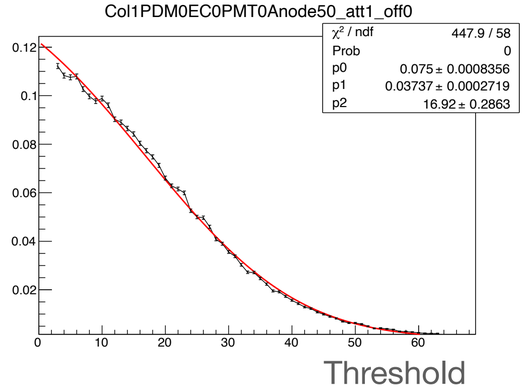

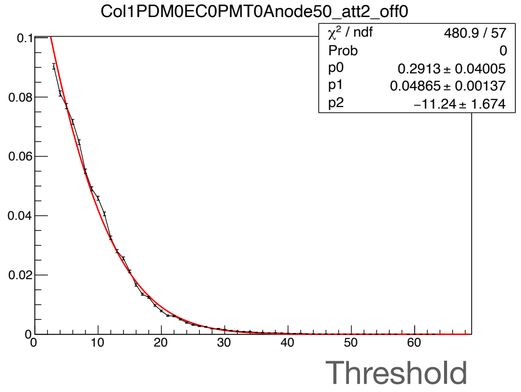

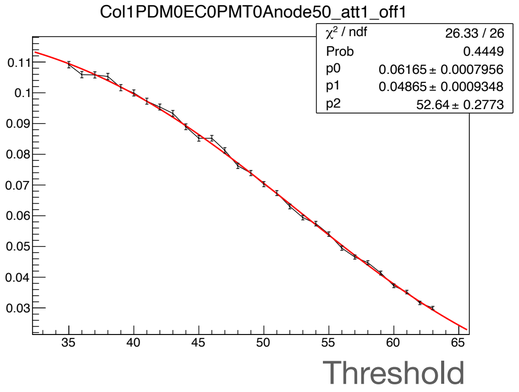

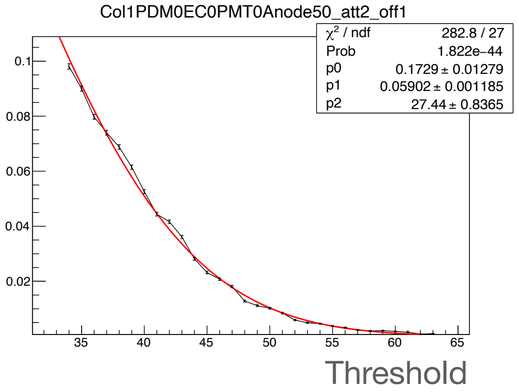

Threshold scans analysis

Fit quality checks:

I perform the fit with no range limits.

If the reduced χ^2 is higher than 30, I remove one point from the lower limit of the range, up to 3 points.

If after this procedure the reduced χ^2 is higher than 30 still, I change the fit parameters settings.

att=1 off=0

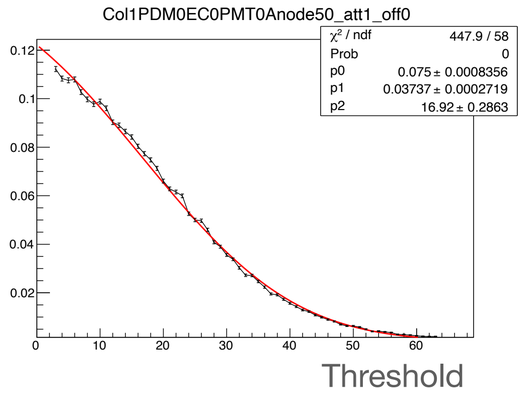

att=2 off=0

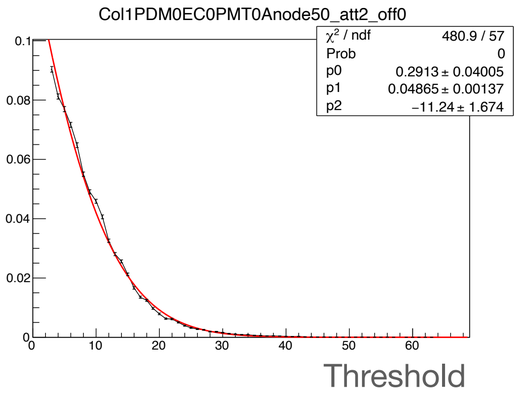

att=1 off=1

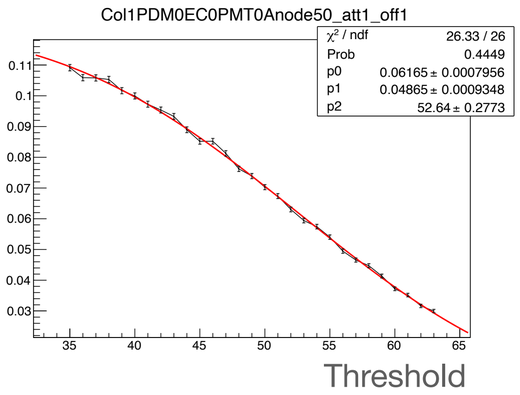

att=2 off=1

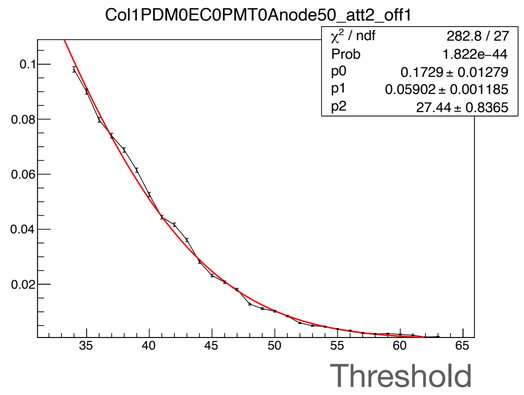

Once I **have the flex**, I **convert** from threshold **to charge by means of the DAC scan**.

Which configurations to choose for each anode?

Once a **gain-threshold for all the configurations** is extracted, I take as **default the att=1 off=1** one.

- **Att=1 best precision** measurement (smaller charge step) .
- **Off=1** guarantees that the **baseline is included** in the **integrated charge spectrum**.

In general as default the flex at configuration att=1,off=1 is chosen.
If the flex is too high, the flex at att=1, off=0 is taken.
If the flex is too low, the flex at att=2, off=1 is taken.

att=1 off=0

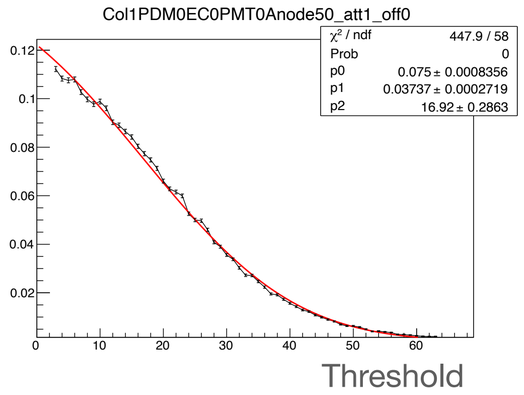

att=2 off=0

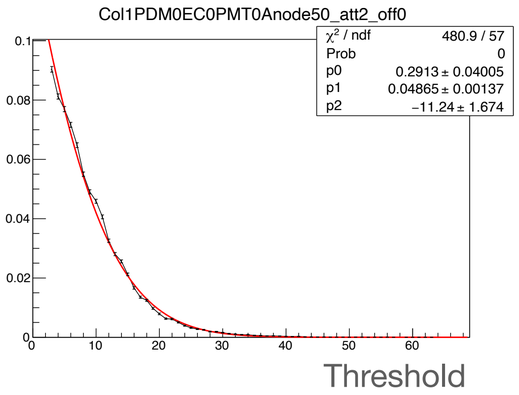

att=1 off=1

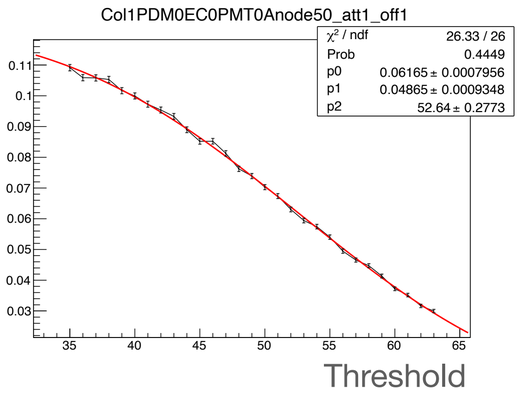

att=2 off=1

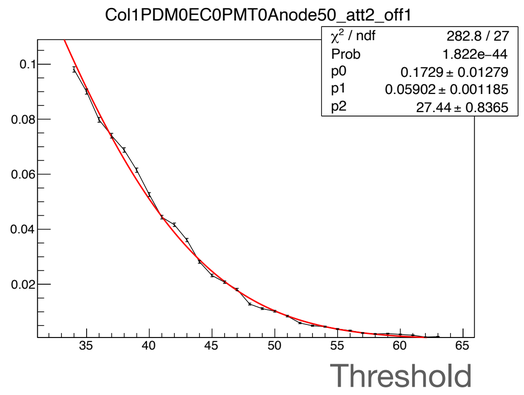

The procedure is repeated for all the anodes of each PMT.

Comparison of QA and DAC+Th scan gains
An example from RICH2, col A02

Finally one can **compare QA and DAC+thr scans anode gains,** both computing the **average gain for each PMT** and the **gain for the single anode**

HV=1000V

QA gain (max from fit)
QA gain (peak finding)
DAC+Thr scan gain
Hamamatsu

Average PMT gain for all A02 PDMs

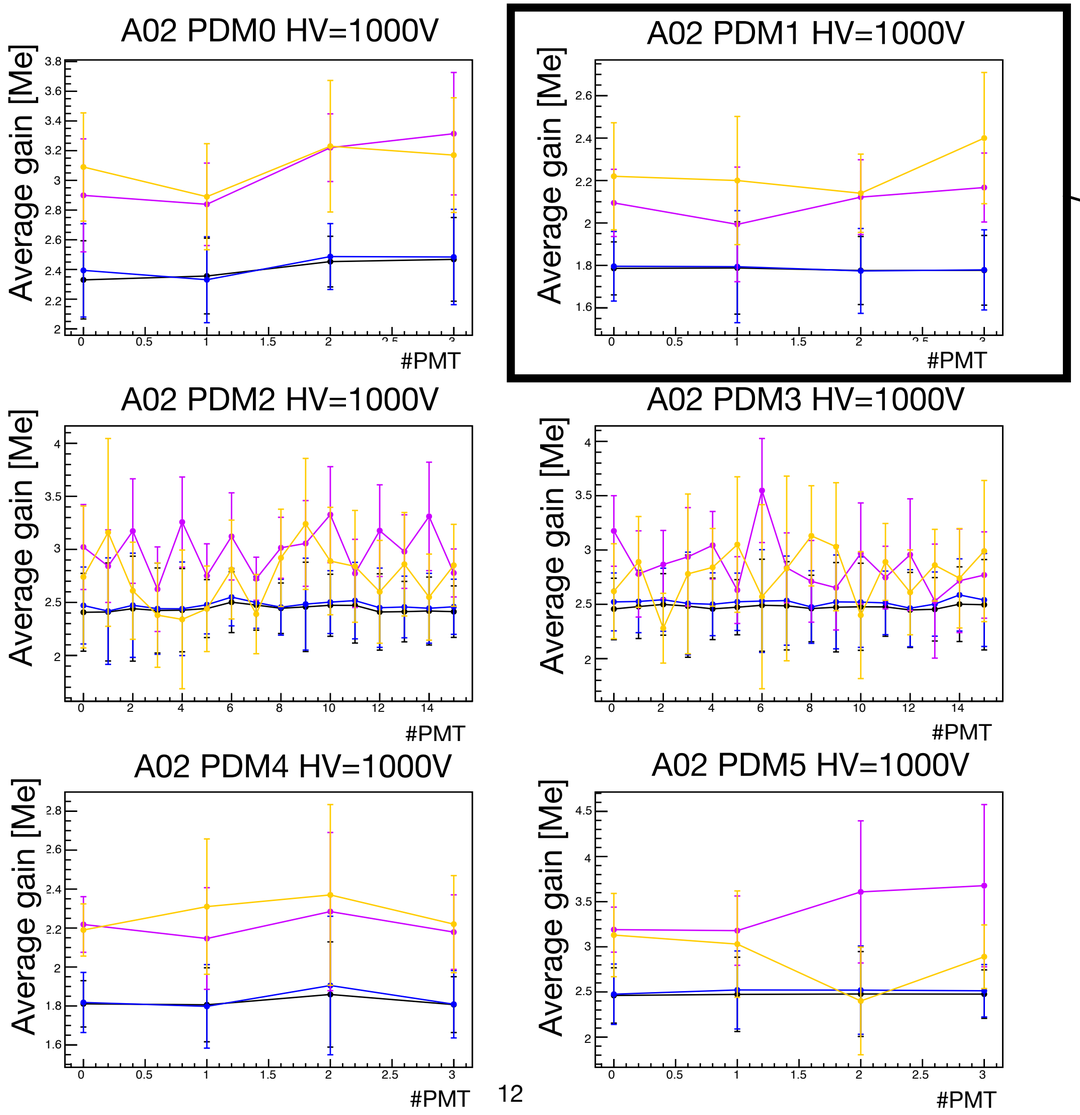

A02 PDM1

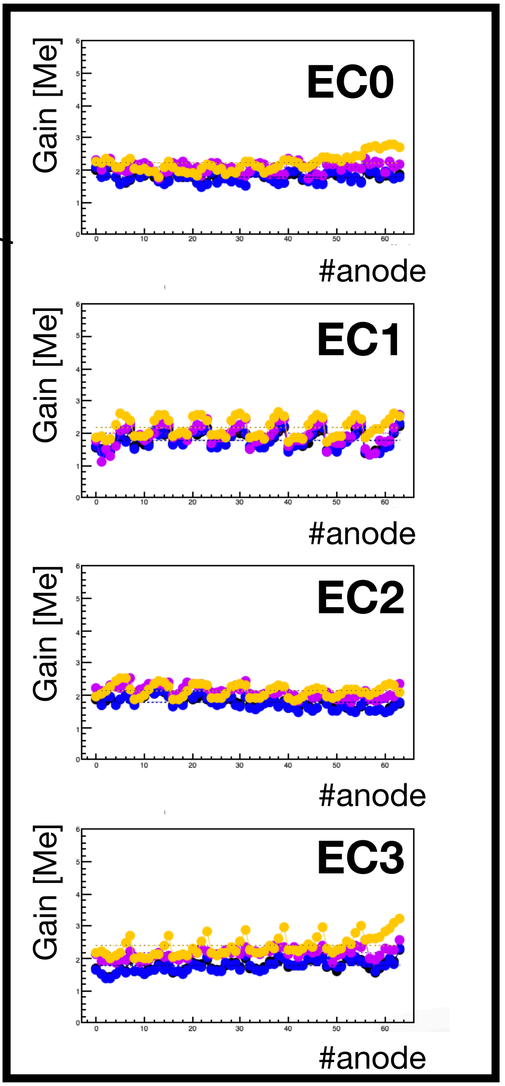

Comparison of ComLab and P8 threshold scan
An example from RICH1, col D04

It is possible **ComLab anode gains with the P8 ones,** both computing the **average gain for each PMT** and the **gain for the single anode**

HV=900V

ComLab gain
P8 gain

Average PMT gain for all D04 PDMs

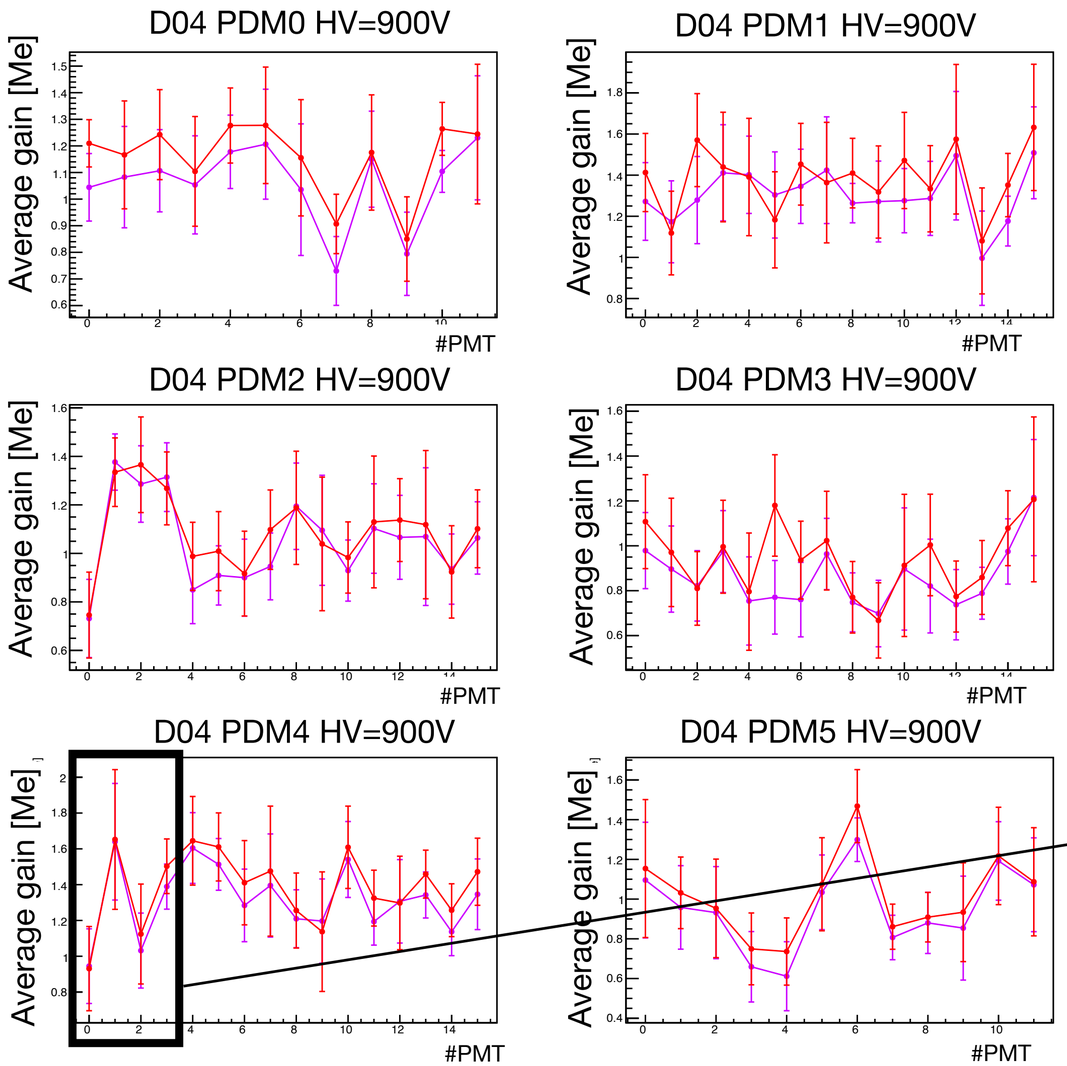

D04 PDM4 EC0

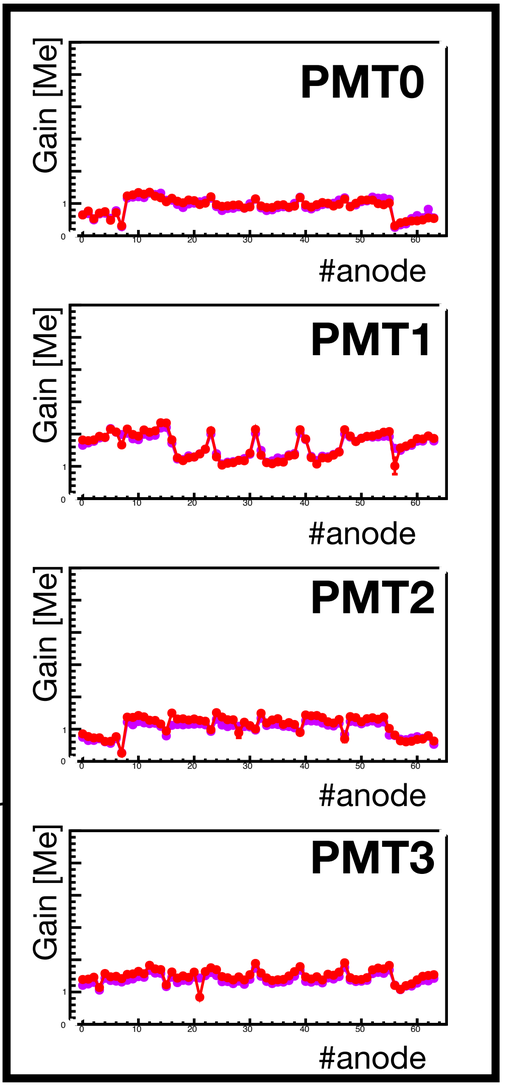

Comparison of ComLab and P8 threshold scan
An example from RICH1, col D04

- **Threshold scan procedure** fully **validated**
- **No aging** observed at all

HV=900V

ComLab gain
P8 gain

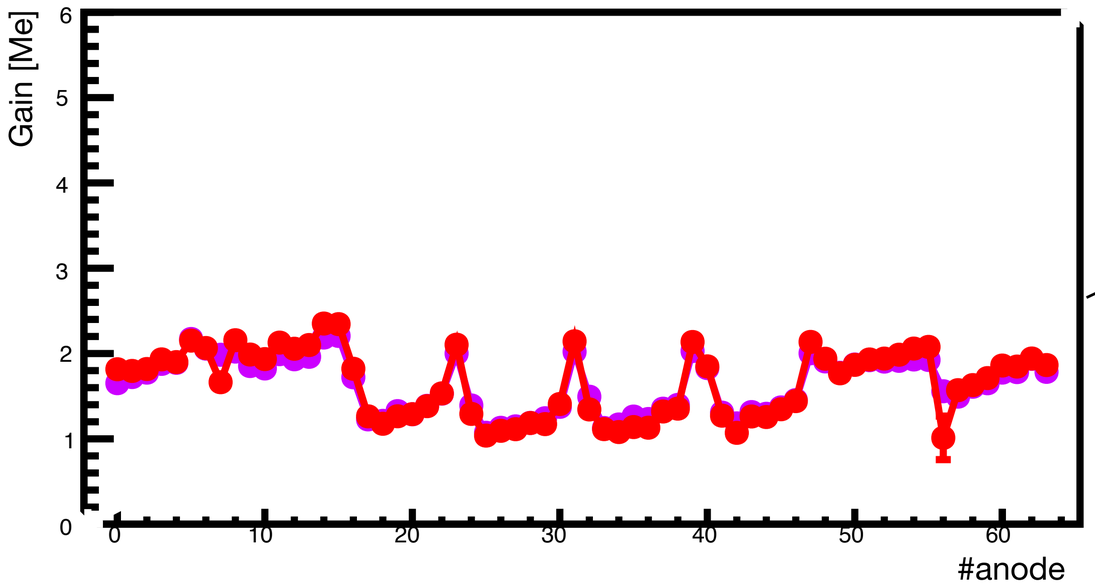

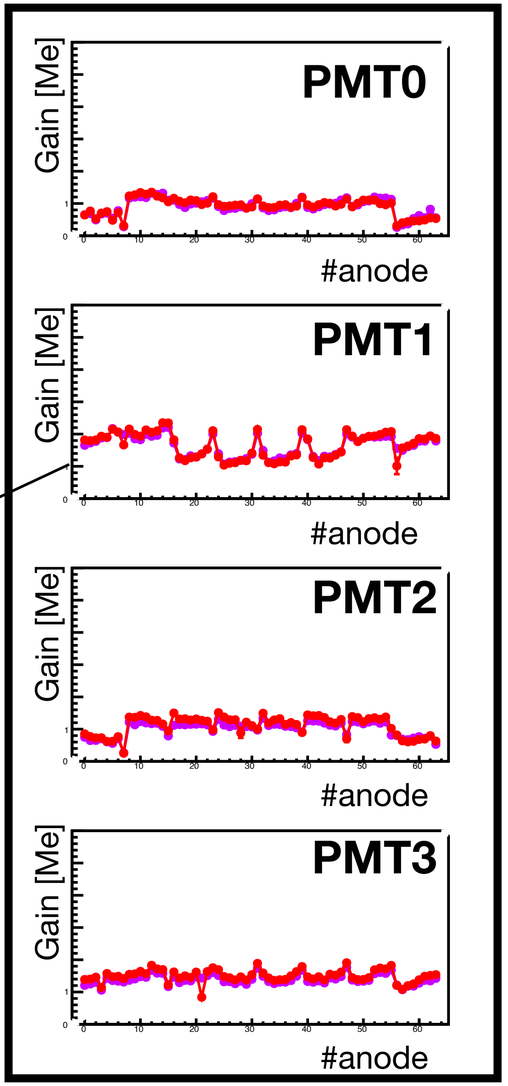

k-factors
An example from RICH1, col D04

The **HV** can be **tuned at the level of the PDMs**, so the **relevant quantity** to study is the **PDM average gain**.

To do so, for the **k-factors study** the **average gain of all the PMTs in a PDM** is considered, with **uncertainty** coming from the **standard deviation of the different PMTs gains**:

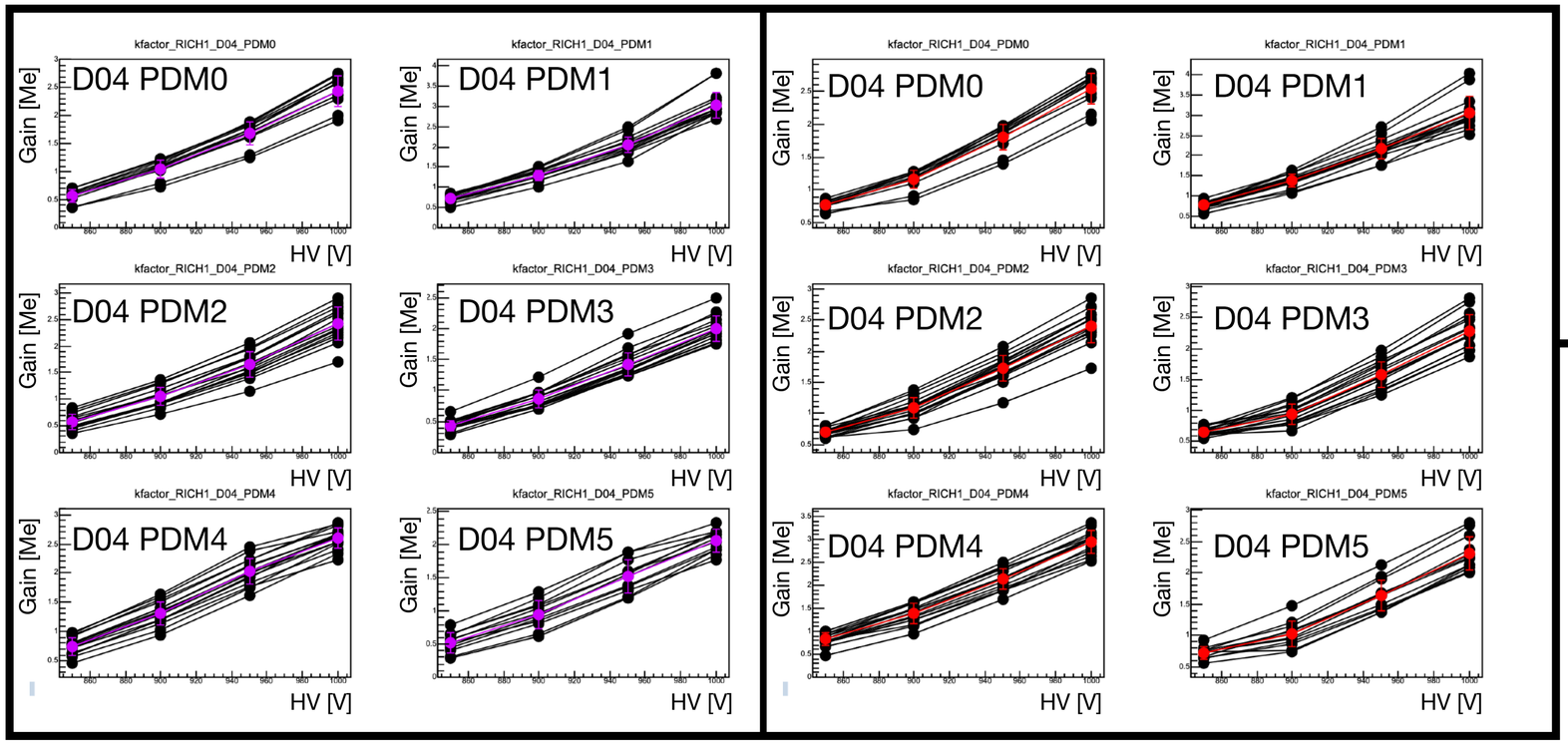

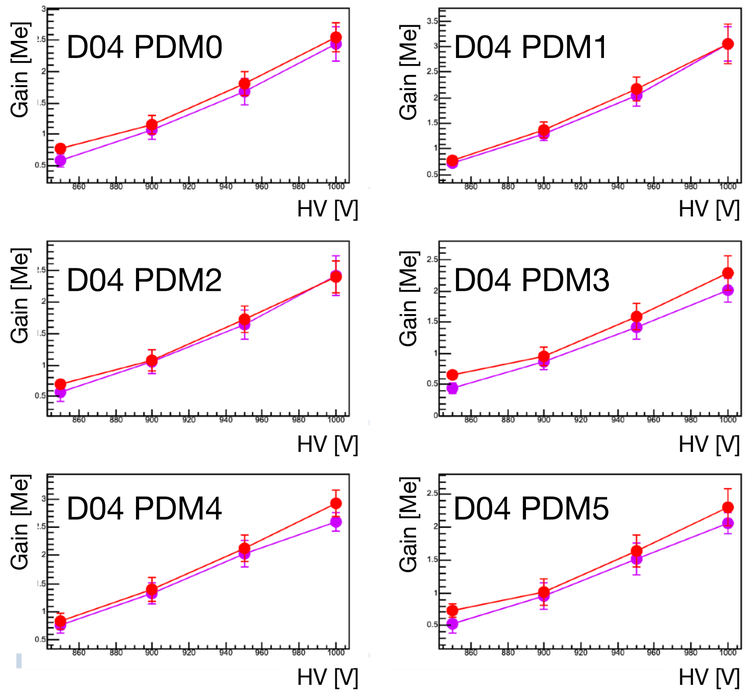

ComLab gain
P8 gain

HV fine tuning: first checks on PDM to PDM gain variations (preliminary)

RICH1 PDM HV [V]

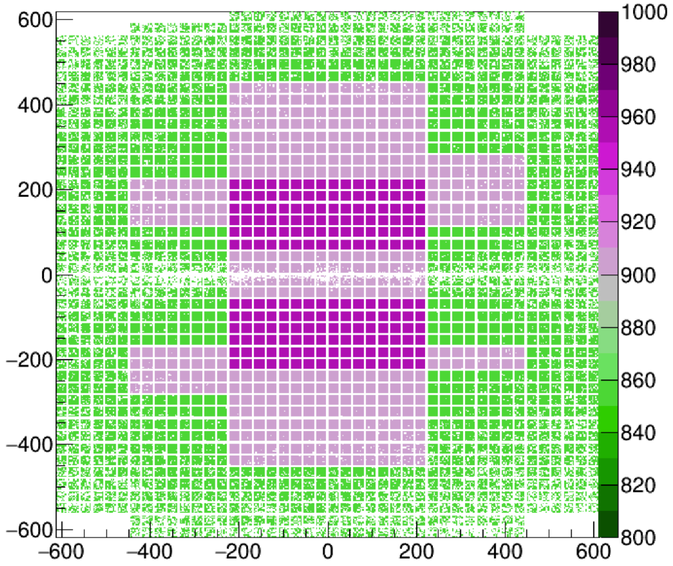

RICH1 PDM average gain [Me]

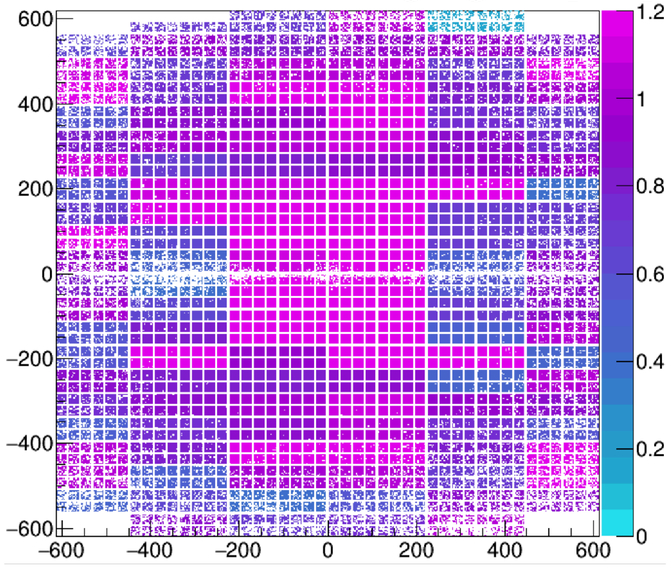

It is possible to visualize the **PDM average gain** across the **RICH1 and RICH2 detector plane**.

In this way one can assess the **gain uniformity** throughout all the PDMs.

In **RICH1** the goal is to **fine tune the HV** in order to get a **uniform gain as in the high occupancy region**, so of about ≈1Me

RICH2 PDM HV [V]

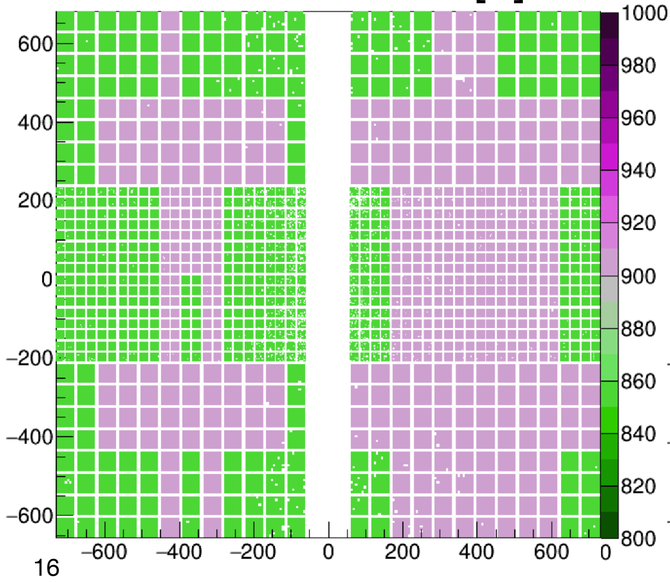

RICH2 PDM average gain [Me]

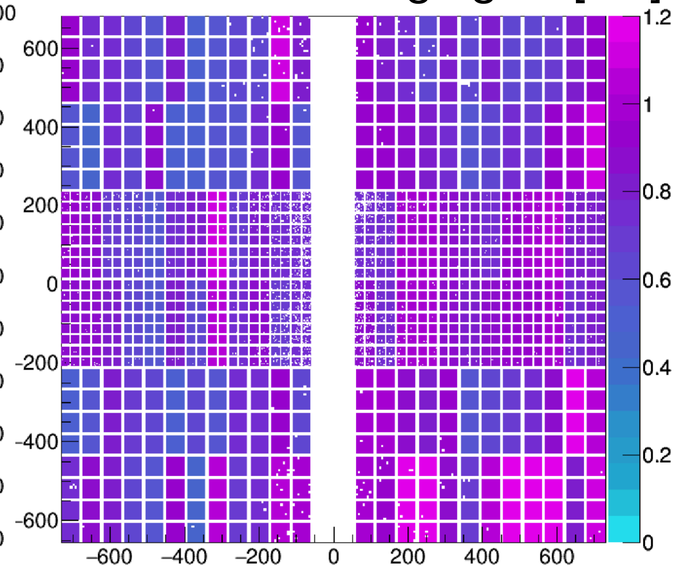

HV fine tuning: first checks on PDM to PDM gain variations (preliminary)

This study is already giving some hints about some features observed in RICH2 C-side:

RICH2 hitmap

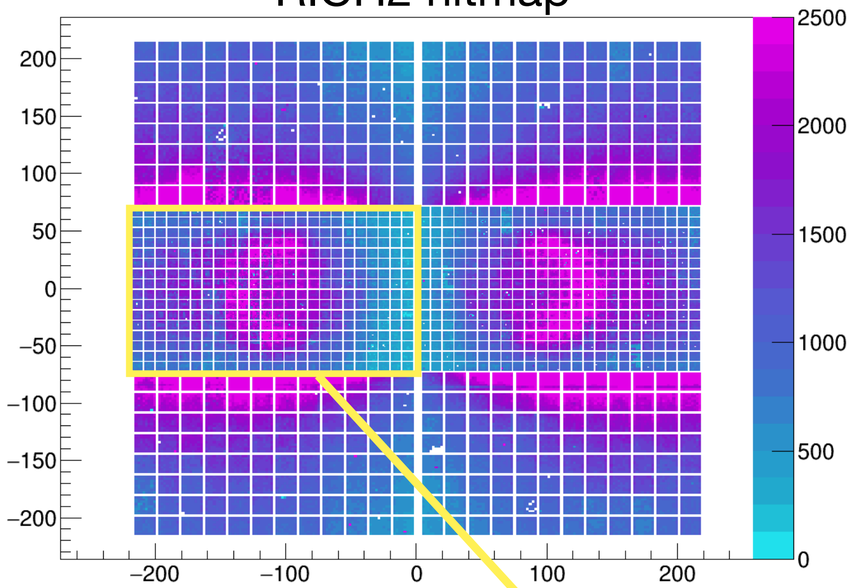

PDM counting less then the nearby ones has also lower gain

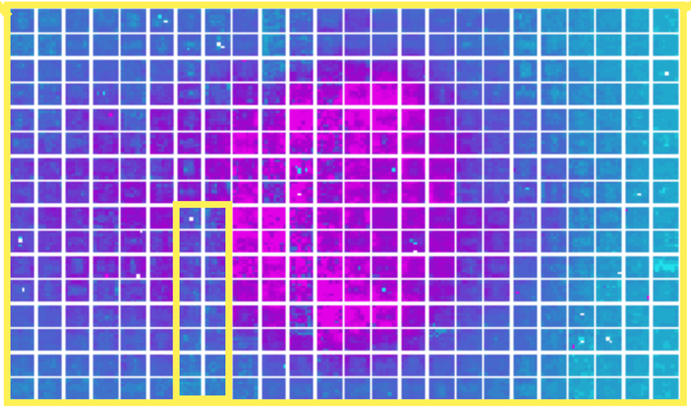

RICH2 PDM average gain [Me]

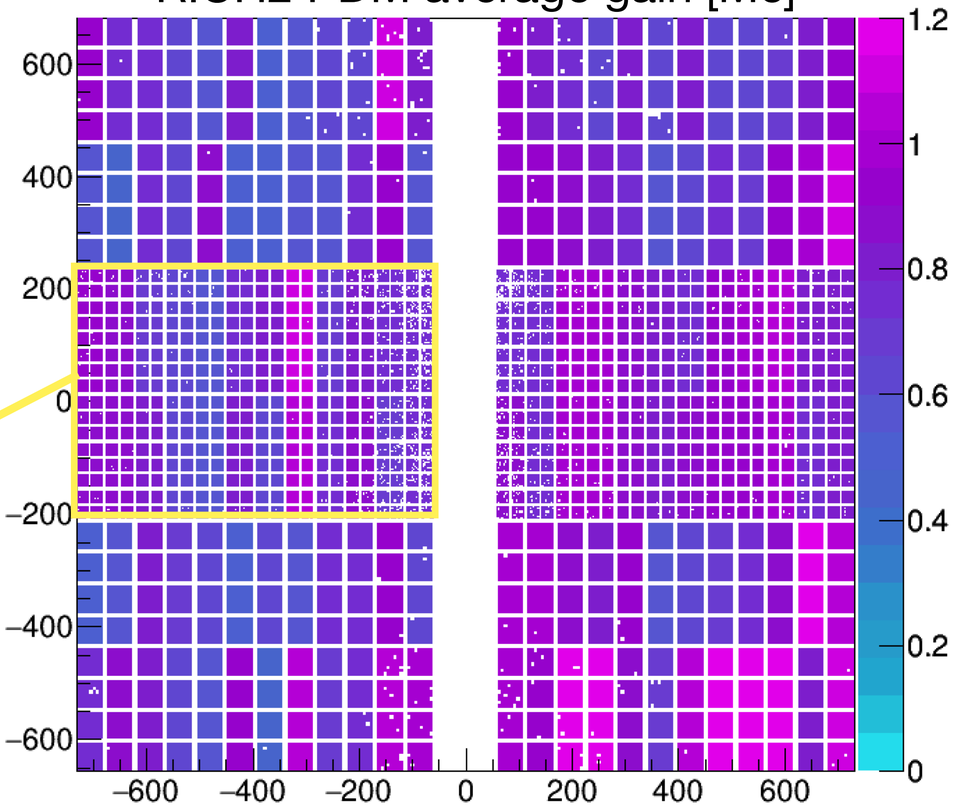

Next steps

- **Finalize the P8 threshold scan** analysis at **HV 800V and 850V**
- **P8 k-factors fits**
- **HV fine tuning** to make the **gains uniform** across the detectors

BR($\Lambda_b \to \Lambda_c^* D_s^{(*)}$ / $\Lambda_b \to \Lambda_c D_s^{(*)}$)

- Talk at LHCb Italy meeting (July 2022), alongside with the other measurement on Flavour Physics of the LHCb Padova group

$\Lambda_b \to \Lambda_c^* \tau \bar{\nu}_\tau$ background studies in the context of R(Λ_c^*)

A dominant background in R(Λ_c^*) is the channel $\Lambda_b \to \Lambda_c^* D_s$, with the D_S which decays semi-leptonically ($D_S \to \mu \nu X$) because the this decay is kinematically similar to the decay $\tau \to \mu \nu \nu$.

In order to reduce the systematic error we are measuring the BR of the process $\Lambda_b \to \Lambda_c^* D_s$, where the D_S is reconstructed in the 3π or KKπ decay mode.

This allows to fix the contribution of this background in the R(Λ_c^*) measurement and it is also the first observation of this decay mode of the Λ_b.

The BR is measured with respect to the normalization channel $\Lambda_b \to \Lambda_c D_s^{(*)}$

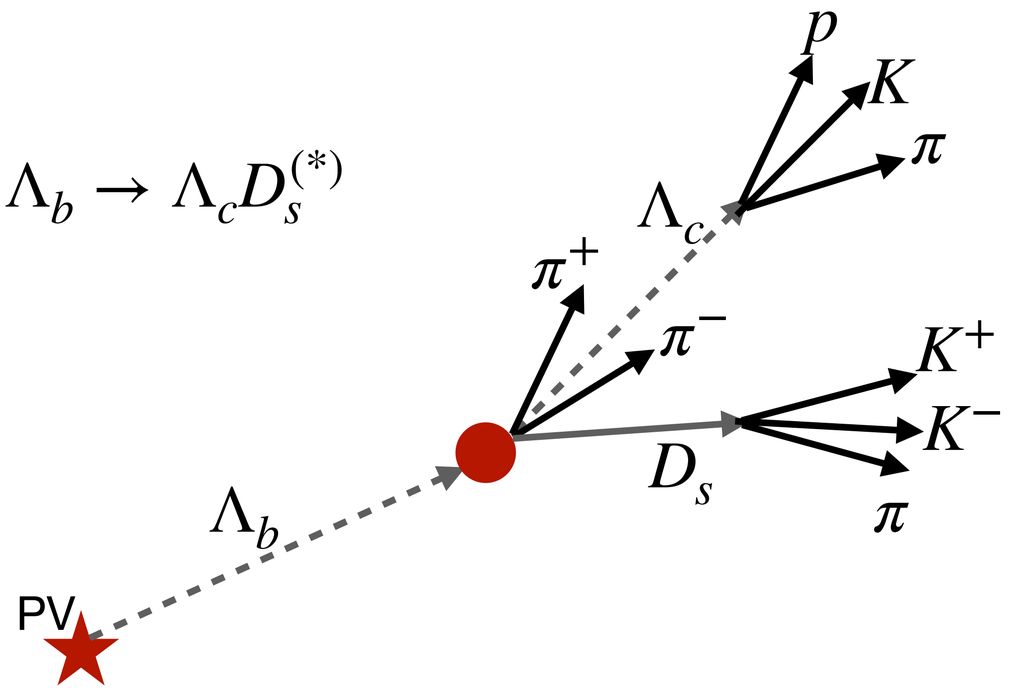

Preliminary studies on $\Lambda_b \to \Lambda_c^* D_s$ with $D_s \to \pi\pi\pi$

Extracting the shape of the Λ_c^* resonances with the MC data:

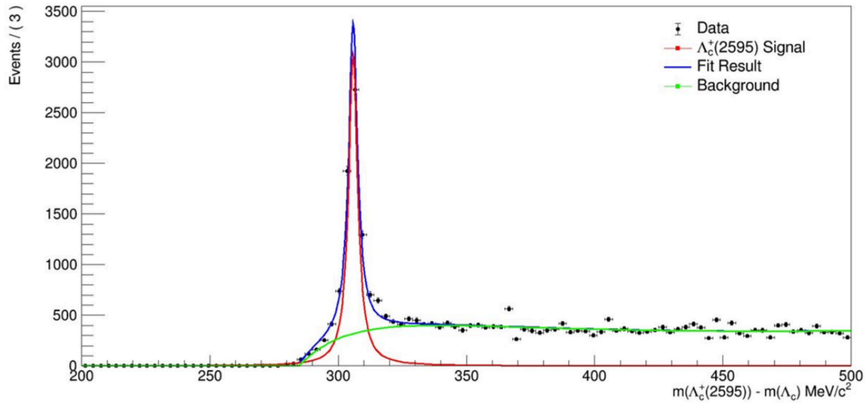

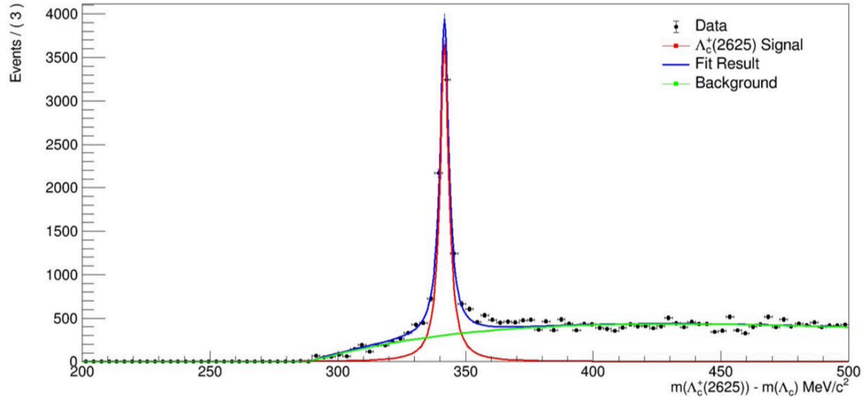

Fitting data and extracting yields:

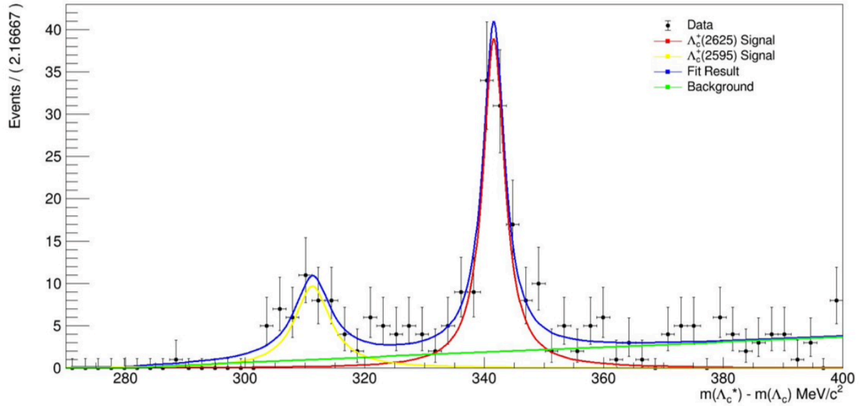

Calculating $\Lambda_b \to \Lambda_c^* D_s$ yields and relative measurement of the BR:

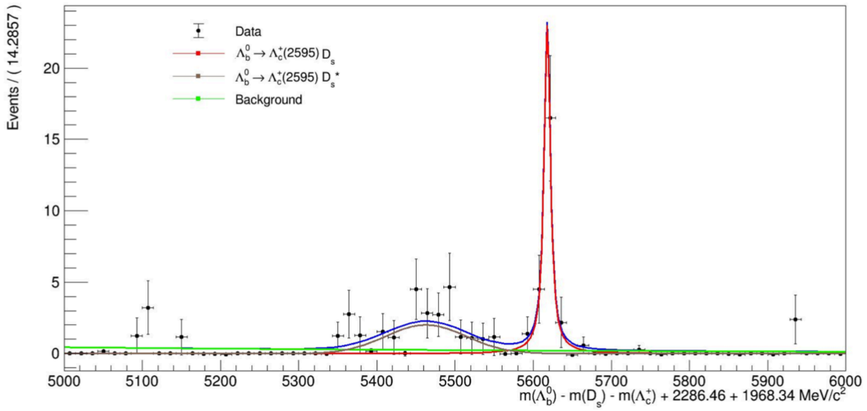

My analysis

My work is focused on the measurement of BR($\Lambda_b \to \Lambda_c^* D_s^{(*)}$ / $\Lambda_b \to \Lambda_c D_s^{(*)}$), with $D_s \to KK\pi$.

To do so several stripping lines have been considered, since currently we do not have a dedicated one.

Stripping line	**Criticalities**
Lb2LcDD2HHHPIDBeauty2CharmLine	Stringent cut on Lambda_b0_AM_MIN>5200MeV
Hlt2CharmHadInclLcpToKmPpPipBDTTurbo	OK but available only for 2018
InclusiveCharmBaryons_LcLine	OK but selection on Lambda_c_BDT at the stripping line level

StrippingLb2LcDD2HHHPIDBeauty2CharmLine cut studies

$\Lambda_c D_s$ invariant mass from TurboLine

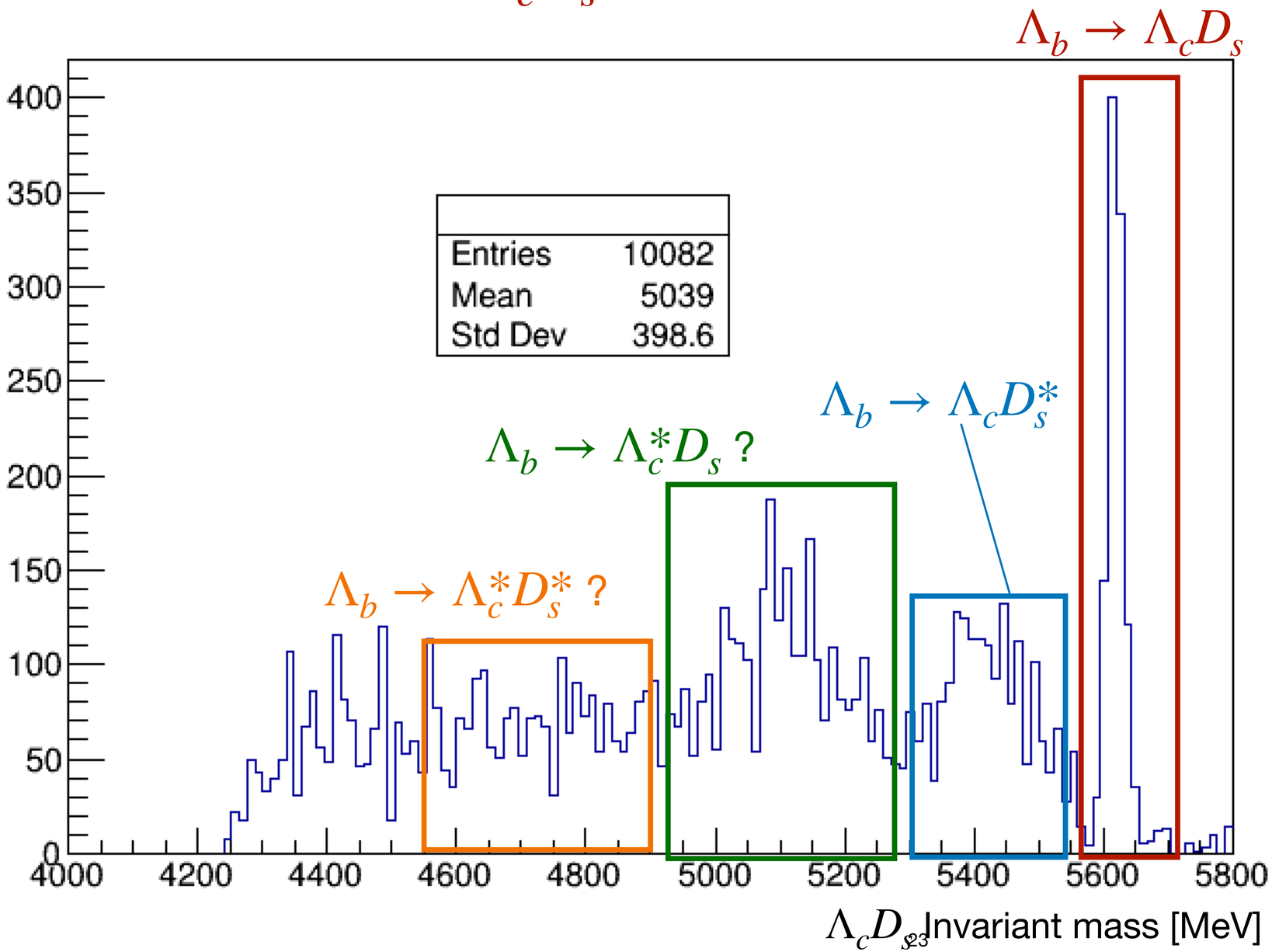

Cuts:

Ds_M in [1940,1990] MeV

Lc in [2280,2290] MeV

Lb_DIRA_OWNPV>0.9999

StrippingLb2LcDD2HHHPIDBeauty2CharmLine cut studies
$\Lambda_c^* D_s$ invariant mass from TurboLine

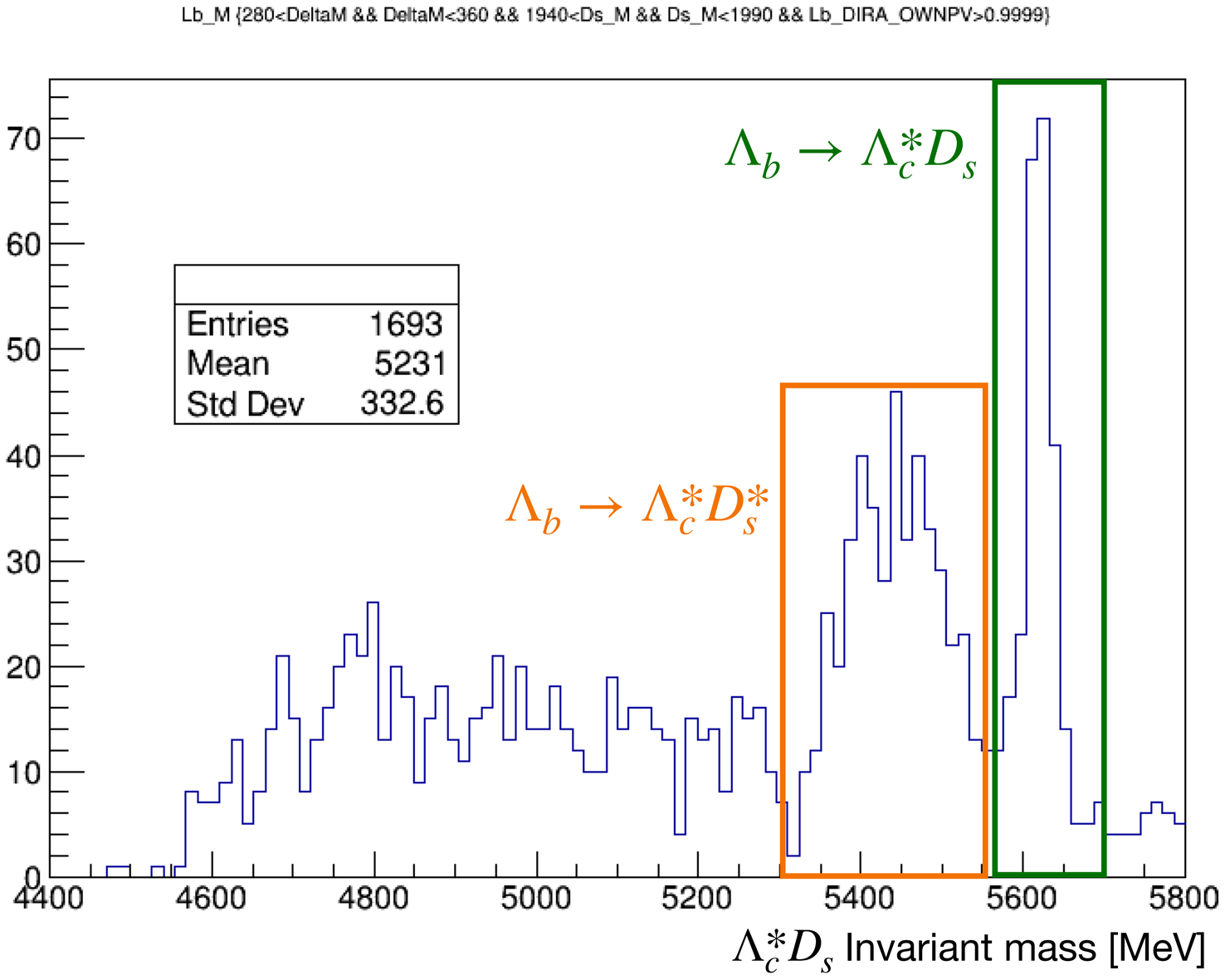

Cuts:

Ds_M in [1940,1990] MeV

DeltaM in [280,360] MeV

Lb_DIRA_OWNPV>0.9999

$\Lambda_c^* D_s$ invariant mass from TurboLine

How to change the cut on $\Lambda_c D_s$ invariant mass in the exclusive stripping line?

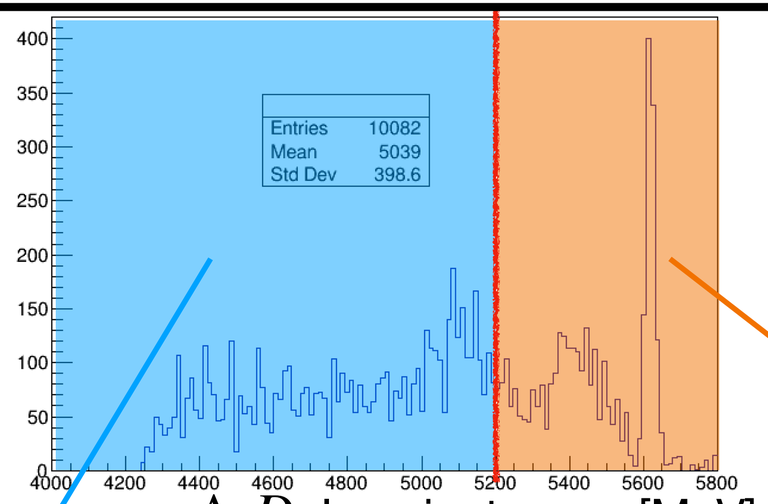

StrippingLb2LcDD2HHHPIDBeauty2CharmLine
$\Lambda_c D_s$ invariant mass >5200

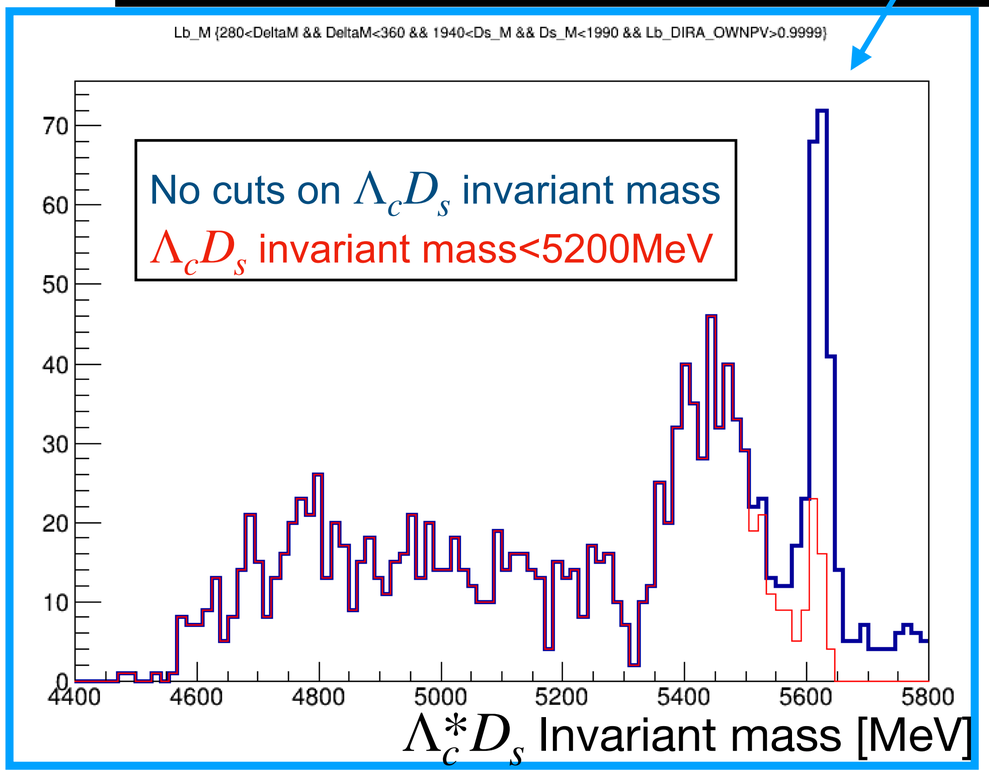

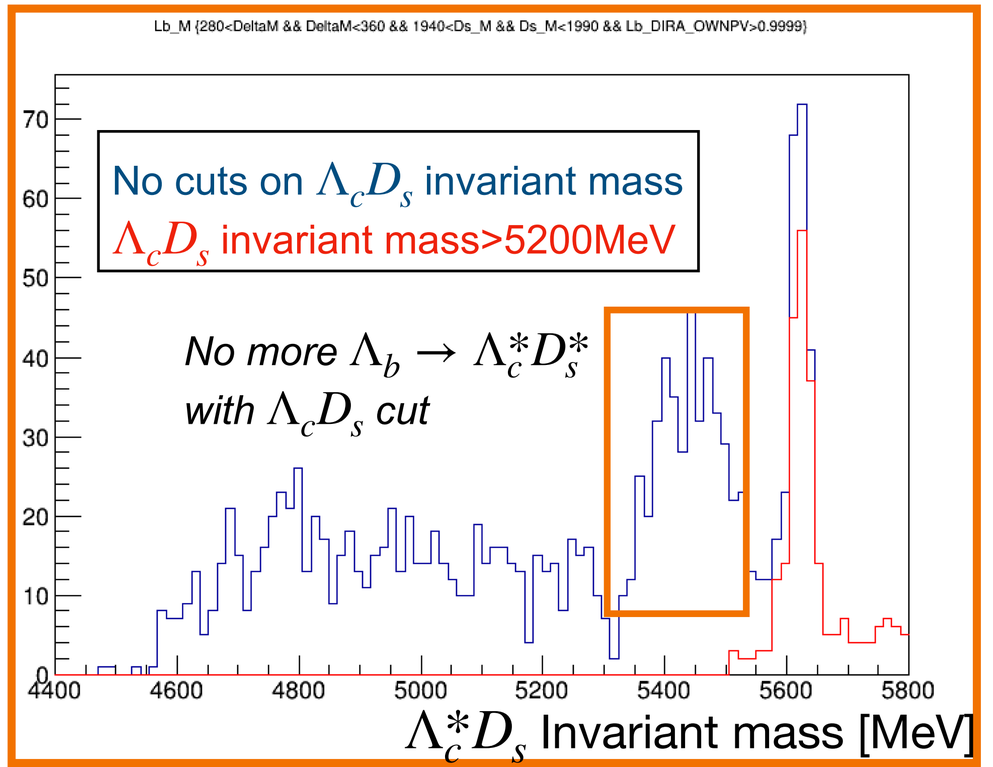

StrippingLb2LcDD2HHHPIDBeauty2CharmLine cut studies

How to set $\Lambda_c D_s$ invariant mass cut ?

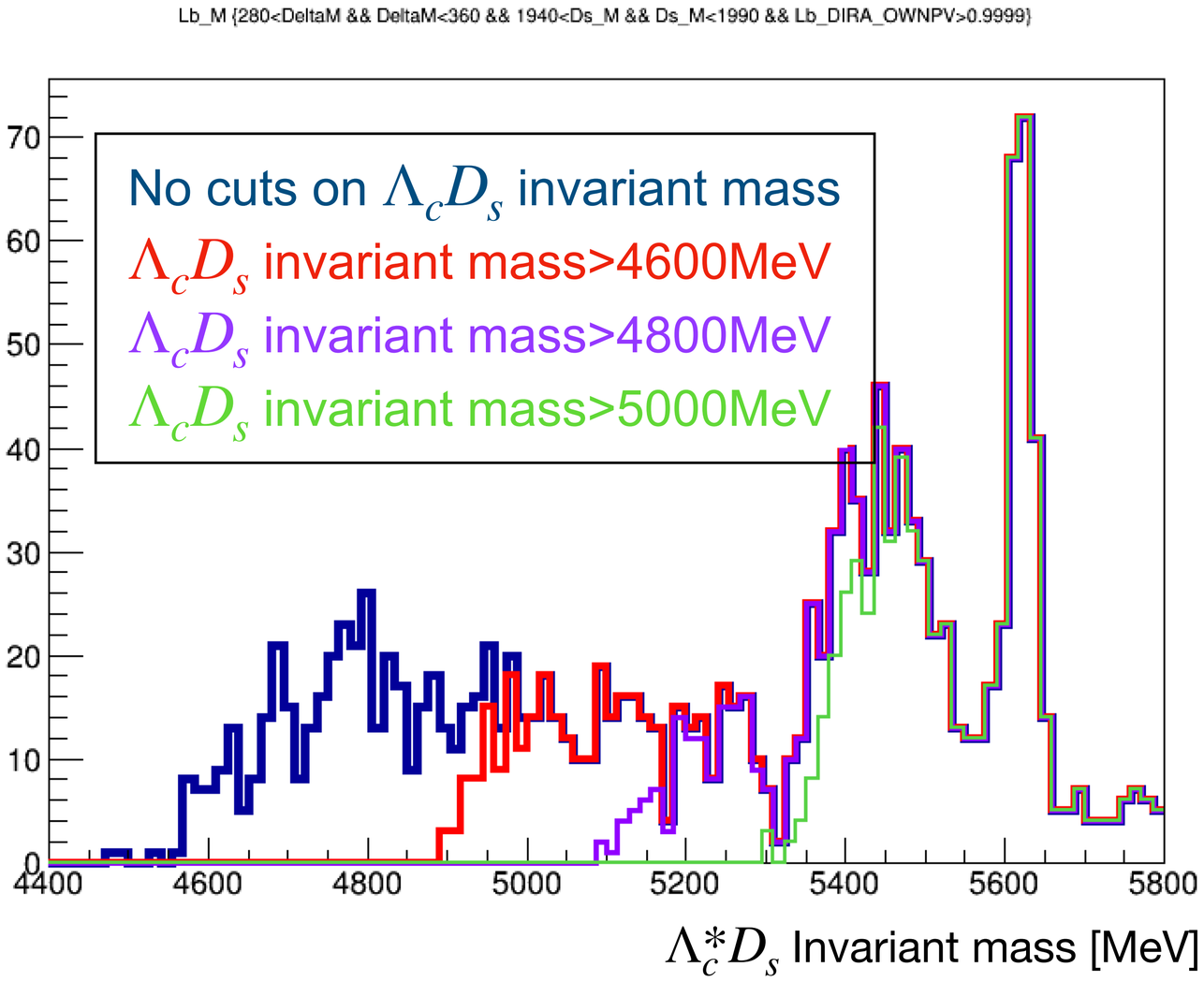

New stripping line campaign

Exploiting the studies performed with the turbo line, we properly modified the previous exclusive Lb2LcDs line (Lb2LcDD2HHHPIDBeauty2CharmLine), writing three other stripping lines:

Stripping line	**Lambda_b0_AM [MeV]**	**Lambda_c (*) sel.**
Lb2LcDsD2HHHPIDBeauty2CharmLine	[4700;6500]	As in previous stripping line
Lb2Lc2625DsD2HHHPIDBeauty2CharmLine		Exploiting cuts from similar lines
Lb2Lc2595DsD2HHHPIDBeauty2CharmLine		

But waiting for the next campaign, now we are focusing on the Inclusive Stripping *StrippingInclusiveCharmBaryons_LcLine.*

StrippingInclusiveCharmBaryons_LcLine

MC ntuples studies: $\Lambda_b \to \Lambda_c^*(2625) D_s$

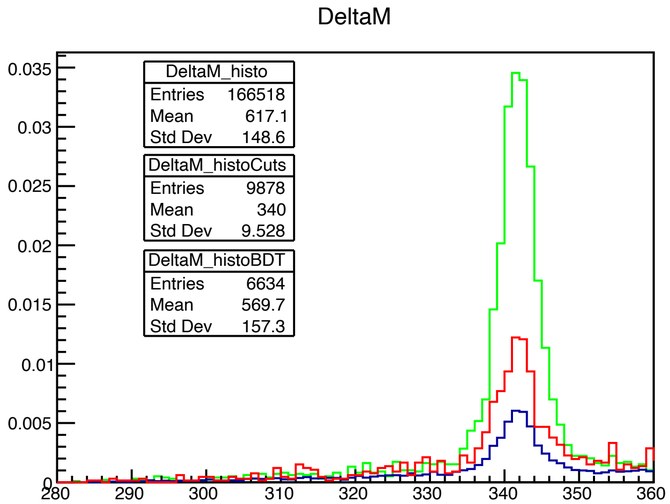

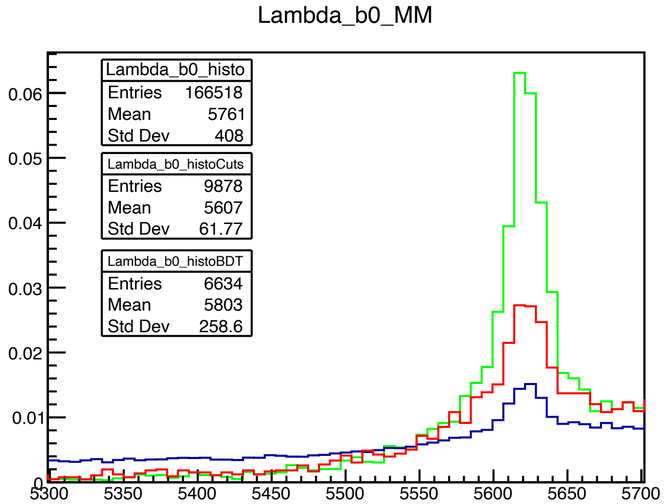

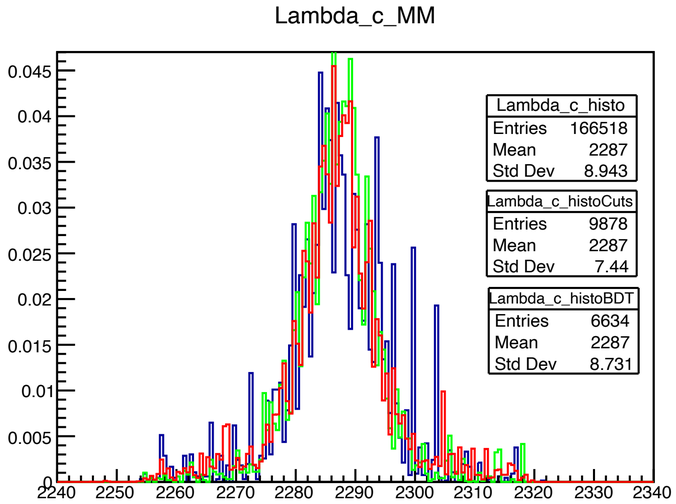

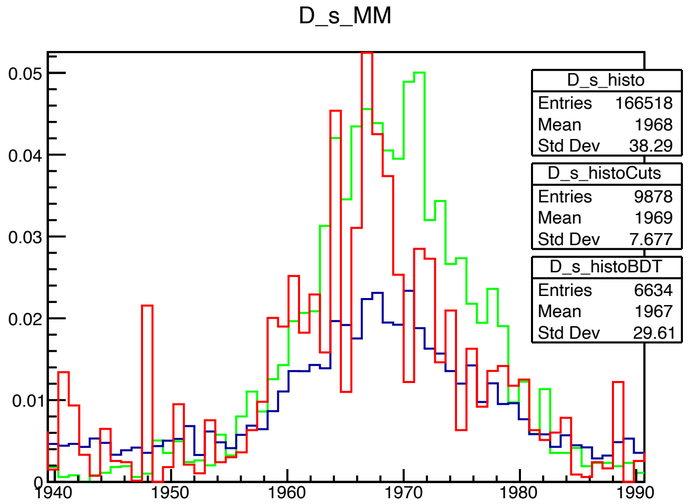

No cuts

BDT cuts:

Lambda_c_BDT>-0.5

D_s_BDT>-0.5

Standard cuts*

Standard cuts*+

stripBDT cut: Lambda_c_BDT>0.45

* Lambda_c_ENDVERTEX_CHI2<20 &&
Lambda_b0_ENDVERTEX_CHI2<15 &&
Lambda_b0_DIRA_OWNPV>0.999 &&
Lambda_c_p_ProbNNp>0.6 &&
Lambda_c_kaon_ProbNNk>0.6 &&
Lambda_c_pion_PIDK<2 &&
Lambda_c_p_PT>250 &&
Lambda_c_kaon_PT>250 &&
Lambda_c_pion_PT>250 &&
Lambda_c_pion_IPCHI2_OWNPV>9 &&
Lambda_c_kaon_IPCHI2_OWNPV>9 &&
Lambda_c_p_IPCHI2_OWNPV>9 &&
Lambda_c_p_ProbNNghost<.6 &&
Lambda_c_pion_ProbNNghost<.6 &&
Lambda_c_kaon_ProbNNghost<.6 &&
Lambda_c_st_pim_ProbNNpi>.2 &&
Lambda_c_st_pip_ProbNNpi>.2 &&
D_s_pi_ProbNNpi>.4 &&
D_s_Km_ProbNNk>.6 &&
D_s_Kp_ProbNNk>.6

StrippingInclusiveCharmBaryons_LcLine

MC request

Campaign	Stripping line	Stripping line efficiency	After DaVinci sel. + PID cuts +MC truth
34r0p1	InclusiveCharmBaryons_LcLine	8.1%	0.3%

MC request to be submitted in the 17th of August at the B2OC meeting:

- Filtered request: 0.3/8.1 * 400k eventi ≈15k events (for both $\Lambda_c^*(2625)$ and $\Lambda_c^*(2595)$)
- Unfiltered request: 0.3% * 5M ≈ 15k events (for both $\Lambda_c^*(2625)$ and $\Lambda_c^*(2595)$)

Timing: RICH LS3 enhancements

- Parallel talk at EPS (August 2023)
- Testbeam paper on 2022 data soon to be published
- Talk at IFD (October 2022) on RICH Upgrades

Introduction

The goal of the beam test is to test a prototype readout chain with fast-timing information.
The MaPMTs/SiPM are coupled with FastICs and read out by a TDC-in-FPGA.

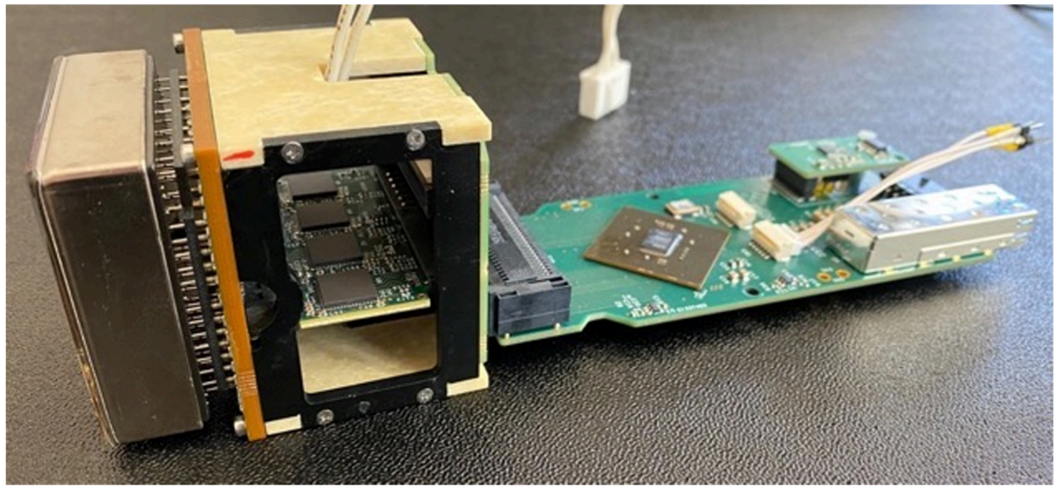

2022 SPS beam tests

Datasets

Test beam data

$2 \cdot 10^6$ events
Ring: focused
MaPMT bias: 1000V
Thresholds:
- EC-R p-18
- EC-H p-10

MCP bias: 2100V

$6 \cdot 10^6$ events
Ring: defocused
MaPMT bias: 1000V
Thresholds:
- EC-R p-18
- EC-H p-10

MCP bias: 2100V

$8 \cdot 10^6$ events
Ring: focused
MaPMT bias: 900V
Thresholds:
- EC-R p-18
- EC-H p-10

MCP bias: 2100V

EC-R

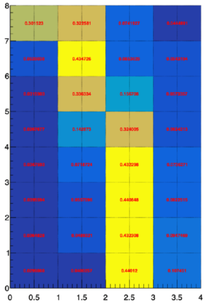

EC-R

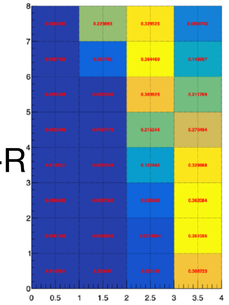

EC-R

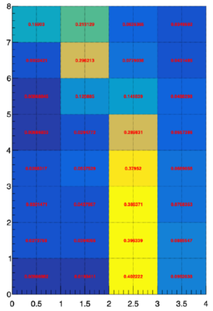

EC-H

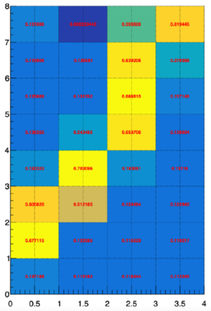

EC-H

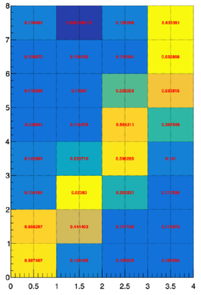

EC-H

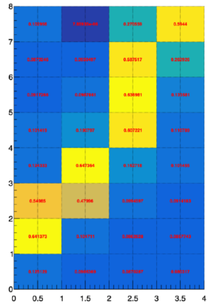

Multiplicity cut on all test beam runs:
pixels on per event higher than 5 and smaller than 10

Laser data

$10 \cdot 10^6$ events
MaPMT bias: 1000V
Thresholds:
- EC-R p-18

Occupancy: ≈2%

$10 \cdot 10^6$ events
MaPMT bias: 1000V
Thresholds:
- EC-R p-18

Occupancy: ≈12%

$10 \cdot 10^6$ events
MaPMT bias: 1000V
Thresholds:
- EC-R p-18

Occupancy: ≈30%

EC-R

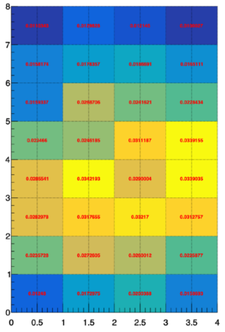

EC-R

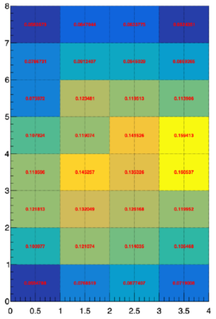

EC-R

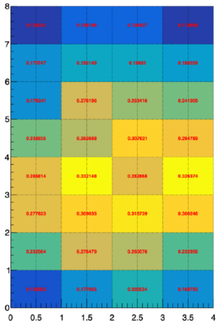

$1 \cdot 10^6$ events
MaPMT bias: 1000V
Thresholds:
- EC-R p-18

Occupancy: 17%
Mask applied, ch22 on only

EC-R

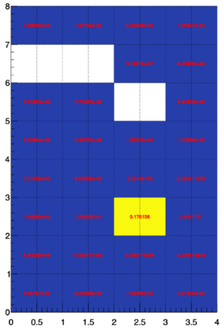

Thanks to Lorenzo Malentacca for the laser runs!

EC-R time resolution 1000V

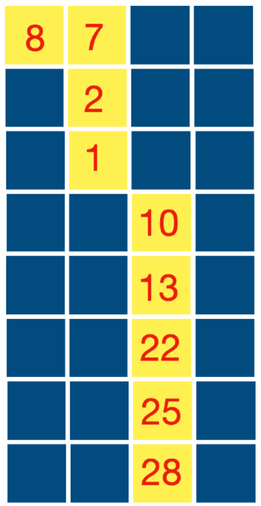

CH 1

$\sigma_t = 180 \pm 13$ ps

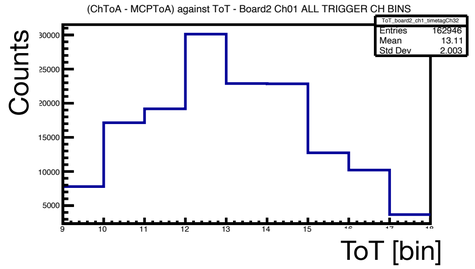

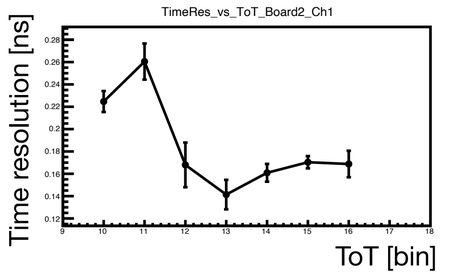

CH 2

$\sigma_t = 210 \pm 10$ ps

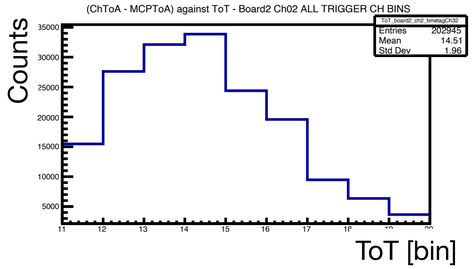

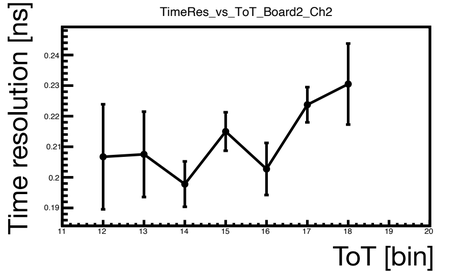

CH 7

$\sigma_t = 427 \pm 11$ ps

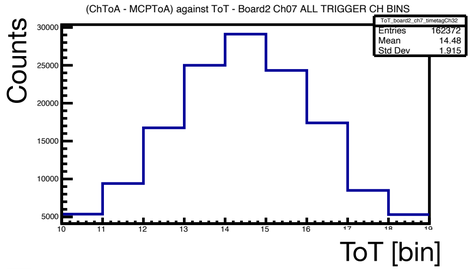

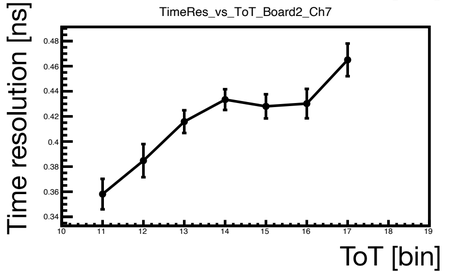

CH 8

$\sigma_t = 318 \pm 15$ ps

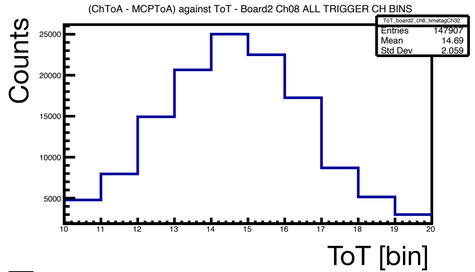

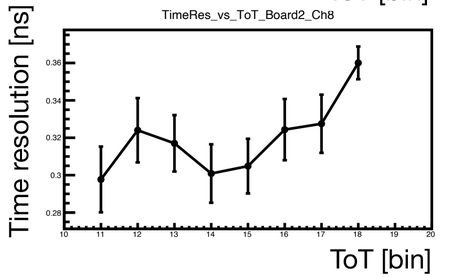

CH 10

$\sigma_t = 226 \pm 14$ ps

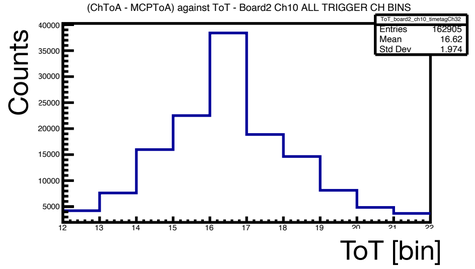

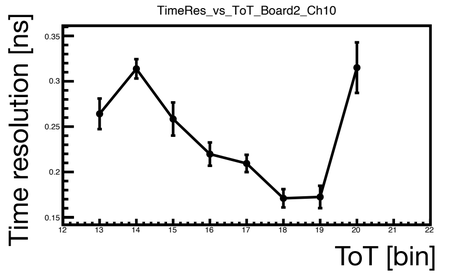

CH 22

$\sigma_t = 187 \pm 11$ ps

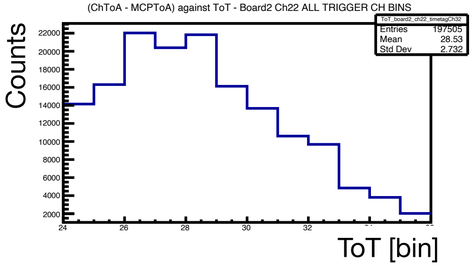

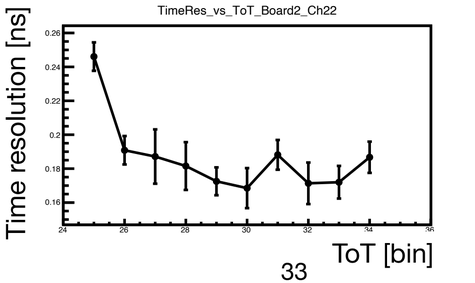

CH 25

$\sigma_t = 239 \pm 12$ ps

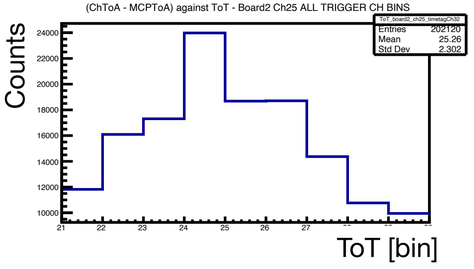

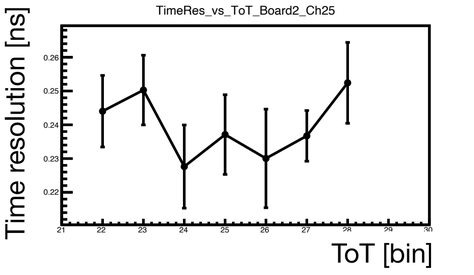

CH 28

$\sigma_t = 263 \pm 20$ ps

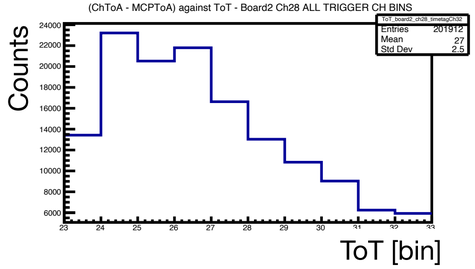

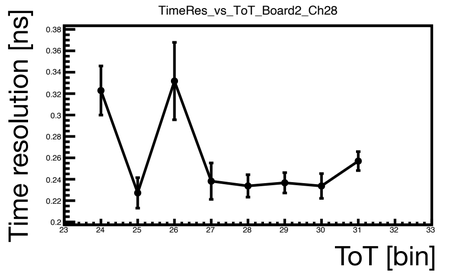

Time resolution contributions

To obtain the time resolutions displayed in the following, to each single channel measurement the various jitter contributions are subtracted.
Namely:

$$\sigma_{ch} = \sqrt{\sigma_{data}^2 - \sigma_{fastIC}^2 - \sigma_{MCP}^2 - \sigma_{TDC}^2}$$

Where $\sigma_{fastIC} \approx 25$ps , $\sigma_{MCP} \approx 110$ps , $\sigma_{TDC} \approx 150/\sqrt{12}$ps.

For the laser measurement σ_{MCP} is substituted by $\sigma_{laser} \approx 20$ ps .

By now, no uncertainty is attributed to σ_{fastIC}, σ_{MCP}, σ_{TDC}, σ_{laser} .

EC-R time resolution: focused/defocused ring

Trend comparison for **EC-R** for **focused/defocused ring**.
The time resolution for the 32 EC-R channels show good agreement, varying slightly depending on the statistics.

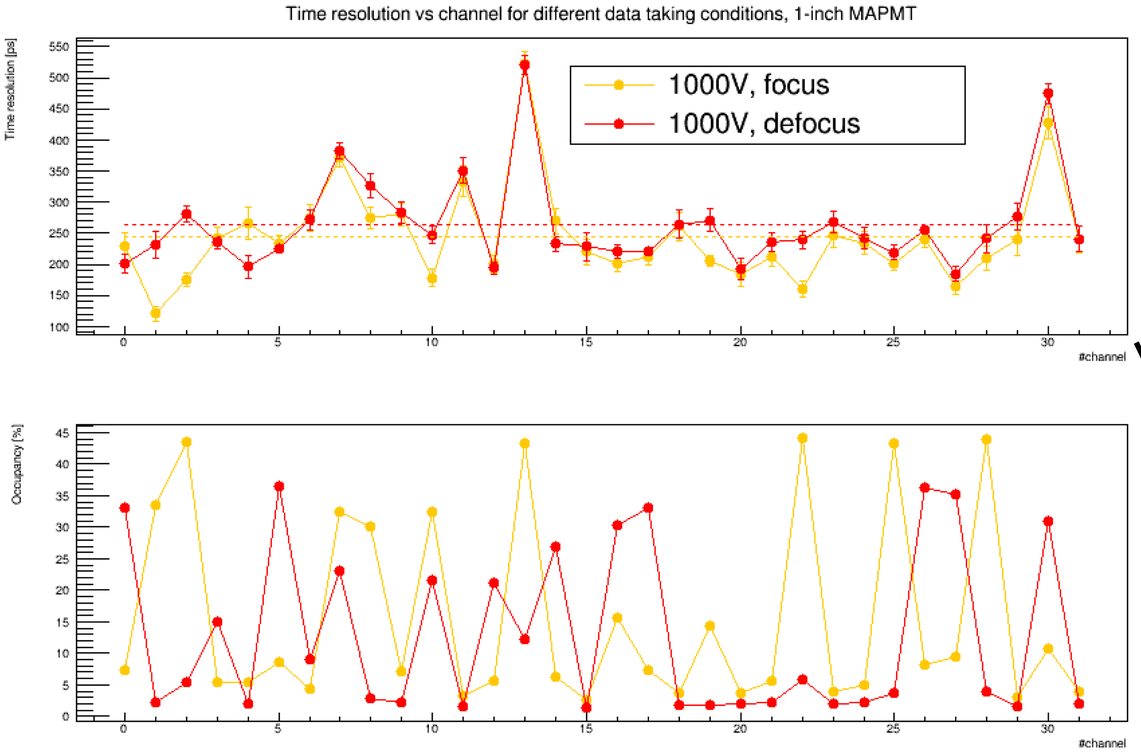

EC-R channels position:

8	7	0	6
4	2	5	3
11	1	16	12
15	19	10	14
18	9	13	17
23	21	22	26
20	24	25	27
29	31	28	30

Excluding ch 7,8 (border pixels) and ch 13 (issues with TDC calibration)
and requiring occupancy>20%:

Settings	Average Time resolution [ps]
1000V, focused ring	174 ± 32
1000V, defocused ring	245 ± 84

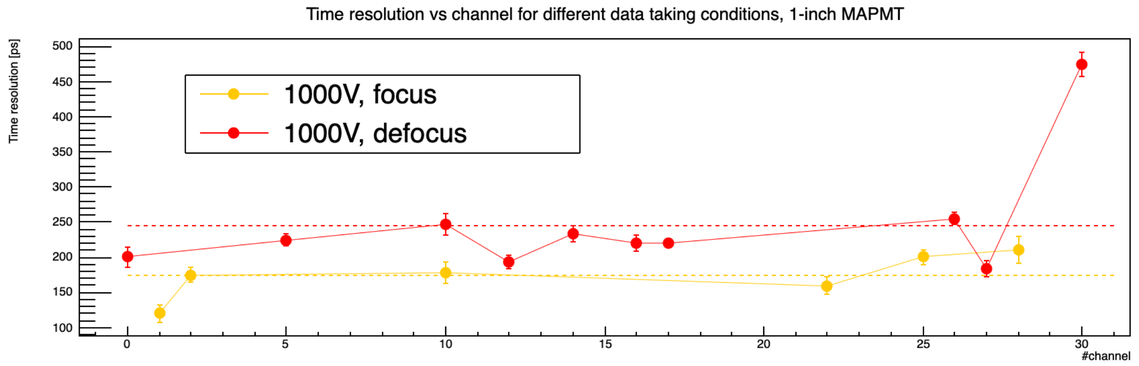

EC-R time resolution: 1000V/900V bias

Trend comparison for **EC-R** for **1000/900V bias**.
The time resolution for the 32 EC-R channels has a consistent trend, showing a slightly degraded time resolution for the 900V bias.

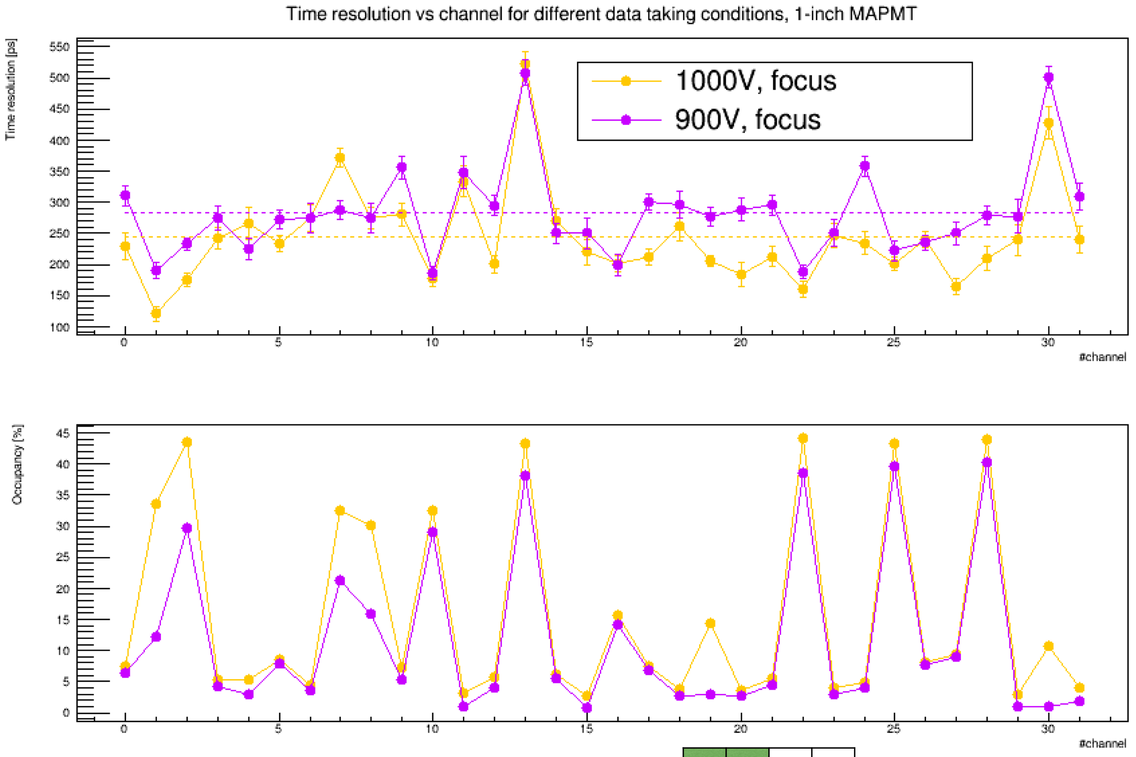

EC-R channels position:

8	7	0	6
4	2	5	3
11	1	16	12
15	19	10	14
18	9	13	17
23	21	22	26
20	24	25	27
29	31	28	30

Excluding ch 7,8 (border pixels) and ch 13 (issues with TDC calibration)
and requiring occupancy>20%:

Settings	Average Time resolution [ps]
1000V, focused ring	174 ± 32
900V, focused ring	222 ± 38

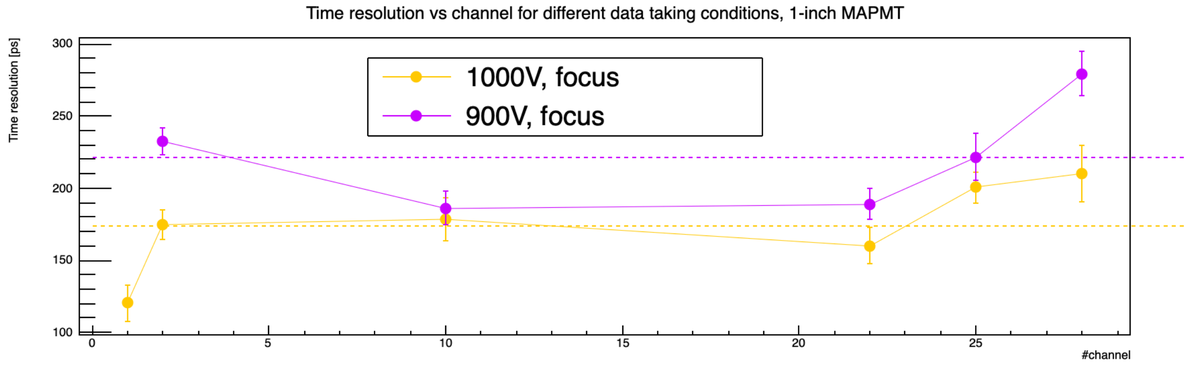

EC-R time resolution: comparison of test beam and laser data

Several **laser runs** were taken in order to get a set of data with an **occupancy comparable to the test beam one**:

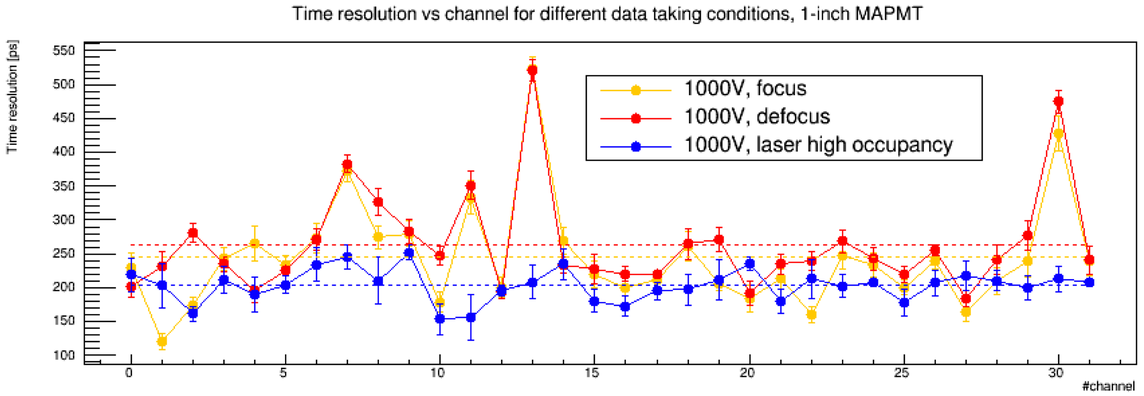

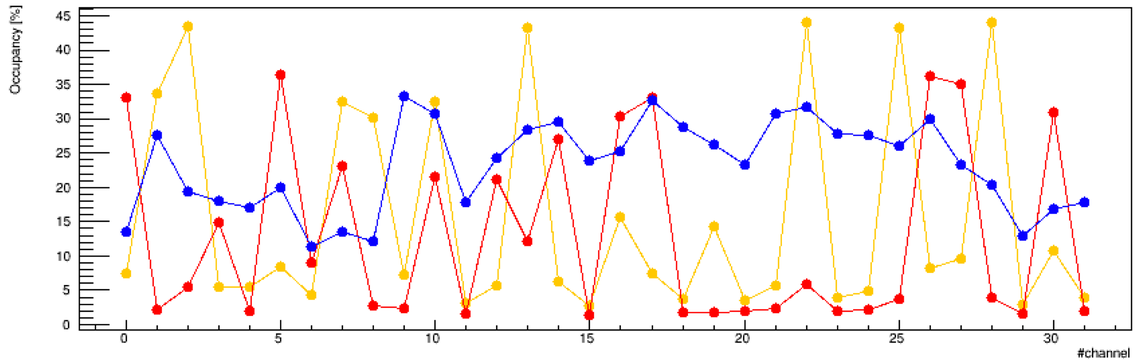

Excluding ch 7,8 (border pixels) and ch 13 (issues with TDC calibration)
and requiring occupancy>20%:

Settings	Average Time resolution [ps]
1000V, focused ring	174 ± 32
1000V, defocused ring	245 ± 84
1000V, laser (occ. about 30%)	202 ± 24

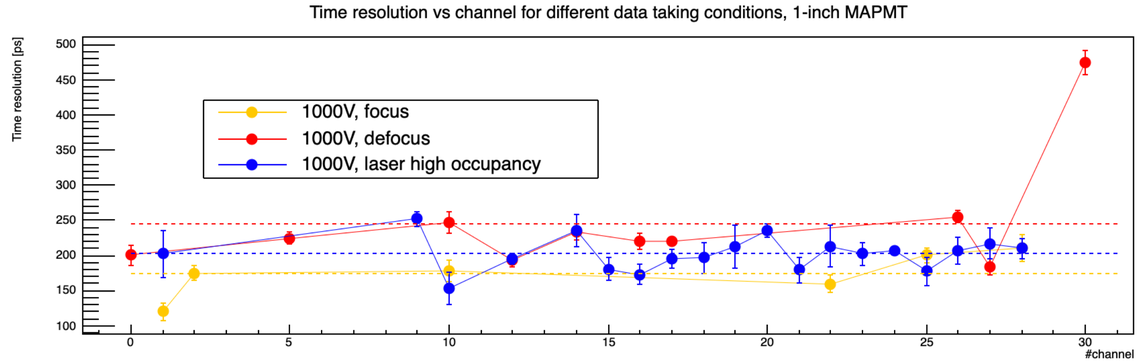

EC-R channels position:

8	7	0	6
4	2	5	3
11	1	16	12
15	19	10	14
18	9	13	17
23	21	22	26
20	24	25	27
29	31	28	30

EC-R time resolution: comparison of test beam and laser data

It was observed that for the **laser data** the **time resolution worsens increasing the occupancy**.
Nevertheless, a **nice uniformity in time resolution** is observed throughout **all the 32 channels**.

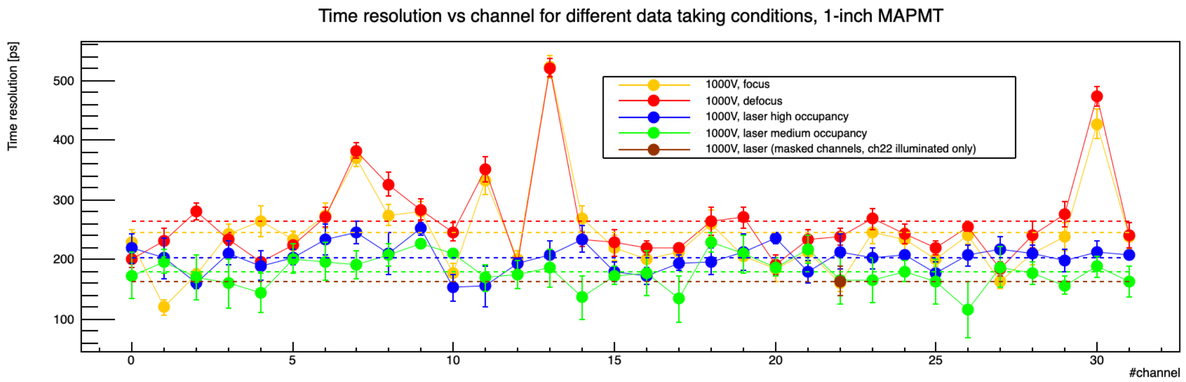

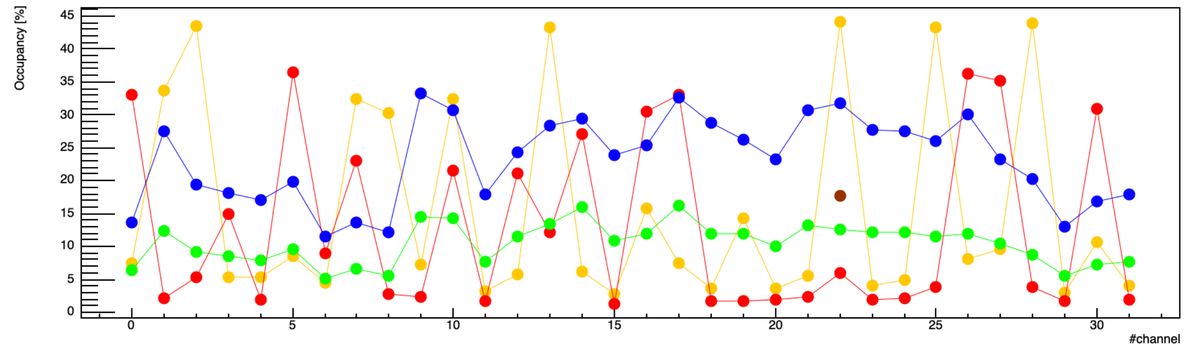

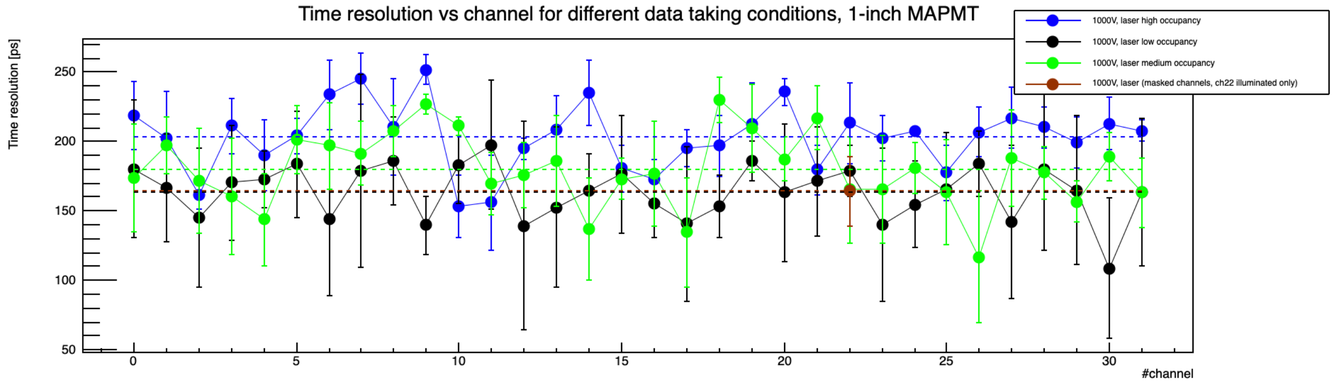

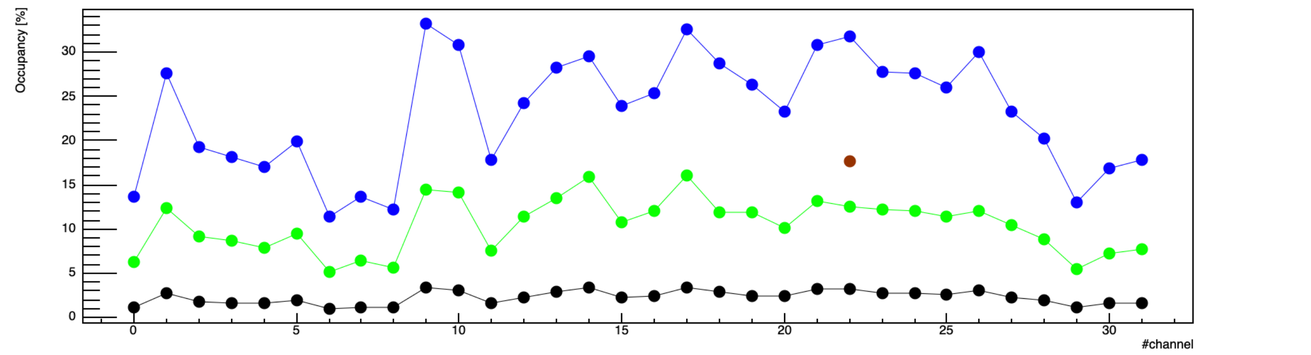

Laser settings	Average Time resolution [ps]
High occupancy (about 30%)	203 ± 24
Medium occupancy (about 12%)	180 ± 26
Low occupancy (about 2%)	164 ± 19
Mask, ch22 on only (about 17%)	164 ± 25

EC-R time resolution: laser threshold scan data

Moreover several **laser runs** were acquired **changing the EC-R channels thresholds** in order to check whether the testbeam threshold was optimal or not (occupancy ≈2% on average).

In the plot one can see the **time resolution** of each EC-R channel as a function of the **threshold in μA**.
The **test beam threshold** is pointed out in **red**: the time resolution reaches a plateau close to that value.

EC-R channels position

8	7	0	6
4	2	5	3
11	1	16	12
15	19	10	14
18	9	13	17
23	21	22	26
20	24	25	27
29	31	28	30

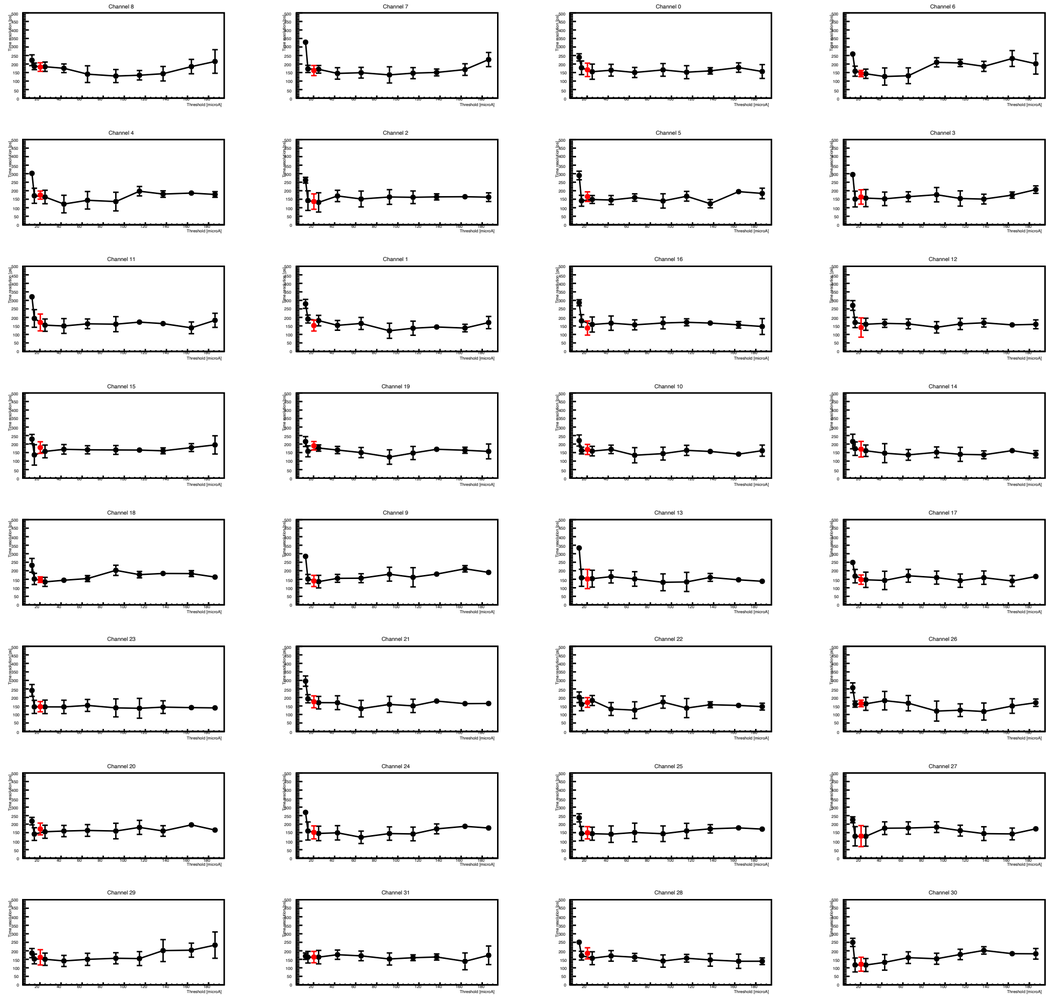

Conclusions

- The **EC-R channels time resolution** obtained at **1000V bias** is **compatible** with the expected **MaPMT time spread**. Moreover the **measurement shows agreement with the acquired laser data**.

- The **EC-R channels time resolution** obtained at **900V bias** degrade slightly with respect to the one obtained at 1000V.

Settings	Average Time resolution [ps]
TESTBEAM, 1000V, focused ring	174 ± 32
TESTBEAM, 1000V, defocused ring	245 ± 84
LASER, High occupancy (about 30%)	203 ± 24
LASER, Medium occupancy (about 12%)	180 ± 26
LASER, Low occupancy (about 2%)	164 ± 19
TESTBEAM, 900V, focused ring	222 ± 38

Next steps

- **Finalize article results**, comparing different methods to extract the time resolution.

- **Start the analysis of the 2023 testbeam data** (?)

Timing: VELO Upgrade 2 R&D

- Parallel talk at ICHEP22 (+ proceeding)
- Paper published in Frontiers of Physics
- Paper on irradiated sensors to be written
- 2 SIF talks + proceedings (SIF best communications)

High Luminosity and Future Colliders

Extremely high instantaneous luminosity planned at today's upgraded and future colliders:

- **High radiation damage** to tracking detectors
- **Difficult event reconstruction** due to large pile-up, implied by:
  - Association of traces to a certain Primary Vertex
  - Correct pattern recognition

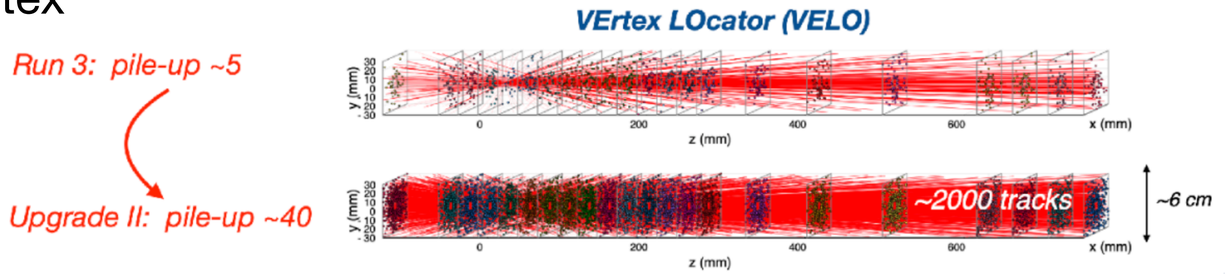

Spatial resolution
Time resolution
Radiation hardness

→ **All required at the same time!**

LHCb Upgrade-2 (2030s) requirements:

- σ_t = 30-50 ps
- σ_s = 10 μm
- F = 10^{16} to 10^{17} 1 MeV n_{eq}/cm^2

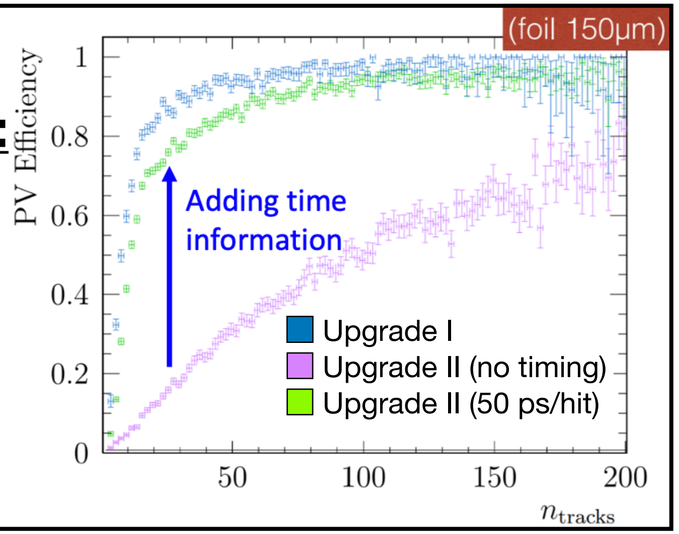

FCC-hh (20??) requirements:

- σ_t = 10-20 ps
- σ_s = 10 μm
- F = 10^{17} to 10^{18} 1 MeV n_{eq}/cm^2

Why 3D sensors?

Original idea by S. Parker, 1997

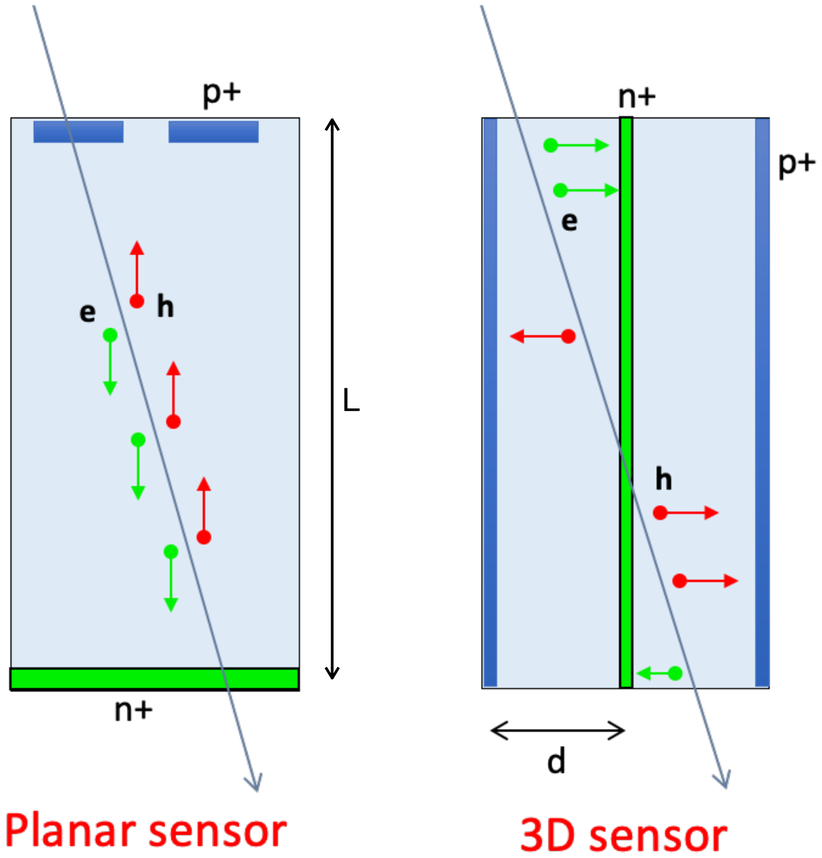

- Short inter-electrode drift distance: **extremely fast signals** (d<<L)
- Active volume and **electrode shape** can be **designed for maximum performance**
- **Unmatched radiation hardness** (>10^{17} 1 MeV n_{eq}/cm^2)
  NIMA, 979 (2020) 164458
- 3D columnar geometry is a production-ready technology (ATLAS IBL, ATLAS-P2)

The optimized 3D sensor design

Current signal is defined as (Ramo's theorem):

$$i = q\,\vec{E}_w \cdot \vec{v}_d$$

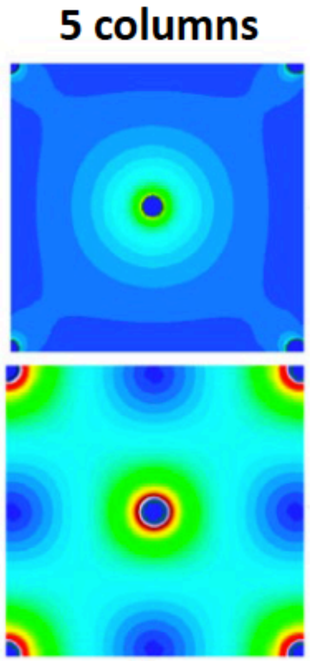

Towards uniformity
in both E_W and velocity

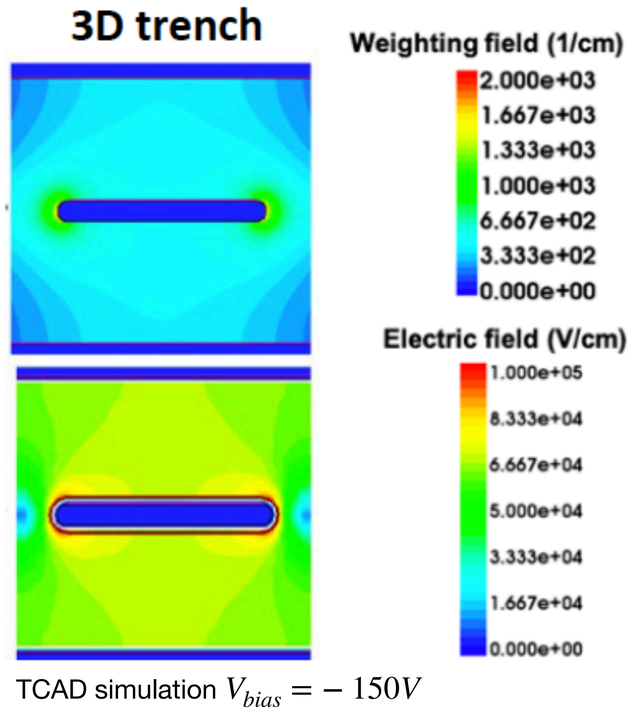

TCAD simulation $V_{bias} = -150V$

Electrode shape optimization
allows the **signals** to be **independent of the hit position**

The trench-type TimeSPT 3D sensors

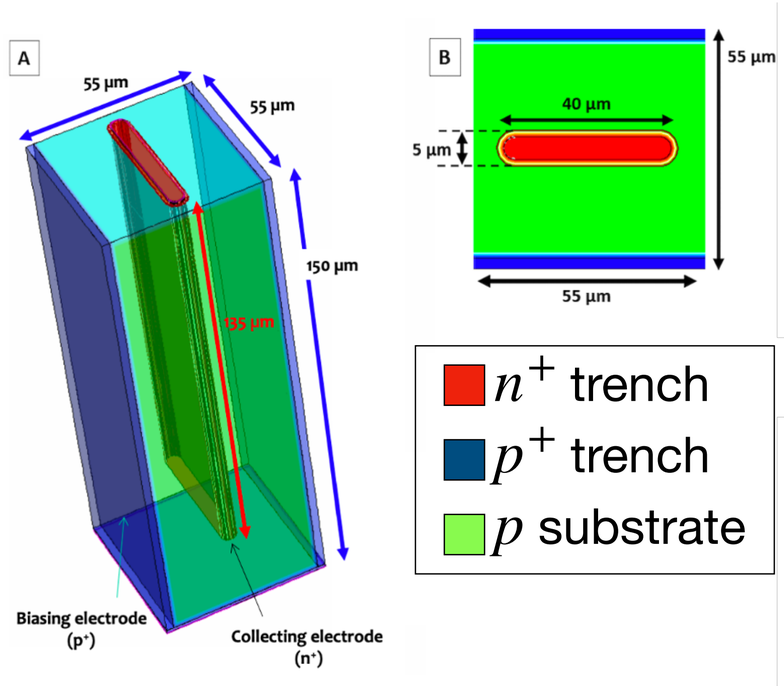

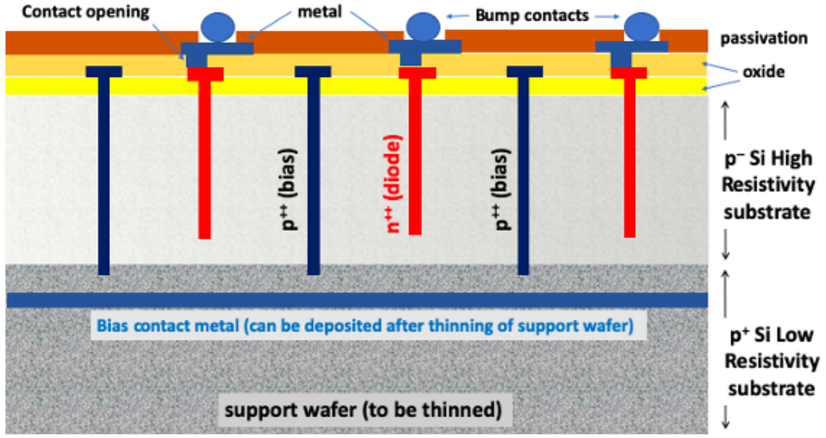

- **55x55 μm^2 pixels** (compatible with existing FEE)
- In each pixel a **40 μm long n++** trench is placed between the continuous p++ trenches for the bias
- **150 μm active thickness**, on a 350 μm-thick support wafer
- Collection electrode **135 μm deep**

3D pixel: timing performance

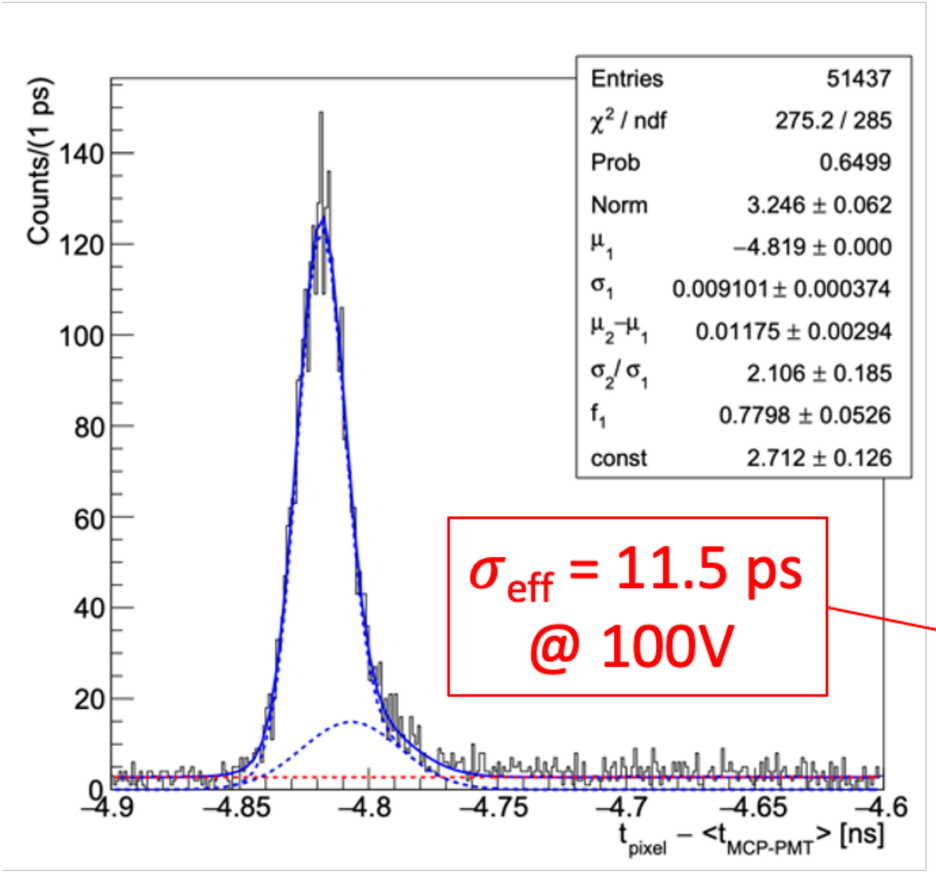

σ_{eff} = 11.5 ps @ 100V

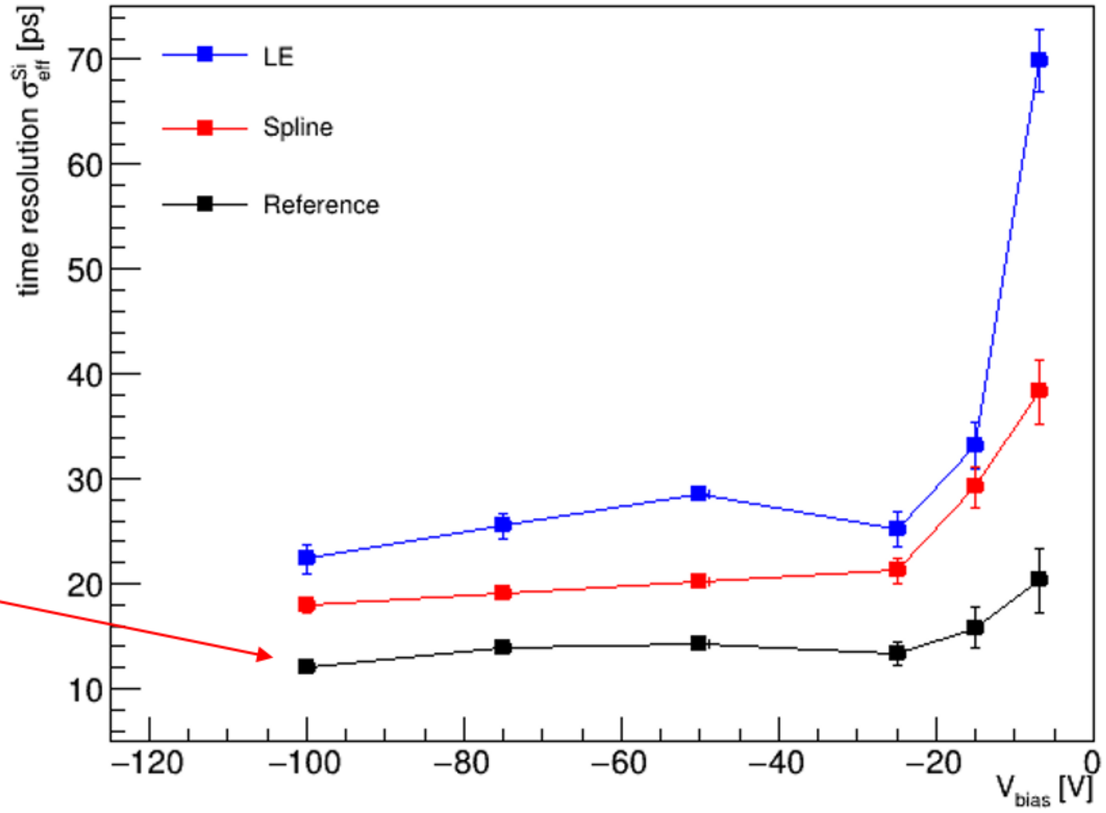

- **Symmetric time distribution**, with only a **small tail** due to late signals
  ⟶ Time distribution fitted with two gaussians to include late signals contributions

- **Excellent performance** with **CFD-based methods**, but also using **leading edge algorithm** (no time walk correction)

Efficiency tests: the method

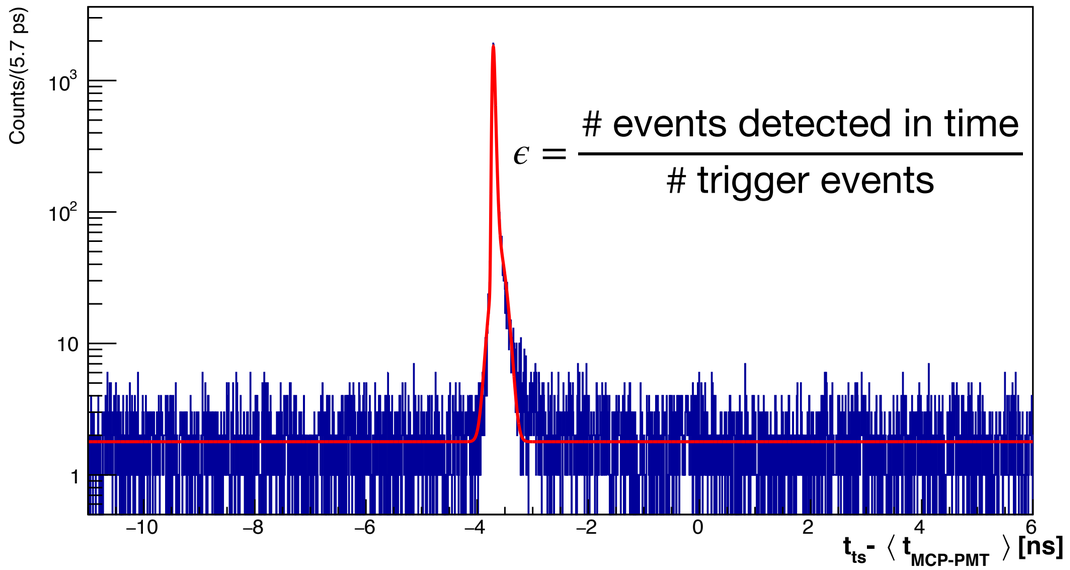

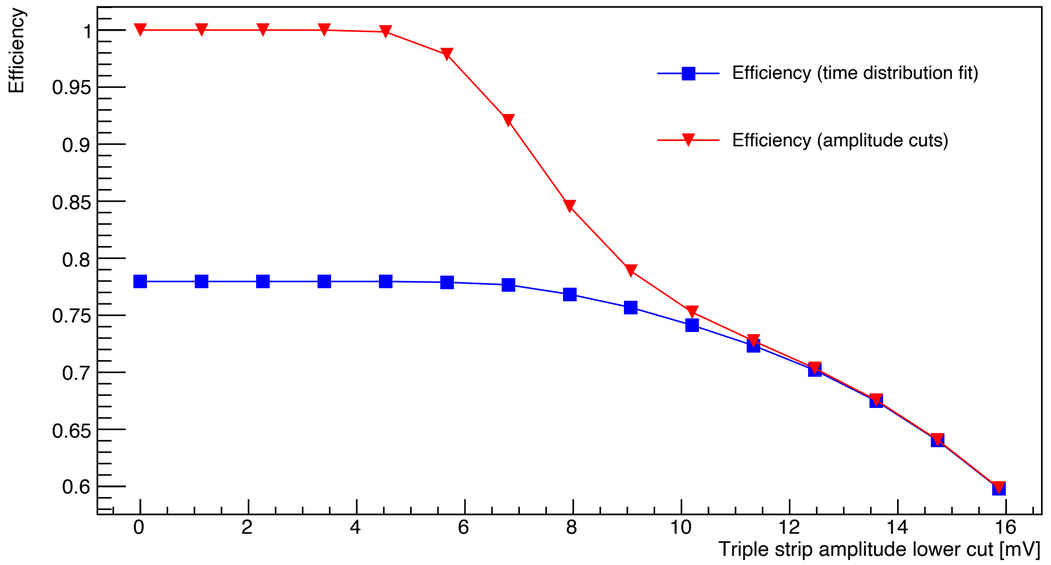

*Red line includes noise contribution

*no correction for the beam divergence

- From the **time distribution of the triple strip signals w.r.t the MCP-PMTs**, the **efficiency** is computed by the number of **events in time** (populating the peak) over the **total number of trigger events**

- **3D pixel detection (geometrical) efficiency** at normal incidence is in **agreement with calculated fraction of active area** ($\approx 80\,\%$)

Efficiency tests: the results

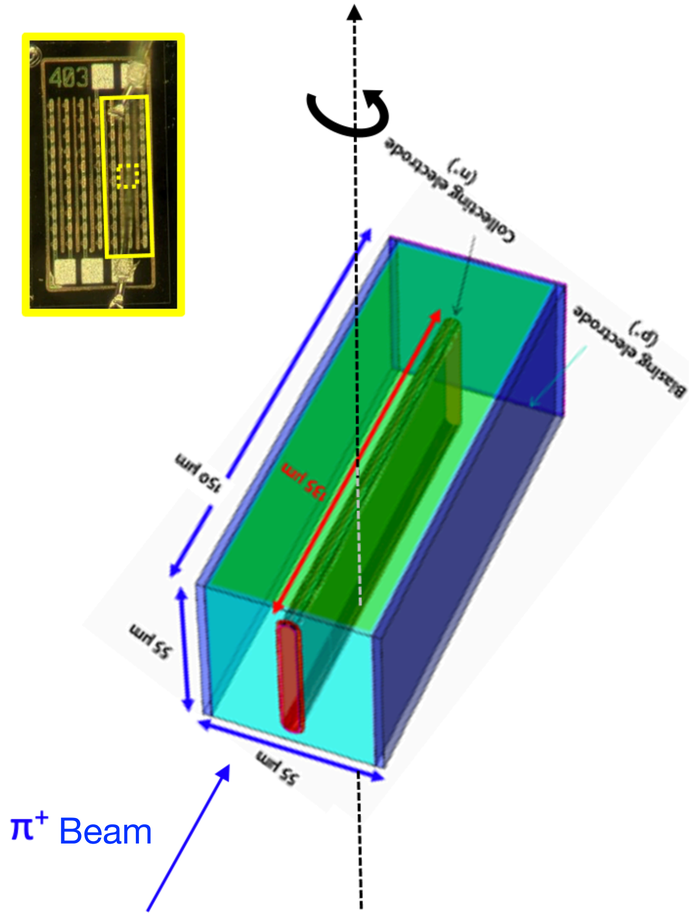

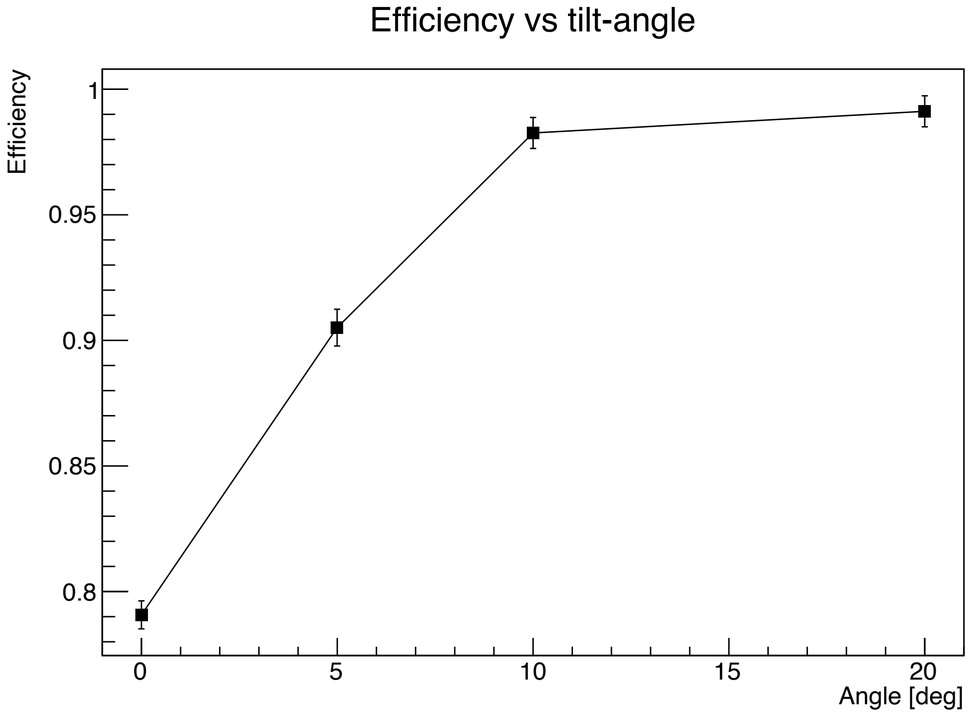

$\epsilon = 99.1 \pm 0.6\,\%$ @20°

The **inefficiency** (at normal incidence) due to the dead-area of the trenches is **fully recovered** by **tilting** the sensors around the trench axis **at angles larger than 10°**

Tilted sensors: timing performances

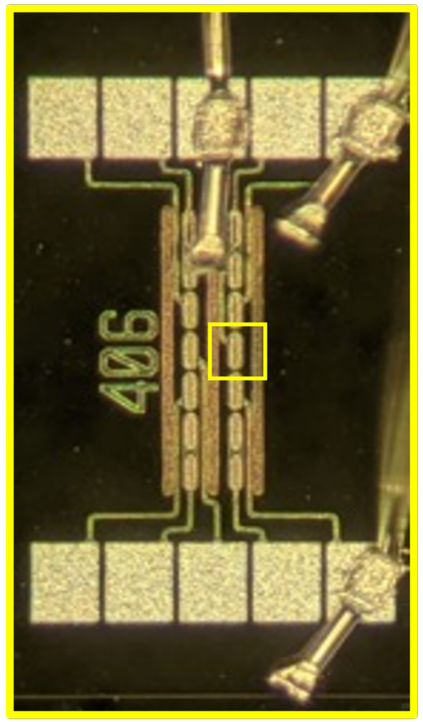

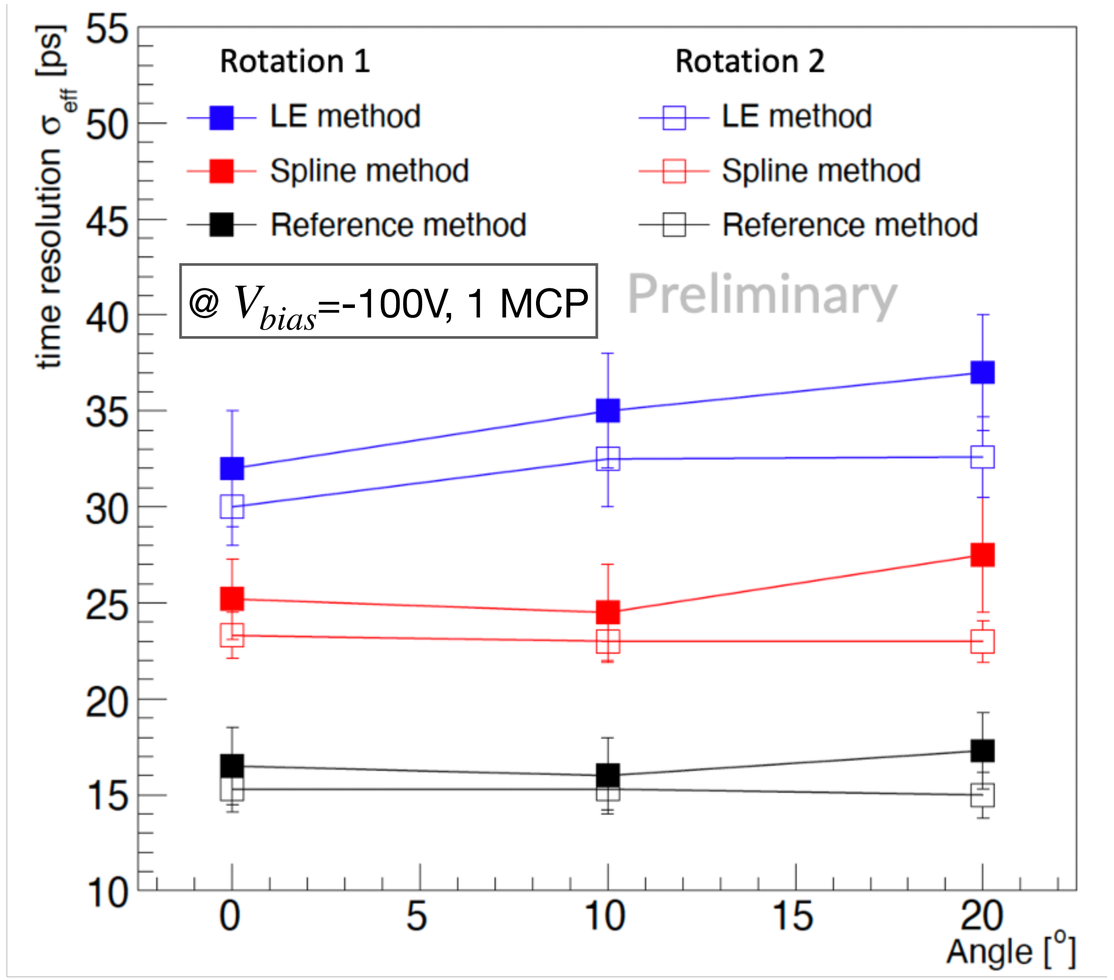

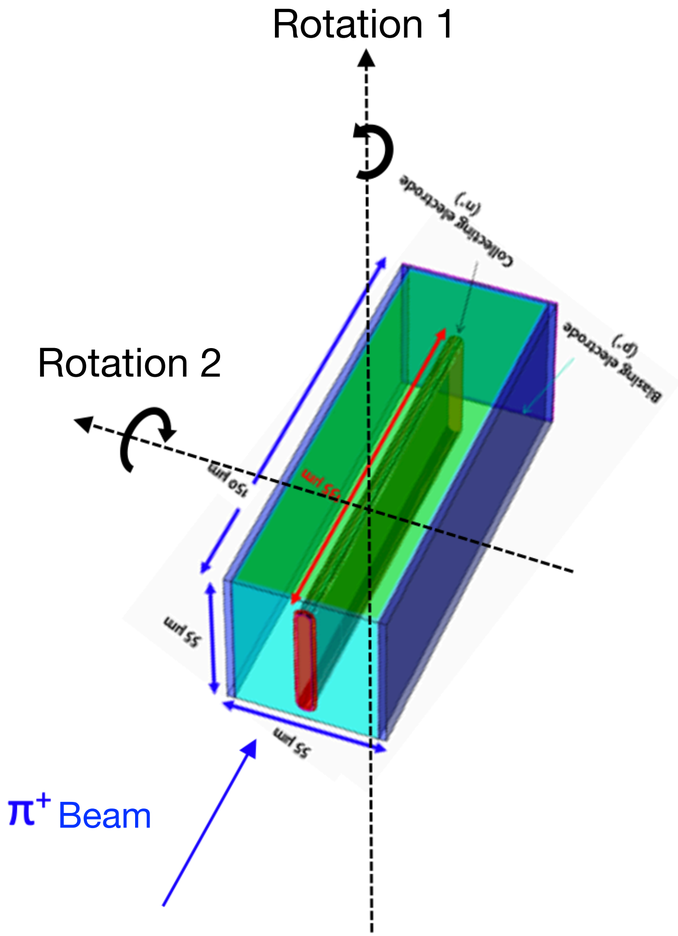

Irradiated sensors: amplitude performance

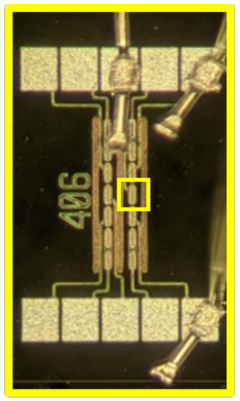

$2.5 \cdot 10^{16}$ 1 MeV n_{eq}/cm^2 - 0°

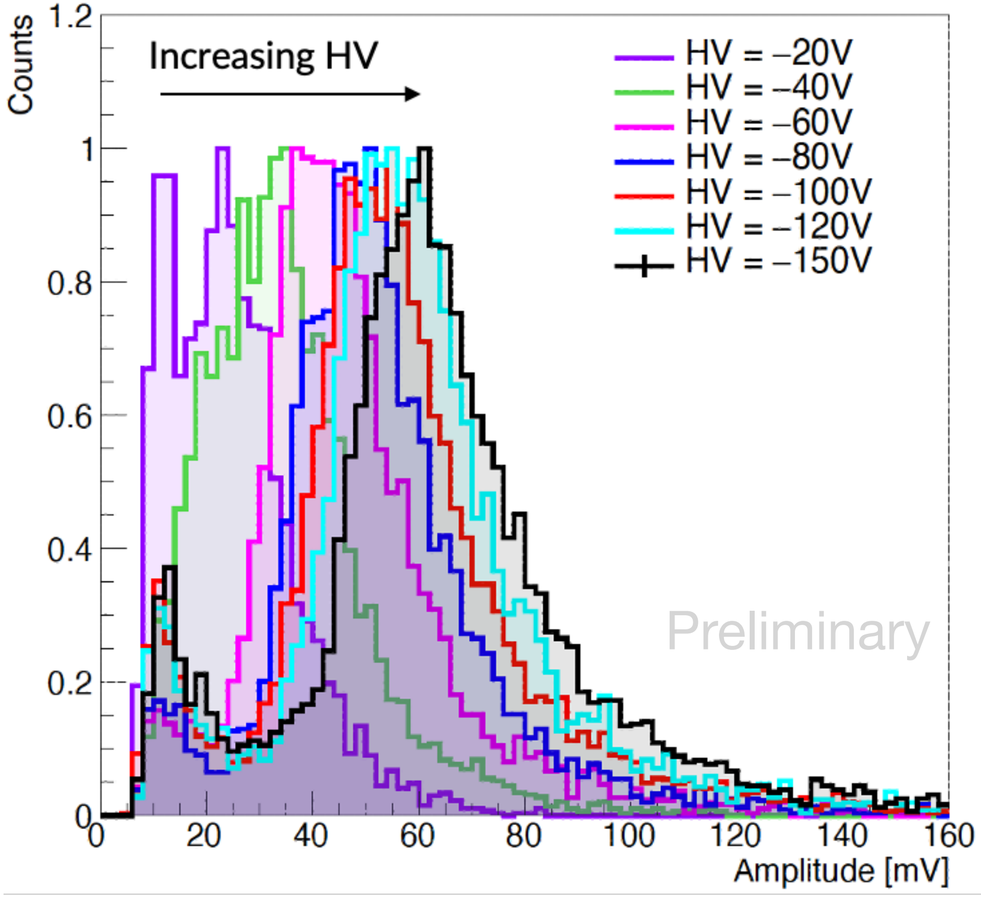

non-irradiated - 0°

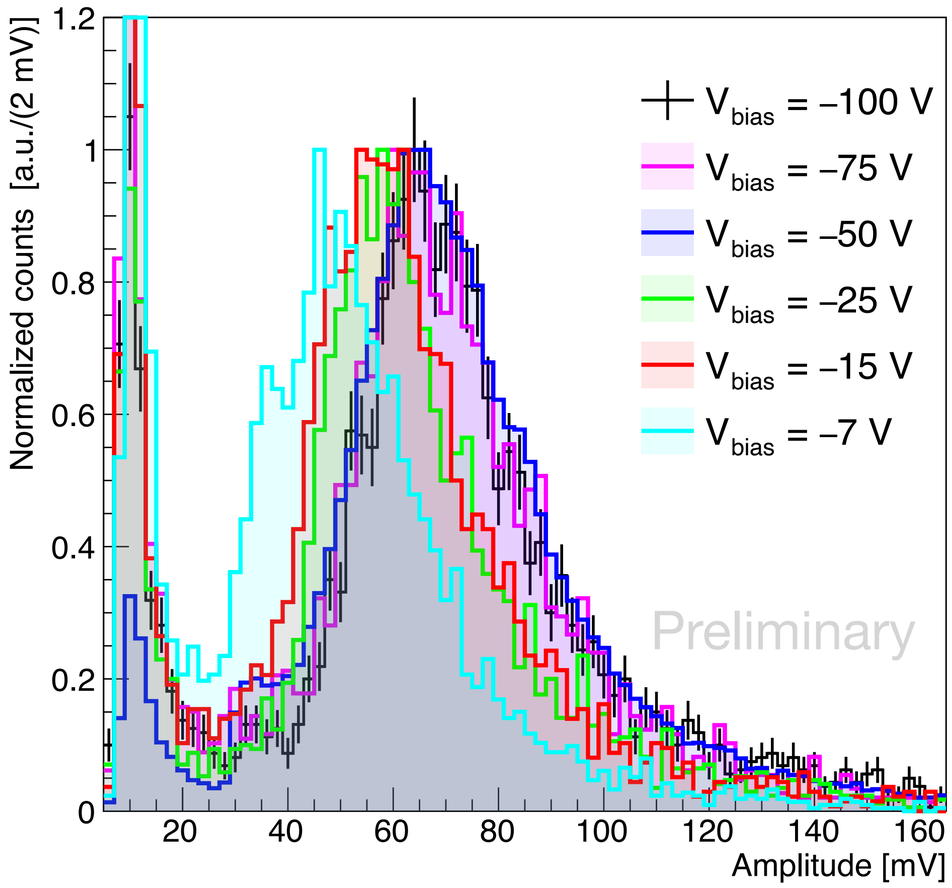

Larger bias voltage is required to **recover the signal amplitude** for irradiated sensors

Irradiated sensors: timing

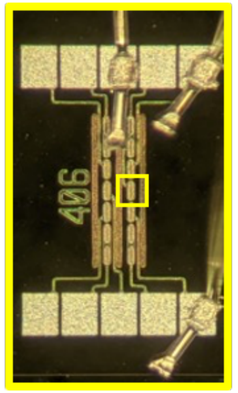

$2.5 \cdot 10^{16}$ 1 MeV n_{eq}/cm^2 - 0°

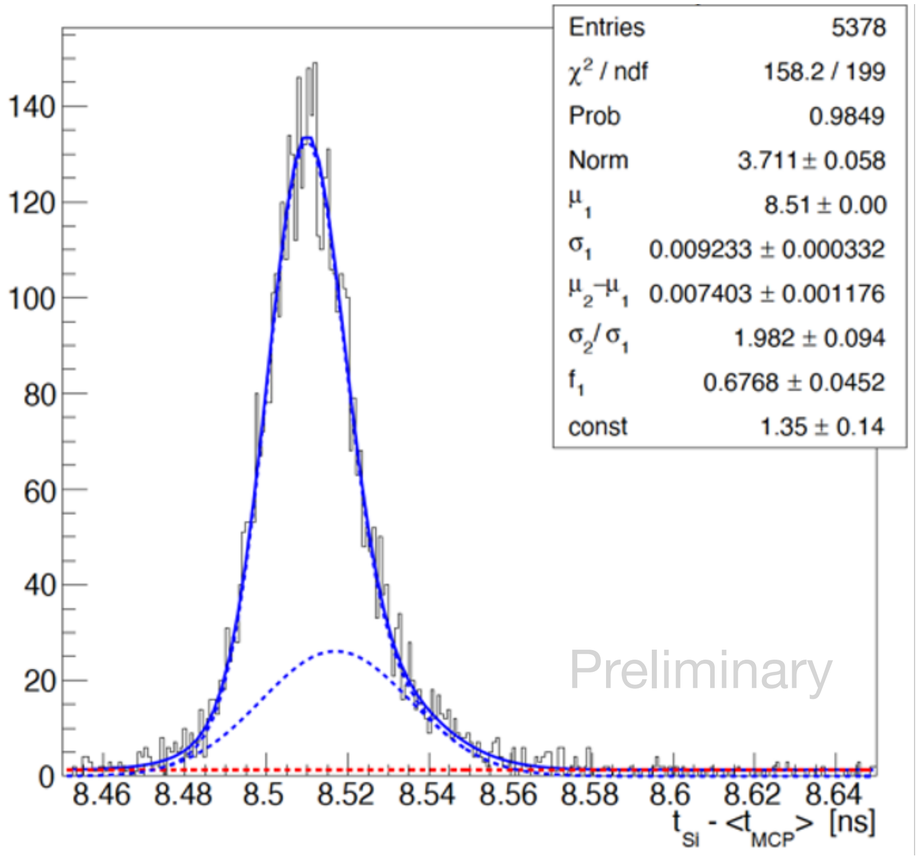

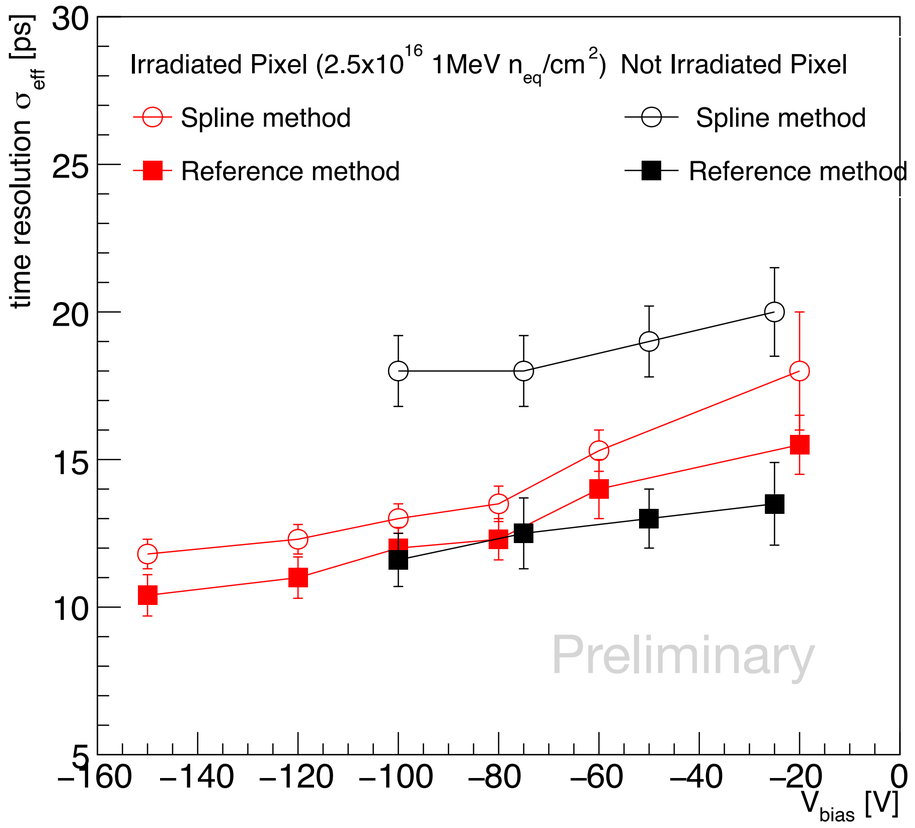

Excellent time resolution measured at 150V on single pixel irradiated $2.5 \cdot 10^{16}$ 1 MeV n_{eq}/cm^2 !

Irradiated sensors: efficiency

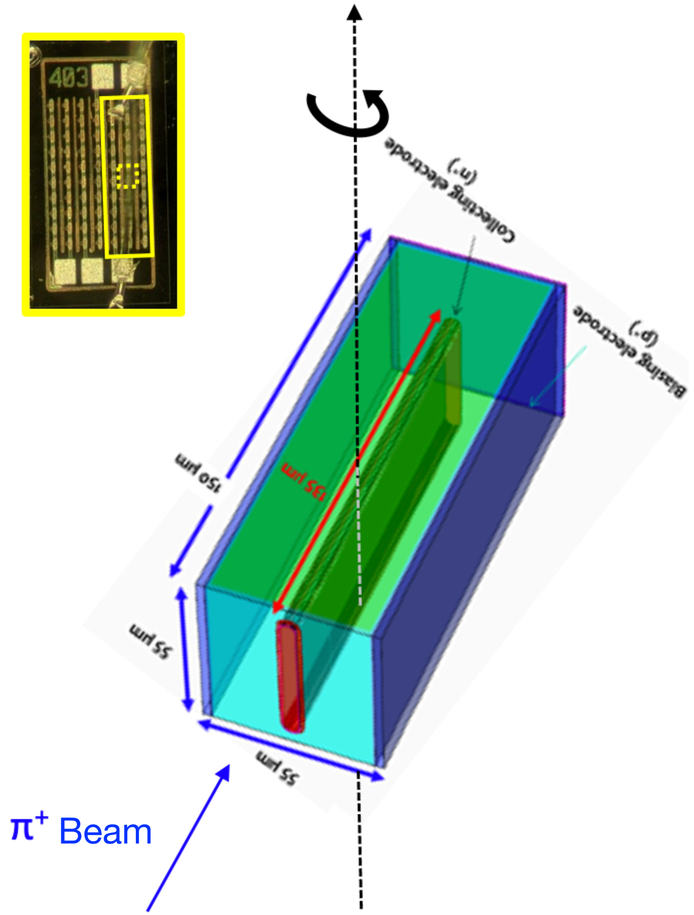

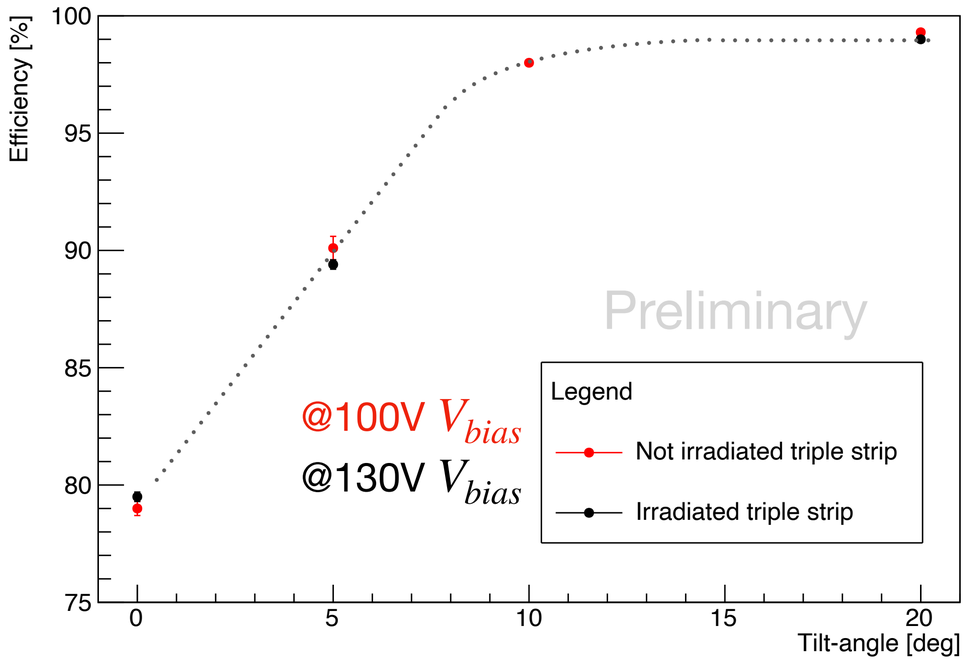

Increasing the **irradiated sensor bias voltage** to 130V allows to **fully recover** the **efficiency @20°** expected for **non-irradiated sensors**

My PhD thesis

- General **introduction** on **LHCb detector and the Upgrades**
- What was done for the **current LHCb detector and collaboration**?
  - RICH Upgrade 1 commissioning
  - BR($\Lambda_b \to \Lambda_c^* D_s^{(*)}$ / $\Lambda_b \to \Lambda_c D_s^{(*)}$) measurement
- What was done for the **LHCb detector Upgrades**? Timing!
  - RICH LS3 enhancements
  - VELO Upgrade 2 R&D

Thank you for your attention (and patience)!

Backup slides

EC-R: TDC-in-FPGA working principle

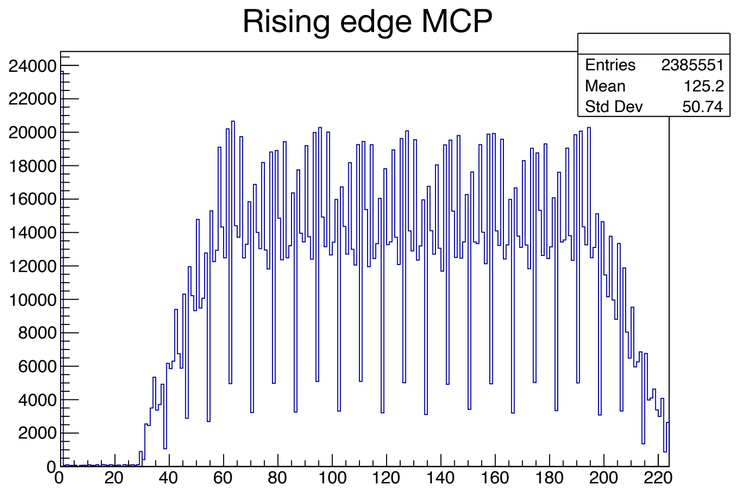

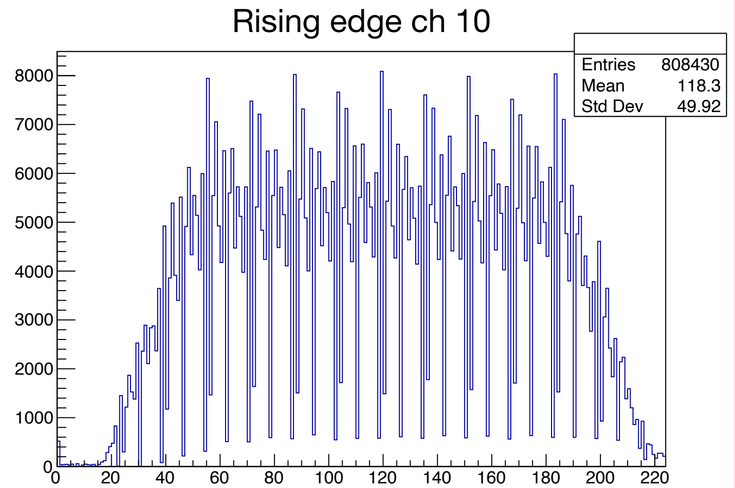

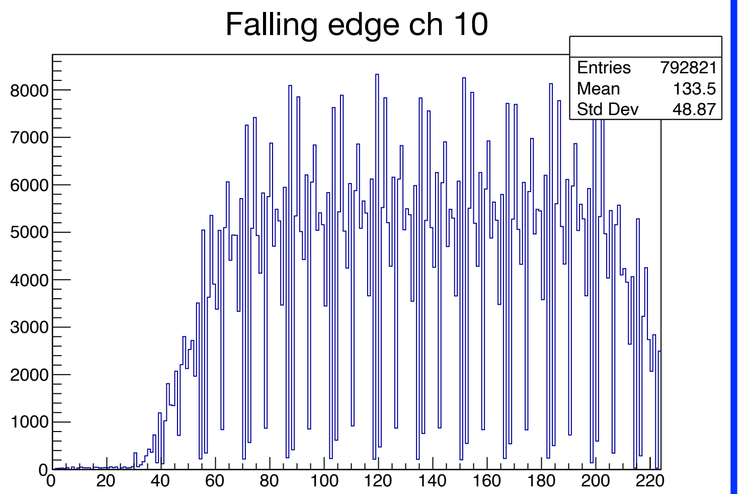

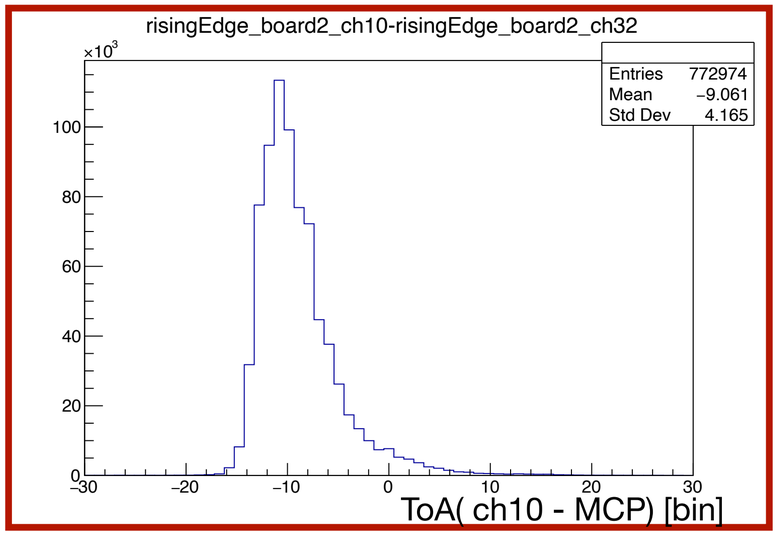

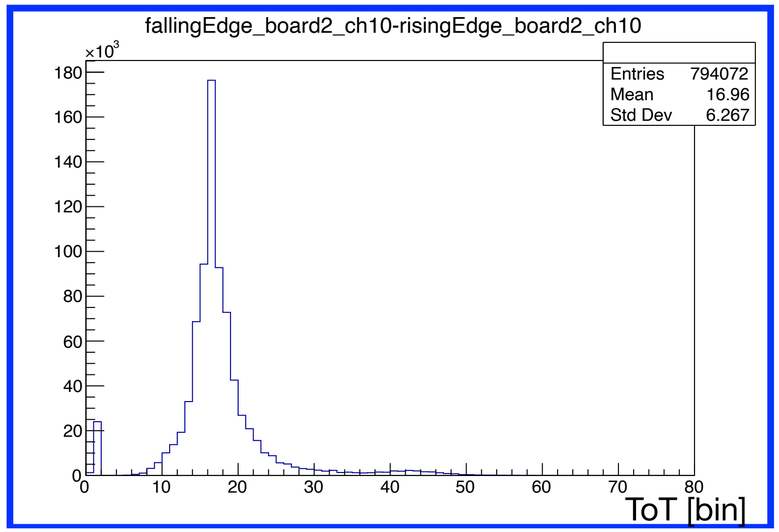

ToA(ch 10 - MCP) = Rising edge ch 10 - Rising edge MCP

ToT = Falling edge ch 10 - Rising edge ch 10

EC-R time resolution: the idea of the analysis approach

The goal of this analysis is looking for the more unbiased way to properly time calibrated our data, considering the fact that our TDC has bin widths which differs one from one another.

Recall: all rising edge bins are grouped by 16 since the TDC is made of a module of 16 bins repeated 14 times (16x14=224 bins).

We can subdivide the data wrt the rising edge (RE) bin of the time reference channel, resulting in 16 subsets of data. In this way each subset is "triggered" by a signal coming from a TDC bin which has always the same length.

Now let's consider the variable ΔToA(ch_x - ch_{ref}) = RE_x - RE_{ref} .

Since RE_{ref} is fixed, the probability that a certain event will have rising edge RE_x will be proportional to its bin width.

It is possible to create histograms with variable bin widths to calibrate correctly the TDC bins to ns

EC-R time resolution: the idea of the analysis approach

Example: ΔToA(ch_{25} - MCP)

Data are subdivided in 16 groups wrt the rising edge bin of the MCP:

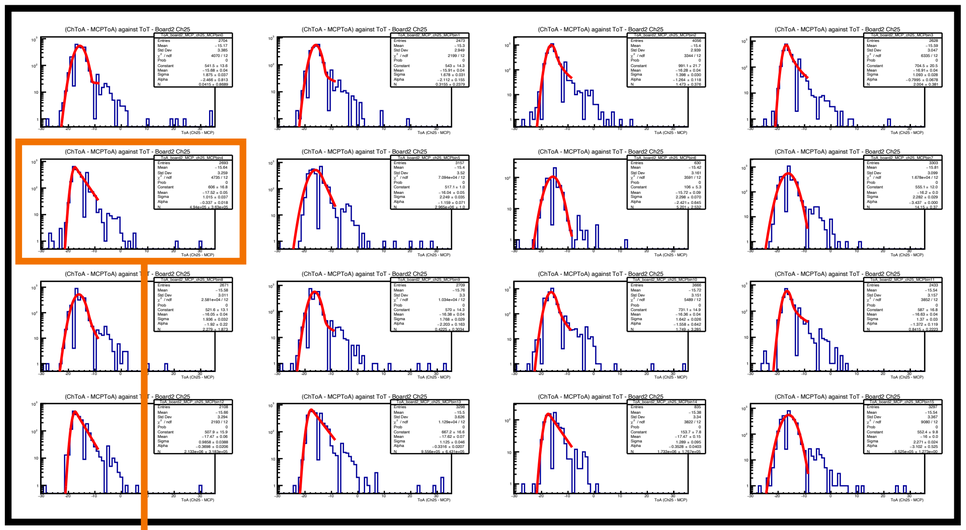

Example: MCP rising edge bin == 5

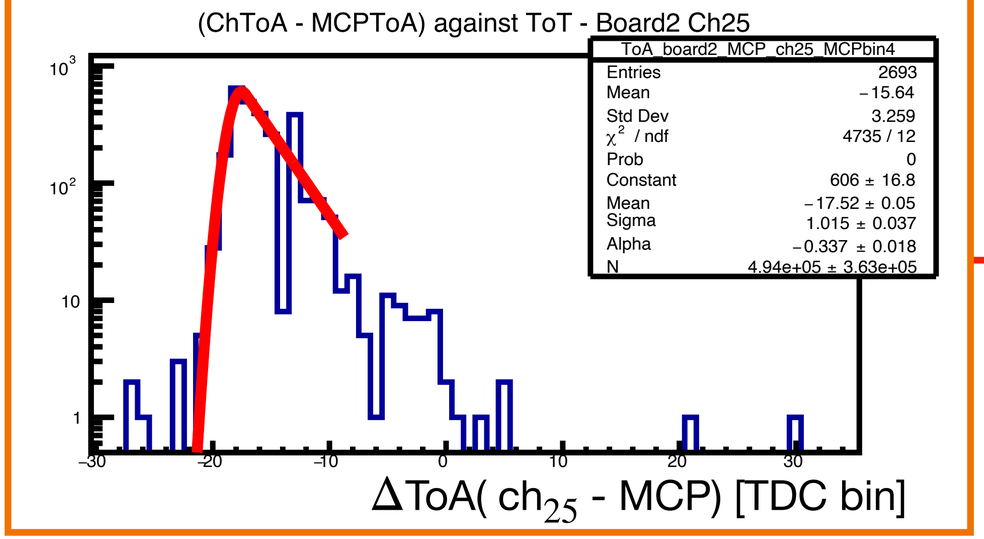

CALIBRATION

We can go from TDC bins to ns units, filling histograms with variable bin widths

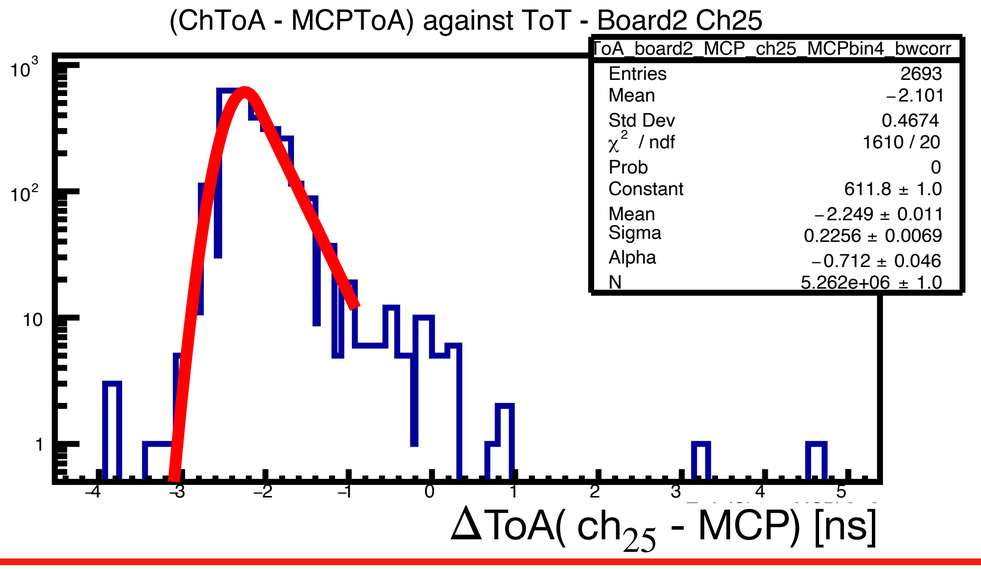

EC-R time resolution: the time walk correction

Currently time walk correction for a certain channel is performed subdividing the data wrt the ToT length in bins of the signals.

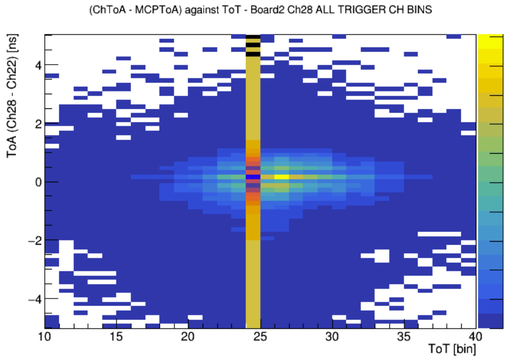

Split data wrt the time reference ToA bin (16 subgroups)

Perform a time calibration generating an histogram with variable bin widths

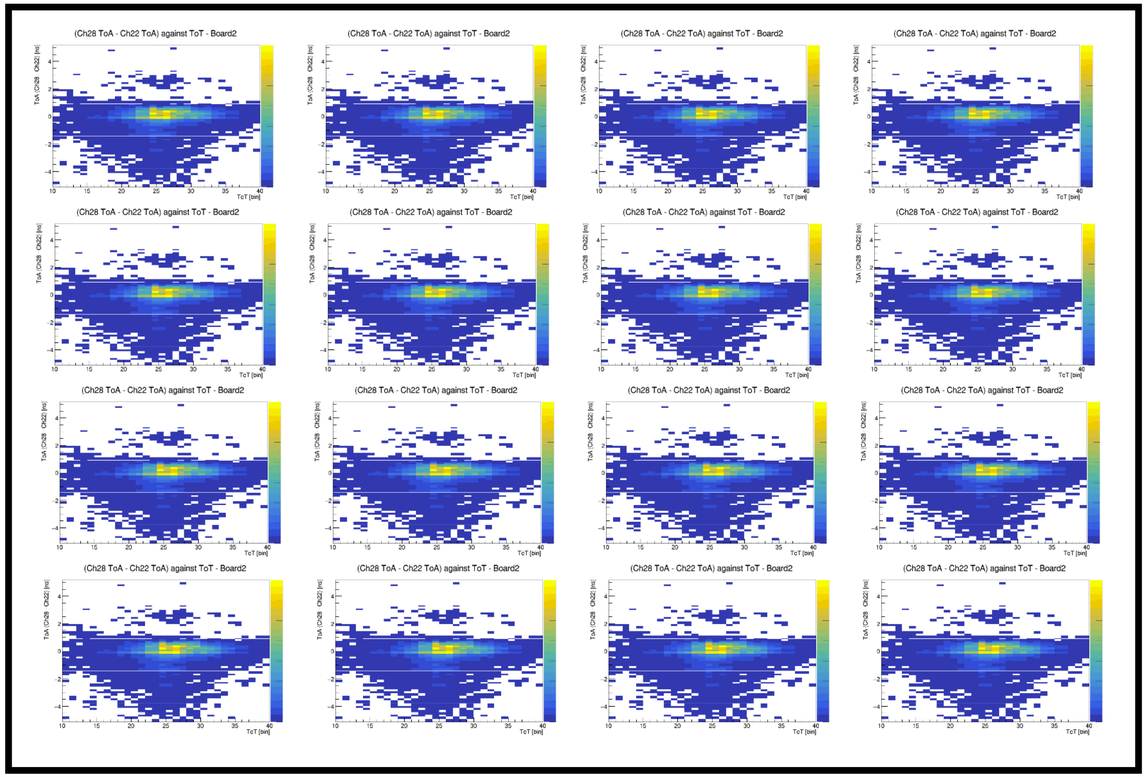

EC-R time resolution: the time walk correction

Currently time walk correction for a certain channel is performed subdividing the data wrt the ToT length in bins of the signals.

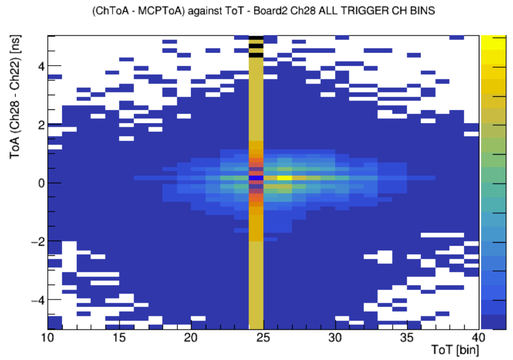

Split data wrt the time reference ToA bin (16 subgroups)

Perform a time calibration generating an histogram with variable bin widths

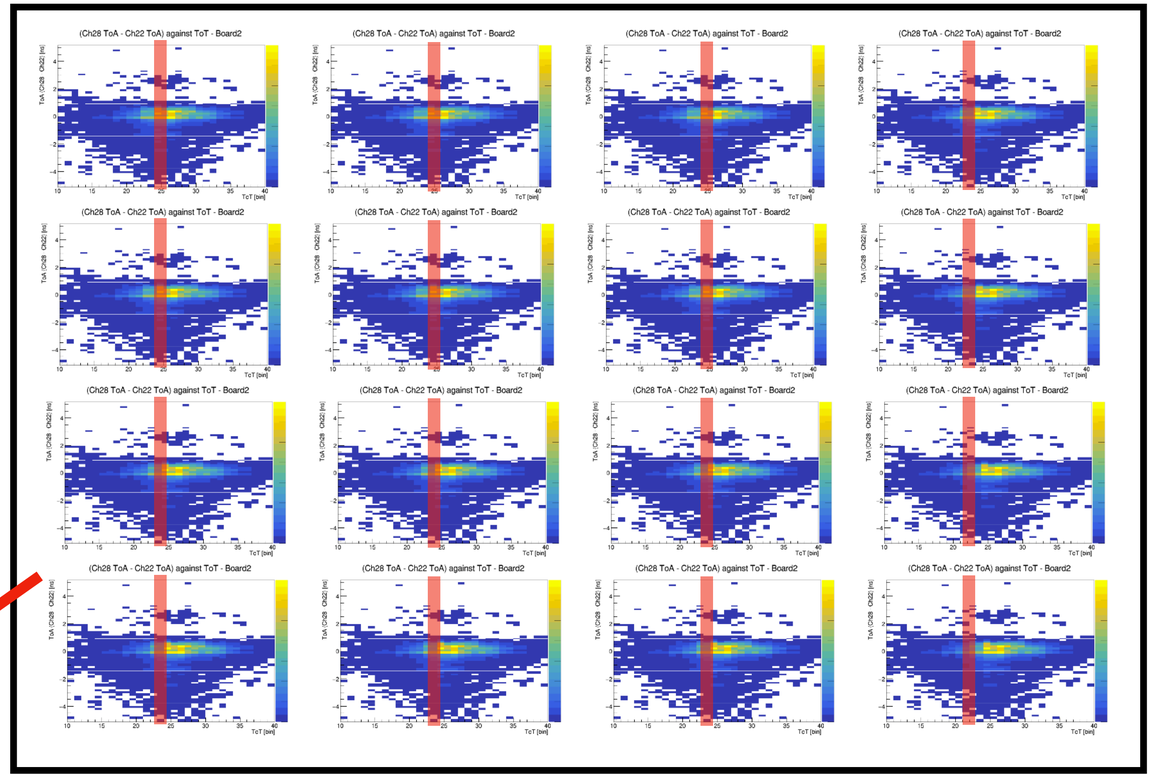

Projection of data in single ToT bins:
16 plots of ΔToA(ch$_x$ - MCP)

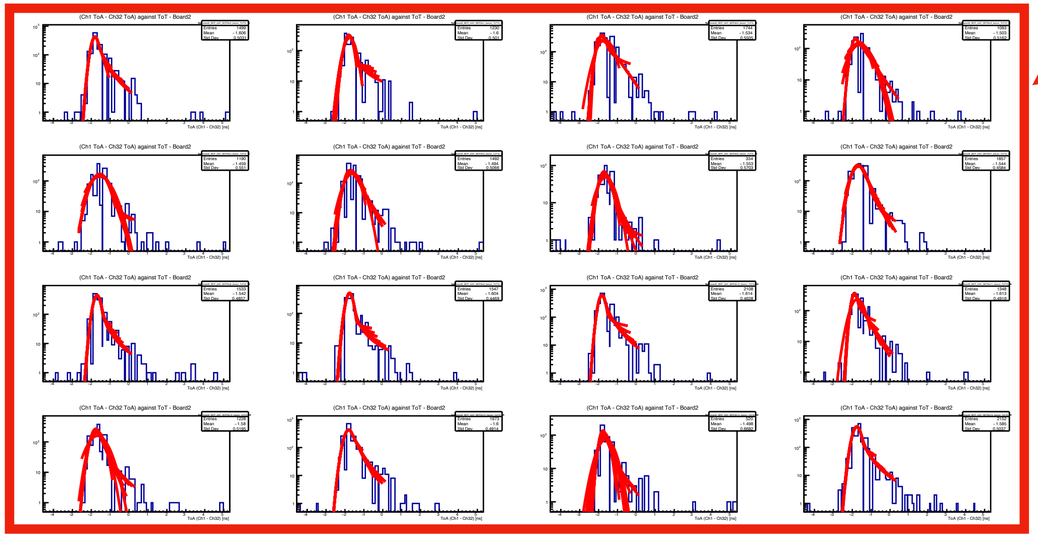

EC-R time resolution: the time walk correction

Currently time walk correction for a certain channel is performed subdividing the data wrt the ToT length in bins of the signals.

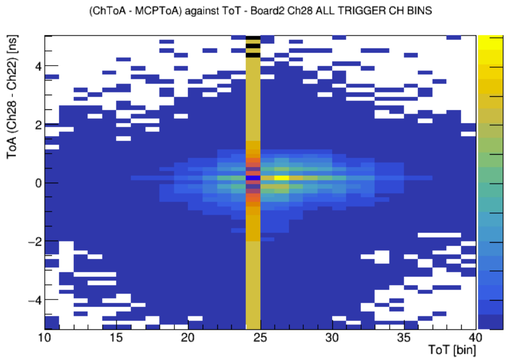

Split data wrt the time reference ToA bin (16 subgroups)

Perform a time calibration generating an histogram with variable bin widths

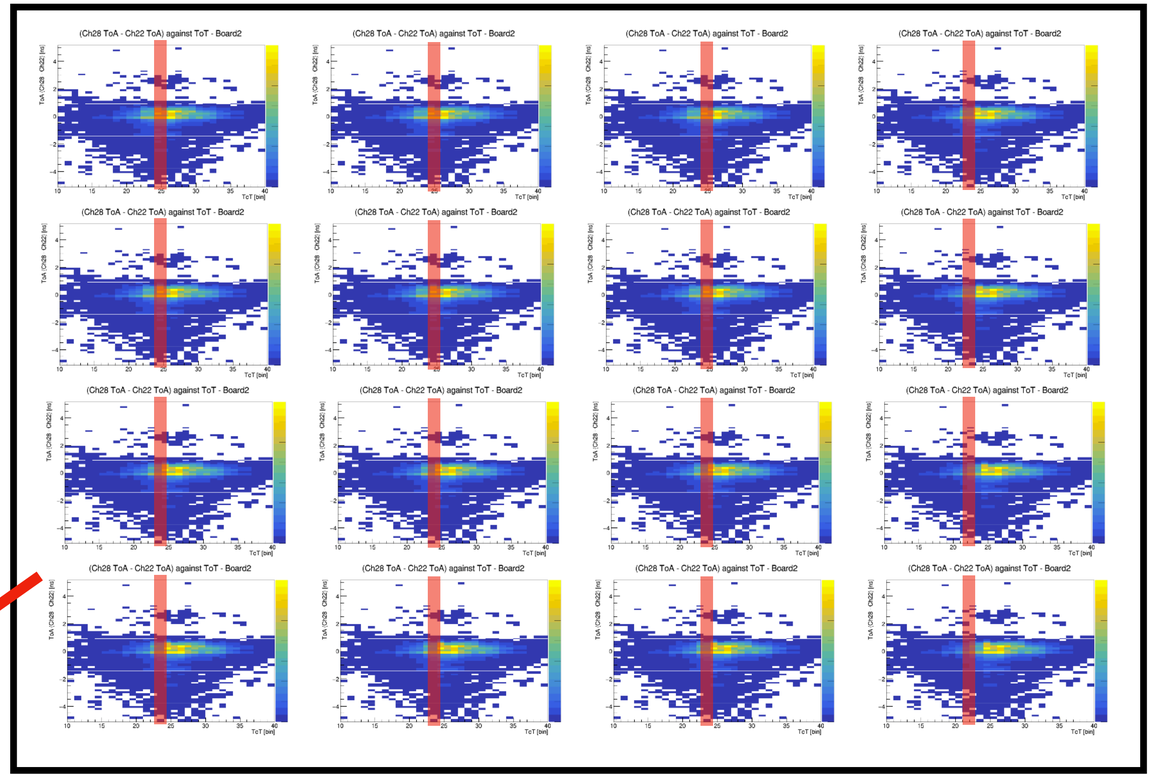

Projection of data in single ToT bins:
16 plots of ΔToA(ch$_x$ - MCP)

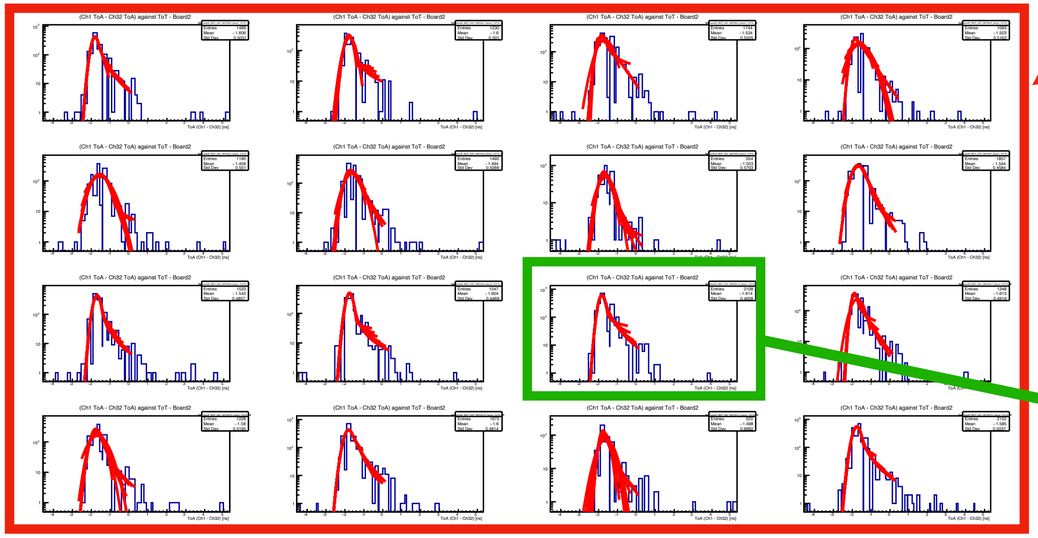

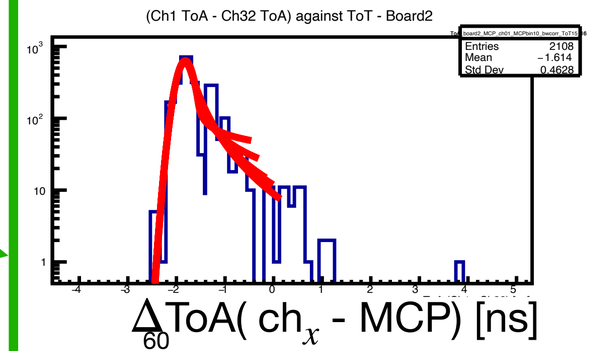

For the single ΔToA(ch$_x$ - MCP) in ns, I perform several fits changing the fit range.

EC-R time resolution: the time walk correction

- The Gaussian sigma of the several CrystallBall fits is taken.
- A subset of sigmas is created selecting only the fits that converged and that satisfy certain parameters ranges conditions.

- The weighted average of the selected CrystallBall is taken: the sigma in the set which is the closest to the mean is taken as the reference one ($\sigma_t^{fit} \pm \sigma_{stat}$).
- I subtract to this value the contribution from the MCP TDC bin:

$$\sigma_{1bin}^{TDCcorr} = \sqrt{\sigma_t^{fit2} - (binwidth/\sqrt{12})^2}$$

- The standard deviation of the set of sigmas is computed wrt the weighted average (std).

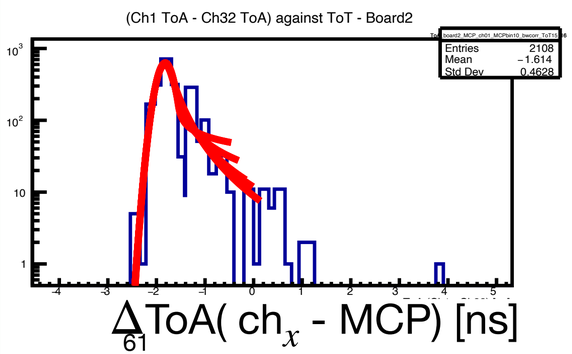

Finally:

$$\sigma_t^{1bin} = \sigma_t^{TDCcorr} \pm \sigma_{\sigma_t^{fit}}^{tot}$$

$$\sigma_{\sigma_t^{fit}}^{tot} = \sqrt{\sigma_{stat}^2 + std^2}$$

EC-R time resolution: the time walk correction

- Now there is a set of 16 independent σ_t^{1bin}.
- I combine those with a weighted average to obtain the time resolution of a single ToT bin:

$$\sigma_{1ToT} = \frac{\sum \sigma_t^{1bin} / \sigma^2_{\sigma_t^{1bin}}}{\sum 1/\sigma^2_{\sigma_t^{1bin}}} \qquad \sigma_{\sigma_{1ToT}} = \sqrt{\frac{1}{\sum 1/\sigma^2_{\sigma_t^{1bin}}}}$$

- I calculate the reduced χ^2 of the 16 σ_t^{1bin} wrt they weighted average. If it is higher than 1, I extrapolate a correction factor to account the uncertainty underestimation

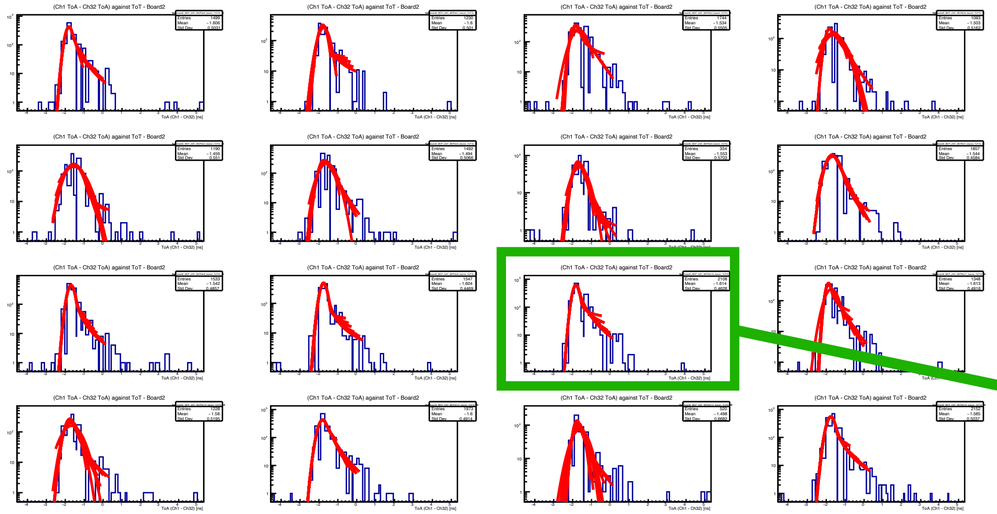

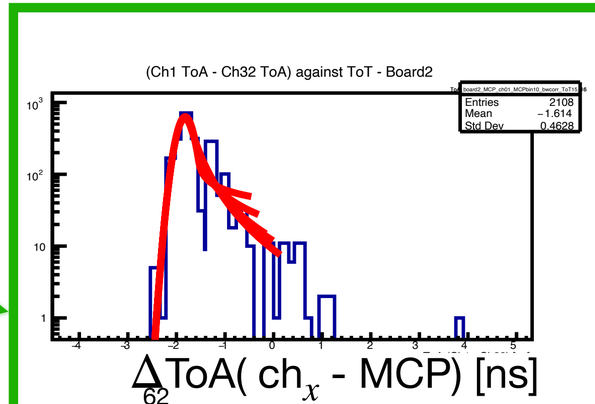

$$\sigma_t^{1bin} = \sigma_t^{TDCcorr} \pm \sigma^{tot}_{\sigma_t^{fit}}$$

$$\sigma^{tot}_{\sigma_t^{fit}} = \sqrt{\sigma^2_{stat} + std^2}$$

EC-R time resolution: the time walk correction

- Now there is a set of 16 independent σ_t^{1bin}.
- I combine those with a weighted average to obtain the time resolution of a single ToT bin:

$$\sigma_{1ToT} = \frac{\sum \sigma_t^{1bin} / \sigma^2_{\sigma_t^{1bin}}}{\sum 1/\sigma^2_{\sigma_t^{1bin}}} \qquad \sigma_{\sigma_{1ToT}} = \sqrt{\frac{1}{\sum 1/\sigma^2_{\sigma_t^{1bin}}}}$$

- I calculate the reduced χ^2 of the 16 σ_t^{1bin} wrt they weighted average. If it is higher than 1, I extrapolate a correction factor to account the uncertainty underestimation

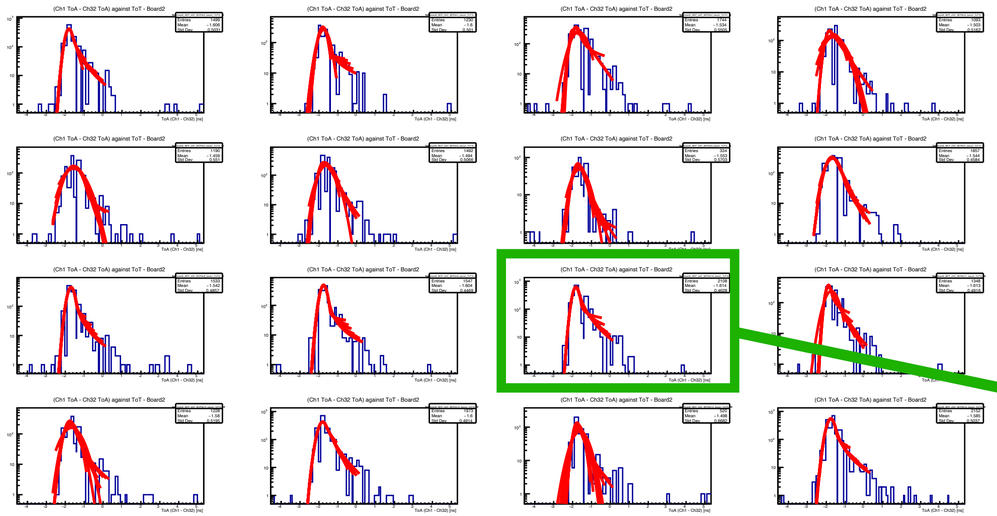

$$\chi^2_r = \sum_{i=0}^{16} \frac{(\sigma_{ti}^{1bin} - \sigma_{1ToT})^2}{\sigma^2_{\sigma_{ti}^{1bin}} \cdot (16-1)} = S$$

$$\sigma^{new}_{\sigma_{ti}^{1bin}} = \sqrt{S} \cdot \sigma_{\sigma_{ti}^{1bin}}$$

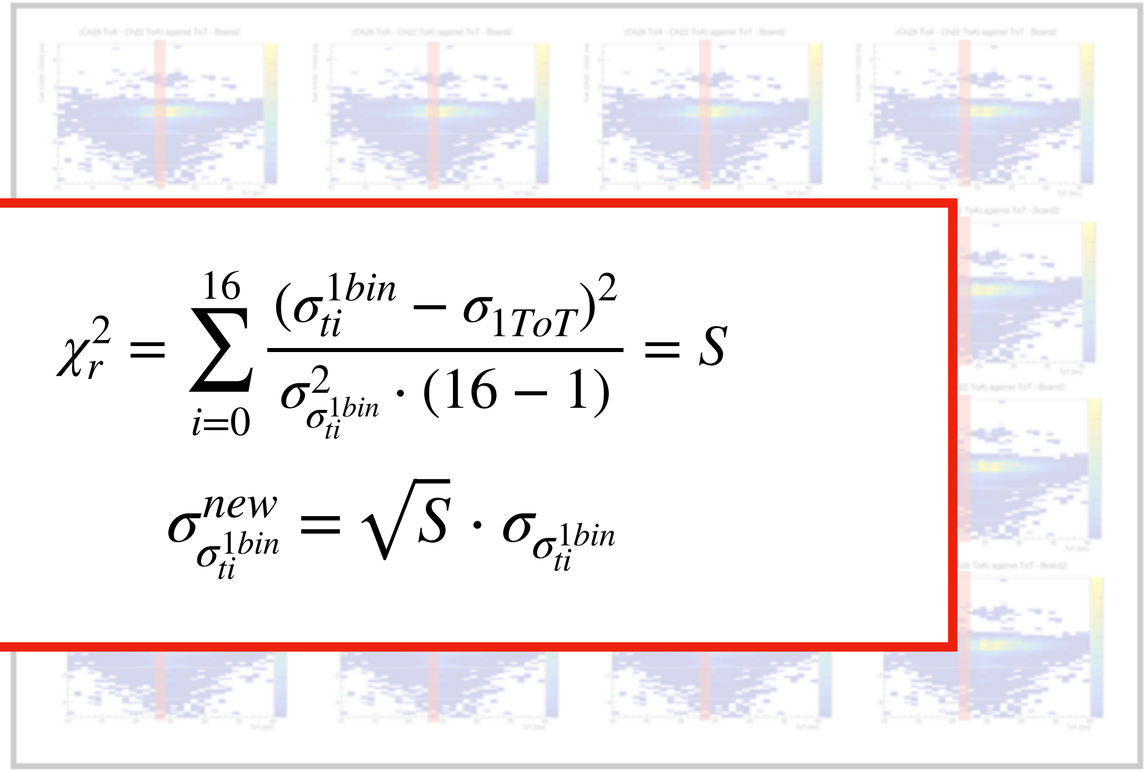

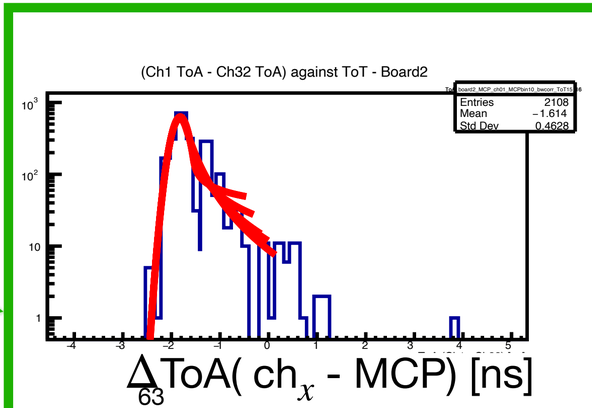

$$\sigma_t^{1bin} = \sigma_t^{TDCcorr} \pm \sigma^{tot}_{\sigma_t^{fit}}$$

$$\sigma^{tot}_{\sigma_t^{fit}} = \sqrt{\sigma^2_{stat} + std^2}$$

EC-R time resolution: the time walk correction

- Finally I can combine the different σ_{1ToT} to obtain the final time resolution according to the statistics inside each ToT bin:

$$\sigma_t^2 = \frac{\sum_{ToTbins} N_{ToT} \cdot \sigma_{t,ToT}^2}{N}$$

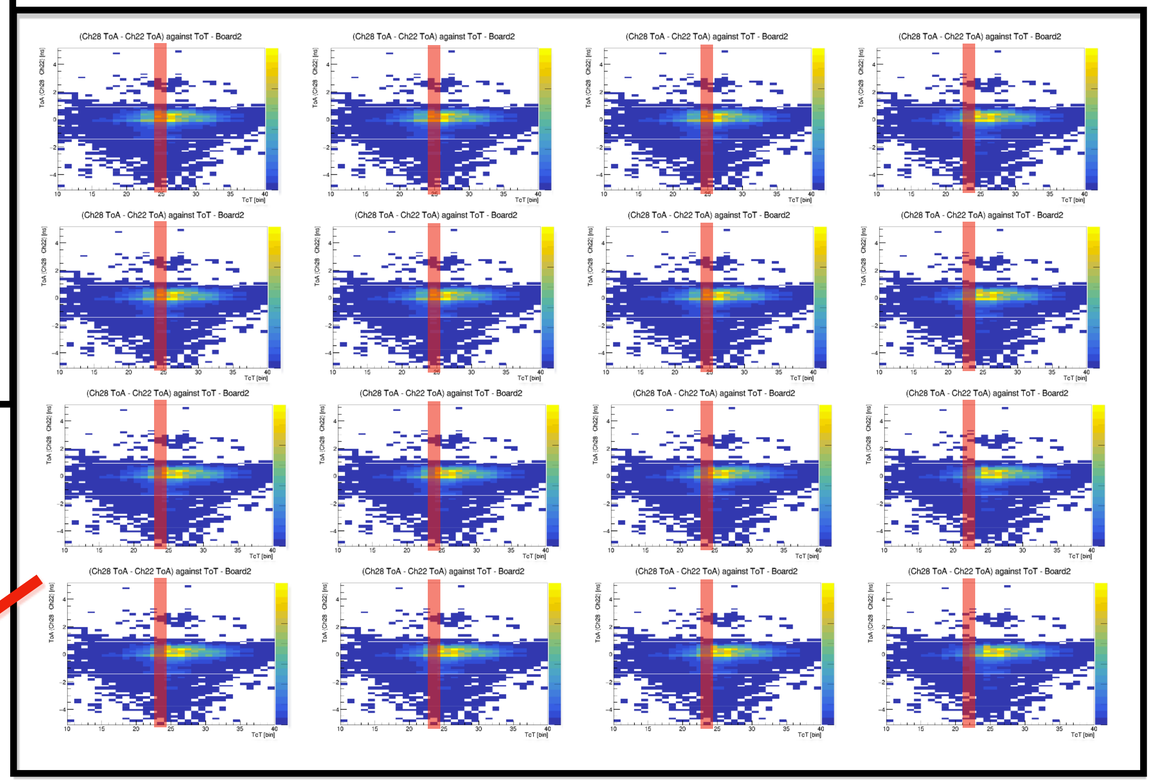

$$\sigma_{1ToT} = \frac{\sum \sigma_t^{1bin} / \sigma^2_{\sigma_t^{1bin}}}{\sum 1/\sigma^2_{\sigma_t^{1bin}}} \qquad \sigma_{\sigma_{1ToT}} = \sqrt{\frac{1}{\sum 1/\sigma^2_{\sigma_t^{1bin}}}}$$

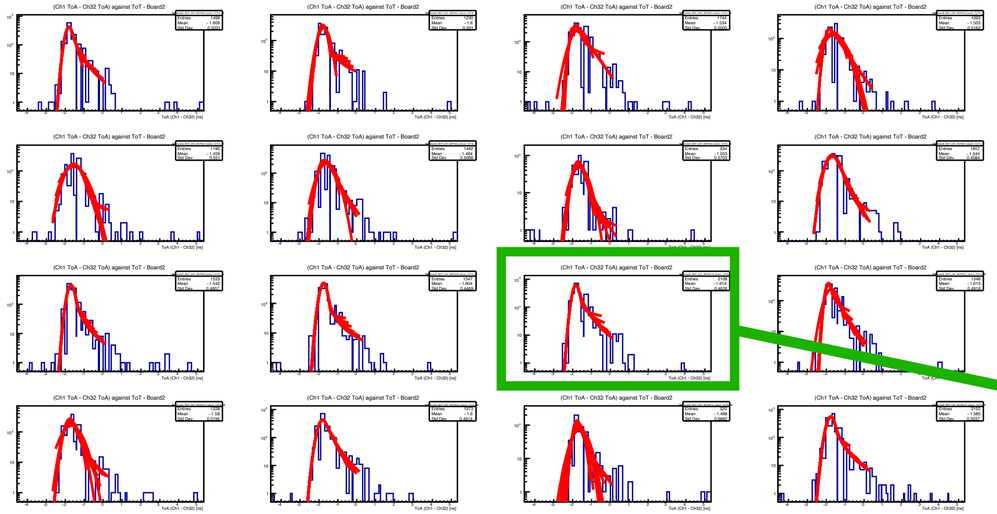

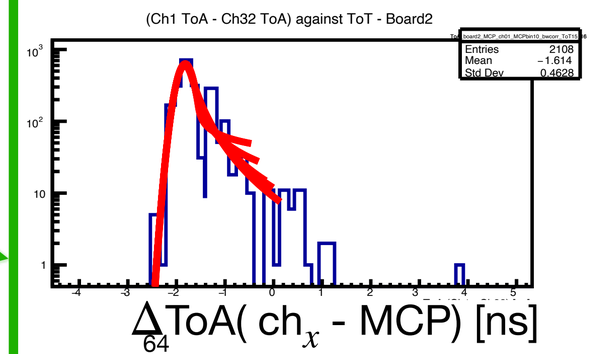

$$\sigma_t^{1bin} = \sigma_t^{TDCcorr} \pm \sigma^{tot}_{\sigma_t^{fit}}$$

$$\sigma^{tot}_{\sigma_t^{fit}} = \sqrt{\sigma^2_{stat} + std^2}$$

The Fabrication Process

Two batches were produced in 2019 and 2021 at Fondazione Bruno Kessler (FBK, Trento, Italy) using the Deep Reactive Ion Etching (DRIE) Bosch process, 6” wafers.

Many devices were designed and fabricated, such as:

Pixels

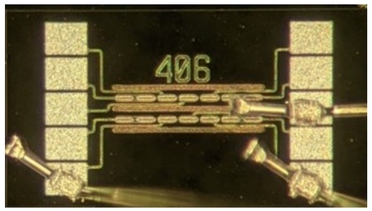

Pixel strips

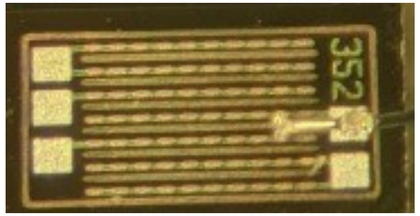

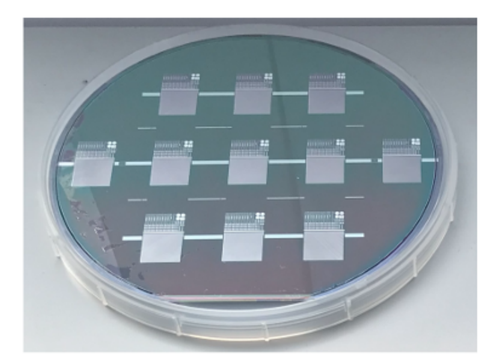

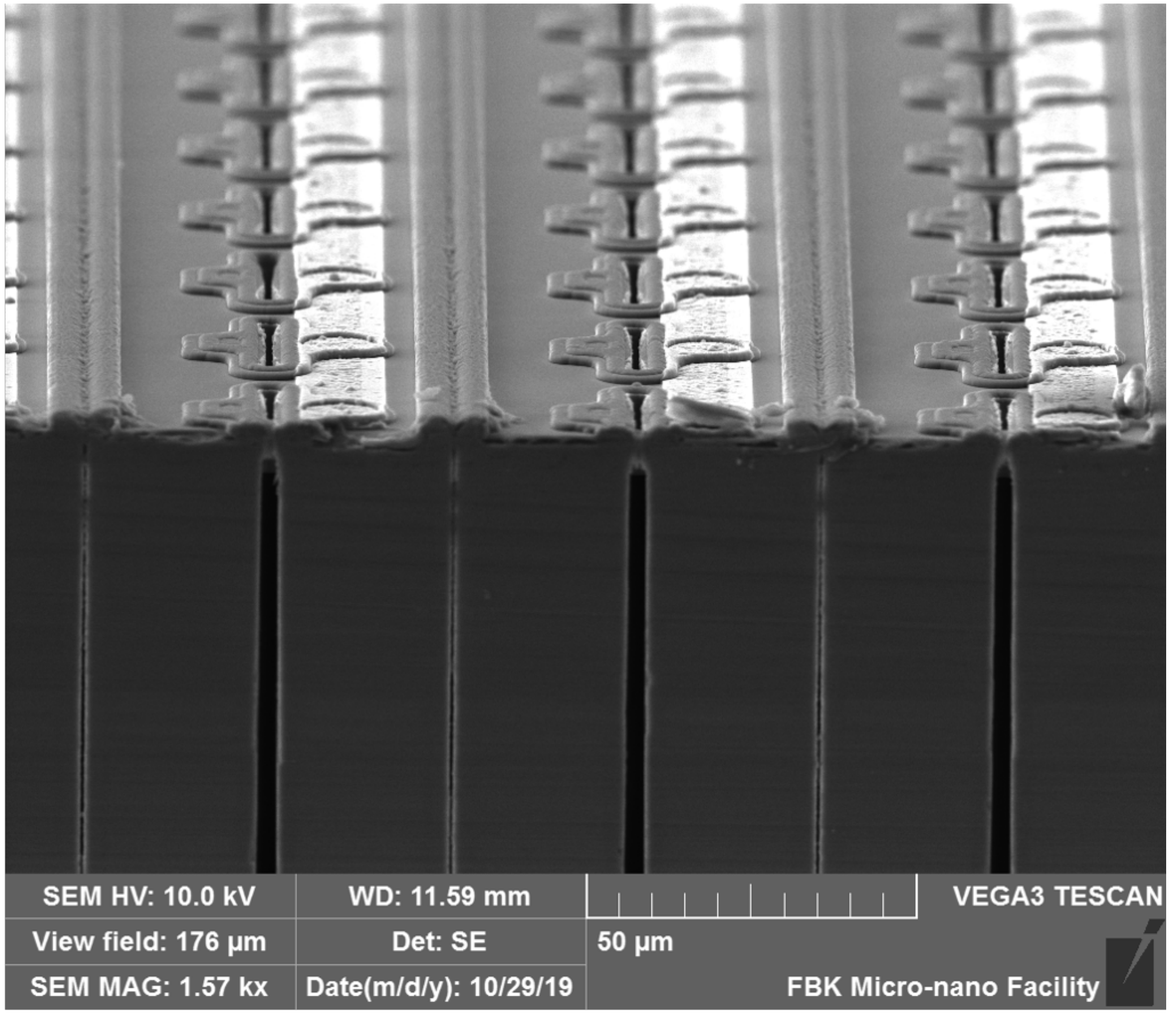

Tested devices: timing and efficiency

- Different devices were tested at **SPS/H8** (November 2021, May 2022)
- Custom made front-end electronic boards featuring a **two stage transimpedance amplifier**

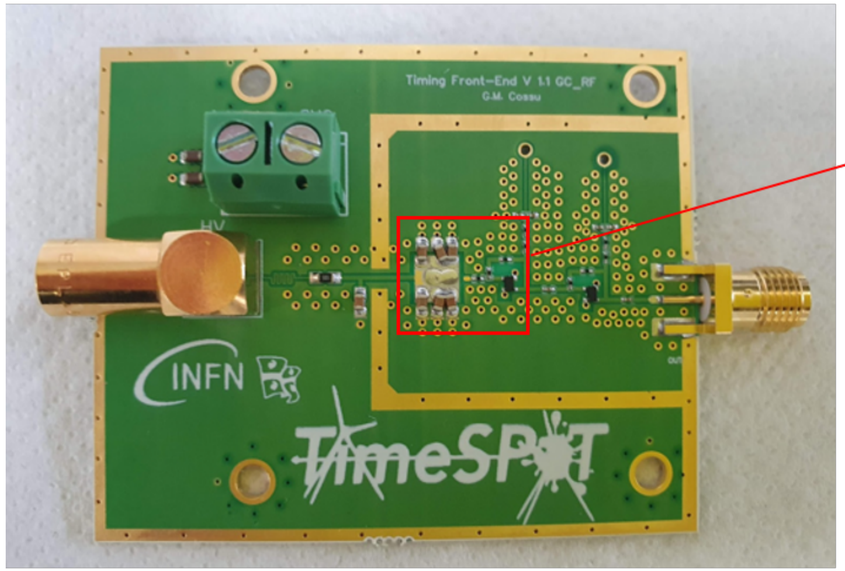

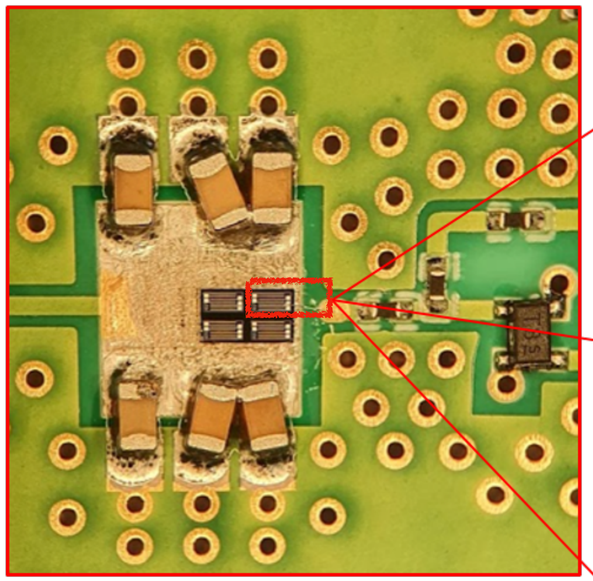

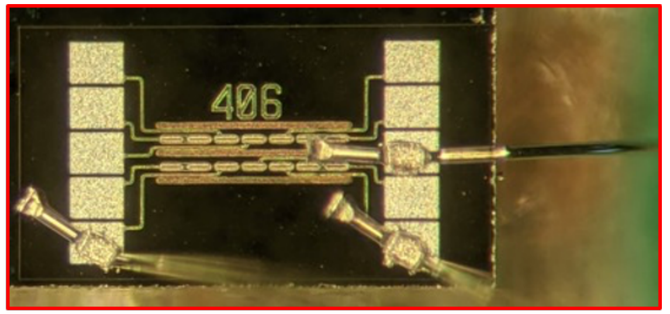

1 PIXEL

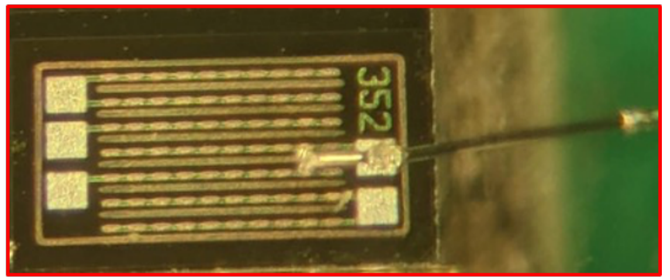

1 STRIP
(10 pixels)

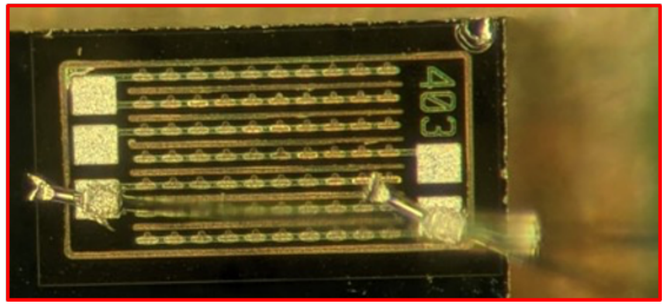

3 STRIPs
(30 pixels)

SPS beam test: Experimental Setup

- **180 GeV/c π^+ beam,** 10^6 pions per spill on a beam spot of 8mm RMS transverse size

- 2 **MCP-PMTs** on the beam line to **time-stamp** the arriving particle (σ_{avg} = 5-7 ps)

- One **sensor fixed** (sensor 1), one **sensor mounted on piezoelectric stages** (sensor 2) to precisely align the two 3D structures, all mounted in a RF-shielded box

- Possibility of operating the fixed sensor down to **-40°C** using dry ice to test **irradiated devices**.

- Readout with **8GHz bandwidth 20GS/s Scope**, trigger on the AND of one 3D sensor and one of the MCP-PMTs

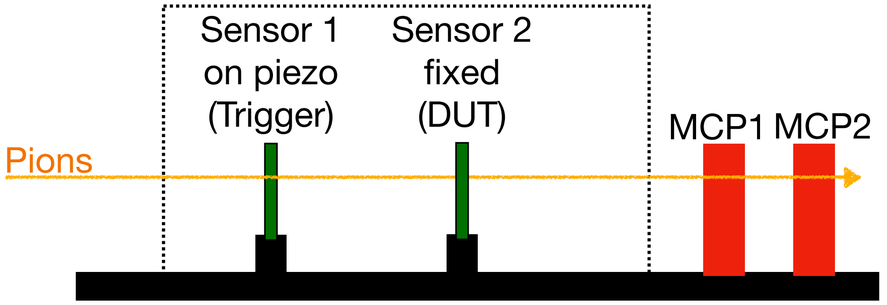

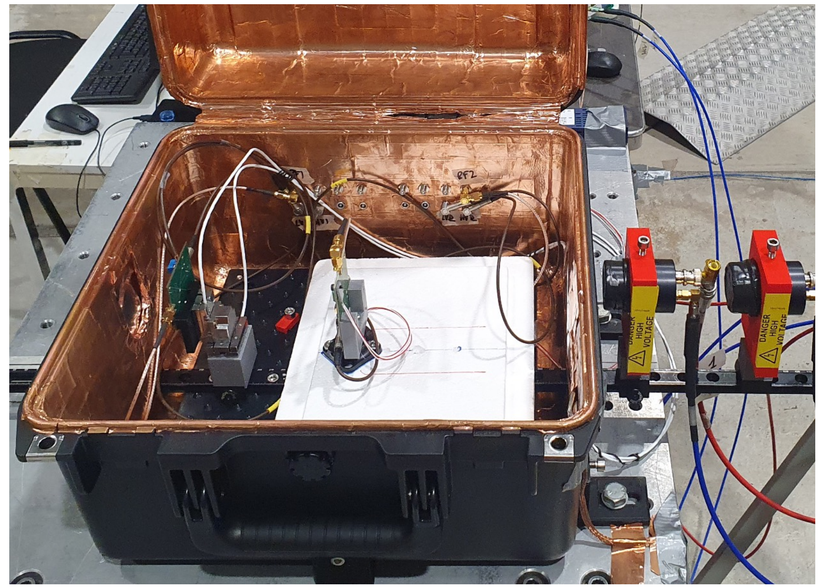

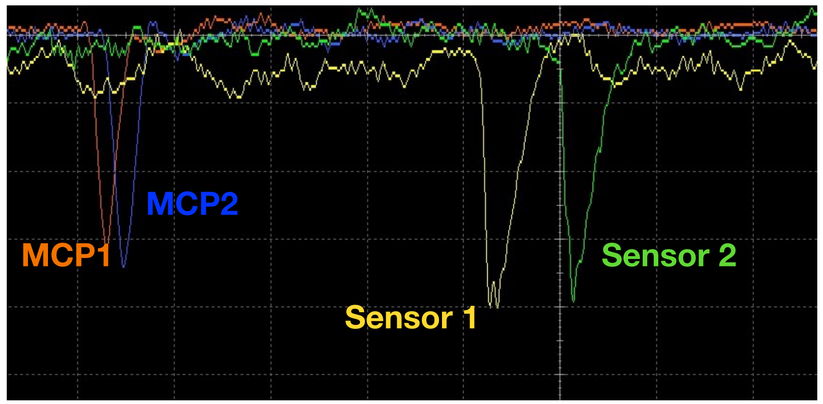

Efficiency tests: the setup

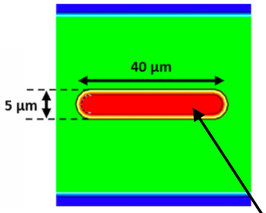

The **trenches** are **non-active volumes**:

to **tilt the sensor** with respect to normal incidence is **needed** to **recover the geometrical efficiency**

To **measure efficiency**:

- Trigger on a **single pixel** (55x55μm^2) **centered** on a **triple strip** (165x550μm^2) and **counting the fraction of signals seen in the triple strip**
- The single **pixel** is mounted on the **piezoelectric stages**, the **triple strip** has fixed position but can **rotate around the trench direction**

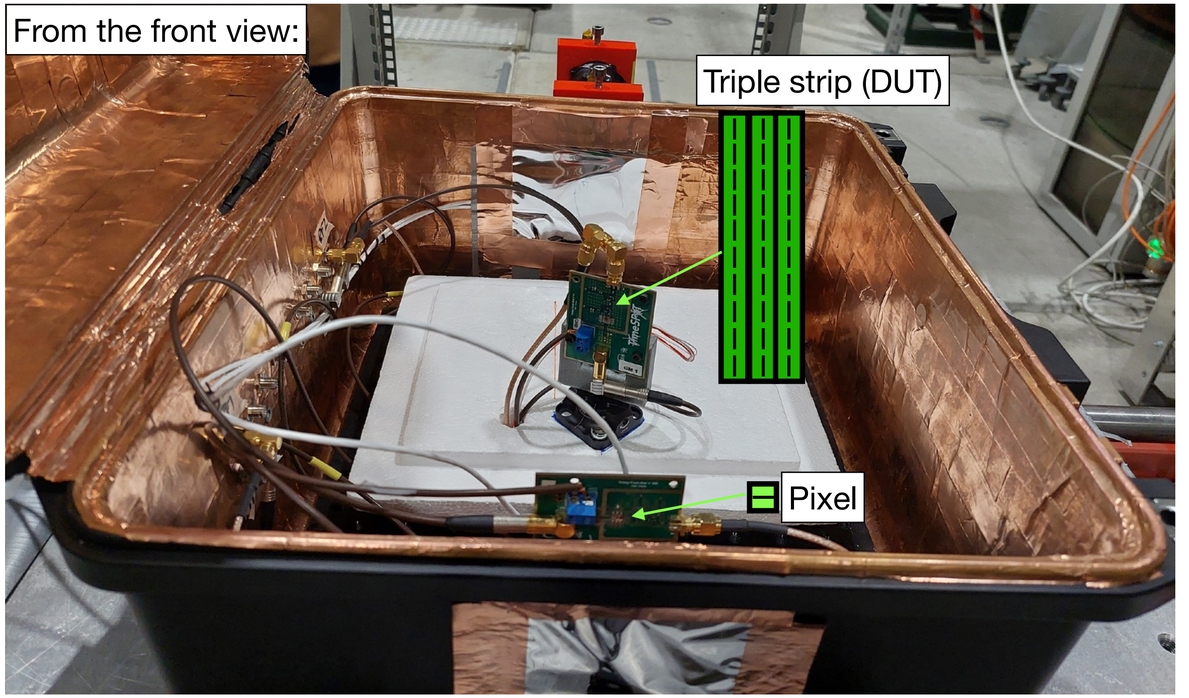

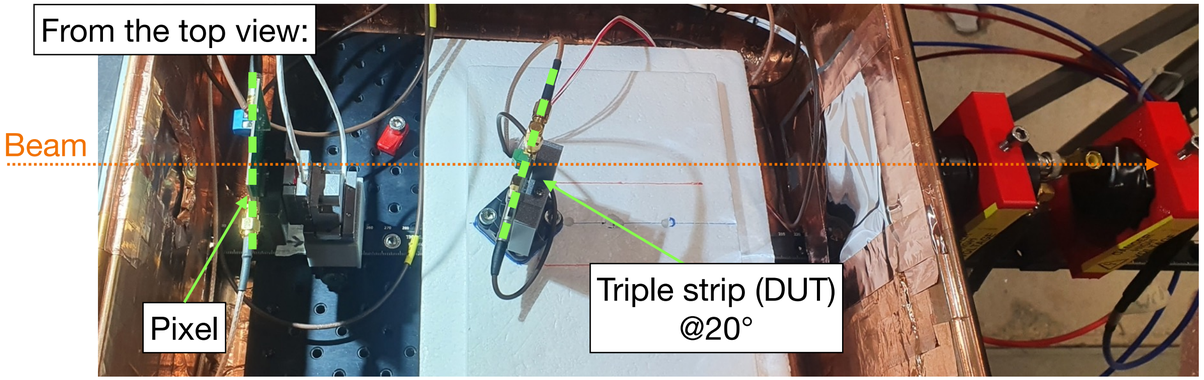

Radiation hardness of 3D-trench silicon sensor studies

- **3D sensors irradiated** at the Triga Mark II reactor at the Jožef Stefan Institute in Lubjiana, Slovenia

- **Fluences:** up to $2.5 \cdot 10^{16}$ 1 MeV n_{eq}/cm^2

  ⟶ Almost expected **fluency on LHCb VELO after LHC Run5** on innermost detectors

- Sensors **tested below -20°C** to reduce **leakage current**

- **Efficiency and timing studies** performed in the irradiated sensors as well

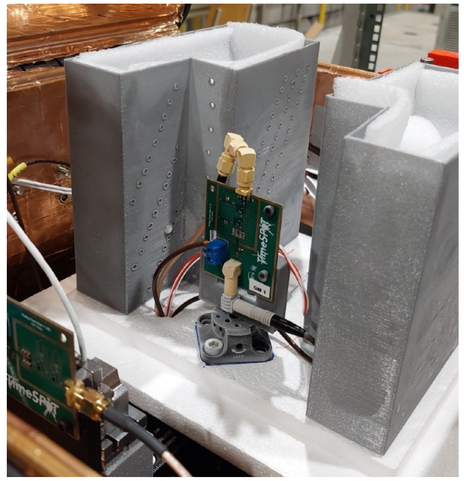

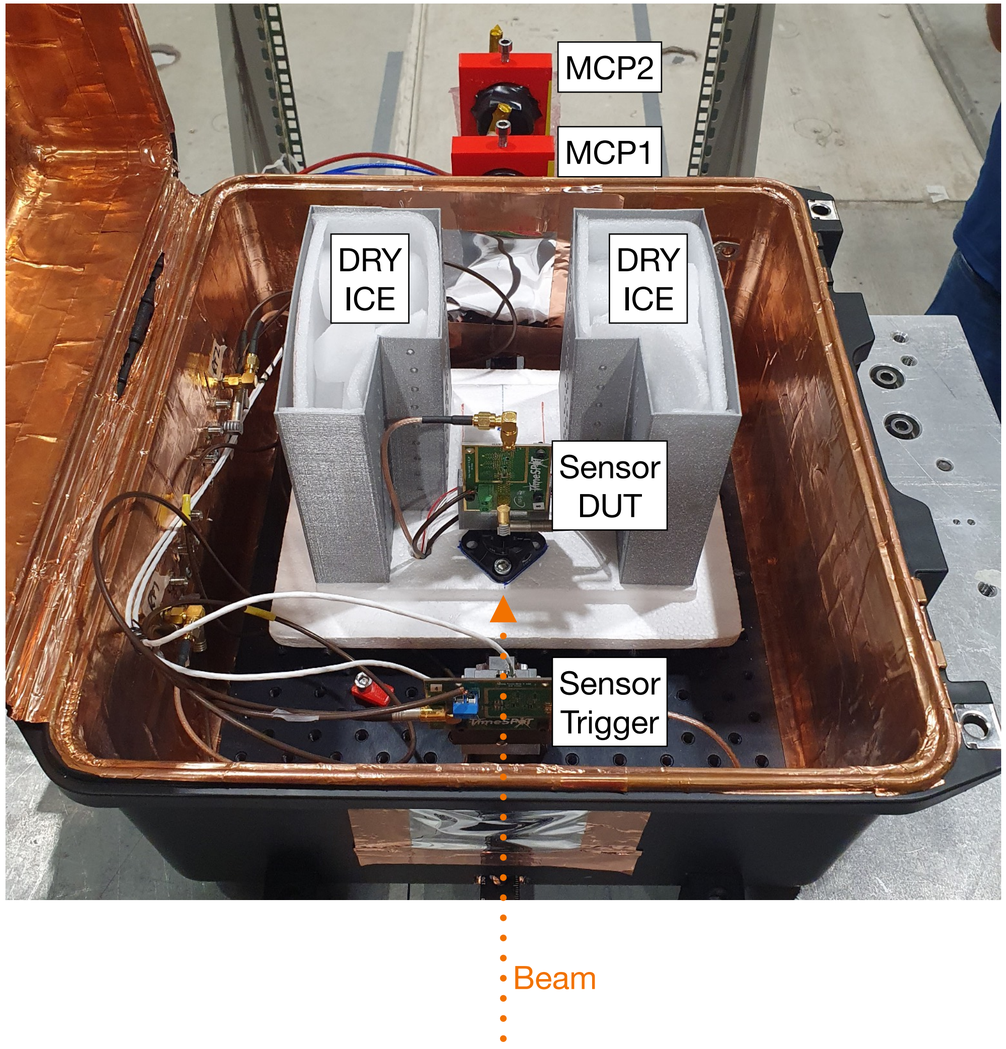

Conclusions

- The **time resolution of a single 3D-trench pixel** sensor was measured at SPS with a 180 GeV/c π^+ beam and found to be about **11 ps** @ V_{bias}=100V (sensor intrinsic + FEE noise)
- The sensor **detection efficiency** is **fully recovered** for incident **angles larger than 10°** with respect to normal incidence
- **Sensors irradiated** at a fluence of $2.5 \cdot 10^{16}$ 1 MeV n_{eq}/cm^2 at V_{bias} exceeding 100V **perform as the non-irradiated sensors, both in timing performances and efficiency**
- **3D devices confirm** their theoretical **excellent performance** in timing and the trench geometry appears to be the right direction to go

The front-end electronics is now the limiting factor to the system performance